課程博士

2017 年 3 月

関西大学審査学位論文

Design and Applications of Intelligent Hydrogels with Controllable Molecular Recognition

分子認識を制御できる インテリジェントゲルの設計と応用

研究科・専攻：理工学研究科・総合理工学専攻

研究領域　　：生体材料化学

学籍番号　　：14D6010

氏名　　：松本　和也

博士論文要旨

理工学研究科総合理工学専攻
研究領域：　生体材料化学
学籍番号：　14D6010
氏名：　松本　和也

【論題】：Design and Applications of Intelligent Hydrogels with Controllable Molecular Recognition
（分子認識を制御できるインテリジェントゲルの設計と応用）

【概要】

刺激応答性ゲルは，温度や pH などの外部環境変化に応答して体積変化することから，ドラッグデリバリーシステム（DDS）やセンサーシステムなど幅広い分野での応用研究が展開されている。これまでに様々な分子複合体を可逆的架橋点としてゲル内に導入することにより，特定分子を認識して体積変化する刺激応答性ゲル（分子応答性ゲル）が合成されてきた。一方，タンパク質はそのアミノ酸配列に応じて特定の高次構造を形成し，それがタンパク質機能の発現を制御している。たとえば，ある種のタンパク質はその特定部位にエフェクター分子が結合することによりそのコンフォメーションが変化し，特定の分子との結合能を大きく変化させるアロステリック効果を示す。本研究では，二次構造が転移するポリペプチドをゲルの高分子主鎖に利用し，分子応答性ゲルの分子認識制御とその応用を目指した。

【各章の要旨】

第 1 章では, 研究の背景と意義を述べ, さらに本論文を理解するための基本的な知識をまとめた。タンパク質の高次構造と機能について述べ，本研究で用いた分子応答性ゲルの基本的設計およびその機能について記した。

第 2 章では，ポリペプチドを高分子主鎖に用いた刺激応答性ゲルの調製とその pH 応答挙動を記した。側鎖にアミノ基を有する poly(L-lysine)（PLL）は，特定の条件下でα-ヘリックスを形成し，pH 変化によってランダムコイルへと可逆的に構造転移することが知られている。そこで，PLL の化学架橋により，PLL ゲルを調製した。このゲルは，外部 pH 変化に応答した体積変化挙動を示した。このゲル中の PLL 鎖は塩基性条件下でα-ヘリックスを形成し，pH 変化によりランダムコイルへと可逆的に構造転移した。また，架橋により PLL のα-ヘリックスが安定化され，ゲルの構造転移点がシフトすることが明らかとなった。

第 3 章では，リガンド分子を PLL ゲルに導入し，二次構造転移による分子の吸着放出挙動の制御を試みた結果について述べた。まず，内分泌かく乱物質の疑いのある bisphenol A（BPA）が，β-cyclodextrin（CD）と 1:2 で包接することを確認した。そこで，PLL にリガンド分子として CD を導入した CD-PLL を合成し，BPA を鋳型とした分子インプリント法により BPA インプリント CD-PLL ゲルを調製した。このゲルは，BPA 存在下では CD と BPA との複合体が形成され，架橋点数が増加することにより収縮した。また，pH 変化により PLL 鎖が構造転移することにより，分子インプリント法により記憶させた分子認識サイトが崩れ，BPA に対する分子認識能が変化した。さらに，分子インプリント法により BPA を固定化させた BPA 内包 CD-PLL ゲルは，pH 変化に応答した PLL の二次構造に依存して BPA を放出した。

第 4 章では，抗酸化物質の放出を制御する薬物固定化ポリペプチドゲルの設計とその薬物放出挙動を記した。抗酸化物質の一種である resveratrol（RSV）は，CD と 1:2 の包接錯体を形成する。そこで，弱酸性条件下で構造転移する poly(L-glutamic acid)（PGA）にリガンドとして CD を導入し，RSV に対する分子インプリント法により，RSV 内包 CD-PGA ゲルを調製した。中性条件下では，分子インプリント法により形成された分子認識サイトにより，CD と RSV の包接錯体が安定化されたため，RSV の放出が抑制された。また，酸性条件下では，PGA 鎖がランダムコイルからα-ヘリックスへ構造転移したことにより，CD と RSV の包接錯体が不安定化され，RSV に対する複合体形成能が低下したため，CD-PGA ゲルは RSV を放出した。

第 5 章では，標的分子を高感度かつ高選択性で検出できる分子インプリントゲル薄膜の設計について述べた。水晶振動子マイクロバランス（QCM）チップ上に BPA インプリント CD-PLL ゲル薄膜を調製した。調製したインプリントゲル薄膜は，ノンインプリントゲル薄膜に比較して 3 倍以上も高感度に BPA を検出できた。さらに，分子インプリント法により形成された BPA 認識サイトは，分子構造のわずかな差異も認識できることが明らかとなった。

第 6 章では, 標的分子に応答して二次構造が転移する BPA インプリント CD-PGA ゲルおよび BPA インプリント CD-PLL ゲルの設計とその応答挙動を記した。BPA インプリント CD-PGA ゲルは，架橋密度が小さかったため，構造転移点はシフトしなかった。一方，BPA インプリント CD-PLL ゲルは，BPA 存在下での分子複合体の形成により，PLL のα-ヘリックスが維持されやすくなり，ゲルの構造転移点がシフトすることが明らかとなった。

第 7 章では，本論文の総括を述べた。分子インプリントゲルの高分子主鎖に二次構造が転移するポリペプチドを用いることにより，分子インプリントゲルはポリペプチドの二次構造に依存した分子吸着挙動を示すことが明らかとなった。また，抗酸化物質を分子インプリン法により内包することにより，構造転移により薬物を放出する DDS キャリアとして応用できることが示された。さらに，QCM チップ上に調製された分子インプリントゲル薄膜は，標的分子を高感度かつ高選択性で検出できるため，診断・分析システムとして医療・環境分野に貢献することが期待できる。したがって，標的分子に応答して構造転移を誘起できるゲルは，新たなバイオインスパイアード材料として期待できる。

以上

References

1) 松本和也，宮田隆志 “生体分子機能を利用した刺激応答性ゲル” *高分子論文集*, 71, 125-142 (2014).
2) Kazuya Matsumoto, Akifumi Kawamura and Takashi Miyata “Structural Transition of pH-responsive Poly(L-lysine) Hydrogel Prepared via Chemical Crosslinking” *Chem. Lett.*, 44, 1284-1286 (2015).
3) Kazuya Matsumoto, Brylee David B. Tiu, Akifumi Kawamura, Rigoberto C. Advincula and Takashi Miyata “QCM sensing of bisphenol A using molecularly imprinted hydrogel/conducting polymer matrix” *Polymer J.*, 48, 525-532 (2016).
4) Kazuya Matsumoto, Akifumi Kawamura and Takashi Miyata “Conformationally Regulated Molecular Binding and Release of Molecularly Imprinted Polypeptide Hydrogels that Undergo Helix-Coil Transition” *submitted*.
5) Kazuya Matsumoto, Nobuki Sakikawa and Takashi Miyata “Thermo-Responsive Gels That Absorb Moisture and Ooze Water” *in preparation*.

Table of Contents

Chapter 1

General Introduction

Page

1.1 Scope of the research 2

1.2 Protein 4

1.2.1 Protein structure 4

1.2.2 Protein function 8

1.2.3 Regulation of protein functions 10

1.3 Intelligent hydrogel 12

1.3.1 Stimuli-responsive hydrogel 12

1.3.2 Molecule-responsive hydrogel 15

1.4 Overview of this thesis 18

1.5 References 21

Chapter 2

Preparation of Polypeptide Hydrogels that Undergo Helix-Coil Transition

2.1 Introduction 28

2.2 Experimental 30

2.2.1 Materials 30

2.2.2 Preparation of PLL hydrogel 30

2.2.3 Measurements of swelling ratio changes 32

2.2.4 Circular dichroism 33

2.3 Results and Discussion 35

2.3.1 pH-Responsive swelling ratio change of PLL hydrogel 35

2.3.2 pH-Responsive structural transition of PLL hydrogel 37

2.4 Conclusions 41

2.5 References 42

Chapter 3

Preparation of Molecularly Imprinted Polypeptide Hydrogels and Their Regulation of Molecular Recognition

3.1 Introduction 46

3.2 Experimental 50

3.2.1 Materials 50

3.2.2 Synthesis of mono-6-carboxy-6-deoxy-β-CD (carboxy-CD) 50

3.2.3 Introduction of CD to PLL 53

3.2.4 Preparation of BPA-imprinted and BPA-loaded CD-PLL hydrogels 54

3.2.5 FT-IR measurement 55

3.2.6 Circular dichroism 55

3.2.7 Measurement of BPA adsorption into hydrogels 56

3.2.8 Measurement of molecularly stimuli-responsive swelling ratio changes 57

3.2.9 Measurements of pH-responsive swelling ratio changes 57

3.2.10 Release of BPA from CD-PLL hydrogels 58

3.3 Results and Discussion 59

3.3.1 Synthesis results of carboxy-CD 59

3.3.2 Characterization of BPA-imprinted CD-PLL hydrogel 61

3.3.3 pH-Responsive structural transition of BPA-imprinted CD-PLL hydrogels 63

3.3.4 Molecule-responsive swelling ratio changes of BPA-imprinted CD-PLL hydrogel 66

3.3.5 BPA adsorption behavior of BPA-imprinted CD-PLL hydrogel 69

3.3.6 Molecular release triggered by structural transition of PLL 74

3.4 Conclusions 80

3.5 References 81

Chapter 4

Preparation of Antioxidant Agent-Loaded Polypeptide Hydrogel and Their Release Behavior by Conformational Change

4.1 Introduction 84

4.2 Experimental 86

4.2.1 Materials 86

4.2.2 Synthesis of NH_2-CD 86

4.2.3 Introduction of CD into PGA 86

4.2.4 Preparation of RSV-loaded CD-PGA hydrogel 87

4.2.5 Circular dichroism 88

4.2.6 Release of RSV from CD-PGA hydrogel 88

4.2.7 Measurement of swelling ratio changes 89

4.3 Results and Discussion 90

4.3.1 Characterization of CD-PGA 90

4.3.2 pH-Responsive structural transition of RSV-loaded CD-PGA hydrogels 91

4.3.3 Antioxidant agent release behavior from RSV-loaded CD-PGA hydrogel 93

4.4 Conclusions 97

4.5 References 99

Chapter 5

Preparation of Molecularly Imprinted Polypeptide Gel Layer for QCM Sensing

5.1 Introduction 102

5.2 Experimental 106

5.2.1 Materials 106

5.2.2 Synthesis of carboxy-CD 106

5.2.3 Introduction of CD to PLL 106

5.2.4 Preparation of poly(G03T-COOH) films 106

5.2.5 Preparation of BPA-imprinted CD-PLL gel layers 107

5.2.6 Characterizations of gel layers on QCM sensor chips 108

5.2.7 QCM measurements 109

5.3 Results and Discussion 111

5.3.1 Characterizations of poly(G03T-COOH) films 111

5.3.2 Characterization of BPA-imprinted CD-PLL gel layers 114

5.3.3 BPA recognition behavior of BPA-imprinted CD-PLL gel layers 118

5.4 Conclusions 126

5.5 References 127

Chapter 6

Molecule-Triggered Structural Transition of Molecularly Imprinted Polypeptide Hydrogel

6.1 Introduction 132

6.2 Experimental 137

6.2.1 Materials 137

6.2.2 Synthesis of NH_2-CD and carboxy-CD 137

6.2.3 Introduction of CD and allyl groups into PGA 137

6.2.4 Preparation of BPA-imprinted CD-PGA hydrogel 138

6.2.5 Introduction of CD to PLL 139

6.2.6 Preparation of BPA-imprinted CD-PLL hydrogel 139

6.2.7 Circular dichroism 140

6.3 Results and Discussion 141

6.3.1 Characterizations of CD-AA-PGA 141

6.3.2 Circular dichroism spectra of PGA in a BPA solution 142

6.3.3 pH-Responsive structural transition of CD-PGA solution 143

6.3.4 pH-Responsive structural transition of BPA-imprinted CD-PGA hydrogel and BPA-imprinted CD-PLL hydrogel 145

6.3.5 BPA-triggered structural transition of BPA-imprinted CD-PLL hydrogel 149

6.4 Conclusions 152

6.5 References 153

Chapter 7

Concluding remarks

Concluding Remarks 155

Appendix

List of publications 160

List of presentations 162

Award 170

Acknowledgement

171

Chapter 1

General Introduction

1.1 Scope of the research

A protein folds into a specific three-dimensional structure which is determined by its amino acid sequence. The three-dimensional structure of the proteins allows their excellent functions such as binding, catalysis and switching.[1] Regulation of molecular recognition of the proteins is an extremely important process to metabolism pathway in biological activity. A protein that changes in conformation and binding capacity by its binding with a specific molecule (effector molecule) is called allosteric protein. For example, a hemoglobin undergoes structural transition by binding with one oxygen, followed by enhancing its binding capacity for second oxygen.[2-4] Furthermore, the binding capacity for additional third and fourth oxygens sequentially increases by conformational changes of remaining subunits. Owing to this unique property, the hemoglobin is efficiently saturated with oxygen at a high oxygen concentration in lung alveoli. When the oxygen-saturated hemoglobin circulates to peripheral tissues with low oxygen concentrations, the hemoglobin efficiently unloads oxygens and its binding capacity for oxygen decreases drastically. The conformation of hemoglobin and its binding capacity for oxygen are also sensitive to hydrogen ion concentration that depends on the blood concentration of carbon dioxide and lactic acid (Bohr effect).[5] The Bohr effect enhances transportation and unloading of oxygen in metabolically active peripheral tissues.

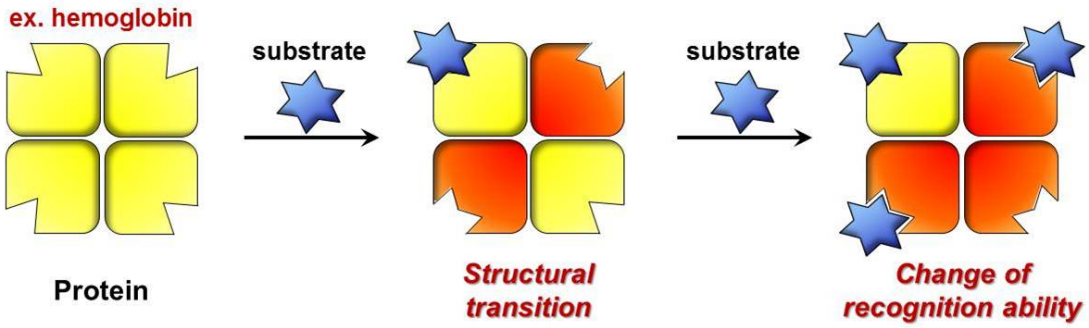

Figure 1-1. Schematic illustration for allosteric effect of a protein.

Intelligent hydrogels have extensively received much attentions in biomedical field because they exhibit swelling/shrinking properties in response to external stimuli such as temperature,[6-8] pH[9,10] and a specific molecule.[11-15] Among the intelligent hydrogels, molecularly imprinted hydrogels that have molecular recognition sites for target molecules during their polymer networks undergo a change in volume in the presence of target molecules.[16,17] However, the polymer networks of the intelligent hydrogel form random coil or globular conformation in water. The structure of the polymer networks has contributed to only swelling/shrinking properties. Thus, the intelligent hydrogels have not achieved the expression of protein-like functions such as allosteric effect and Bohr effect yet.

The goal of this study is to fabricate intelligent hydrogels with controllable molecular recognition as allosteric proteins. Here, the polypeptide that undergoes structural transition to its secondary structure by a stimulus is promising as a main chain for designing molecularly imprinted hydrogels with controllable molecular recognition sites. In this study, molecularly imprinted polypeptide hydrogels were strategically designed to regulate their molecular recognition ability by the structural transition of polypeptide networks. This thesis describes the approach for fabrication of the intelligent hydrogels with controllable molecular recognition using structural transition of polypeptides. The unique property of the hydrogels was demonstrated as smart biomaterials for drug delivery systems and sensor systems.

1.2 Protein

1.2.1 Protein structure

Proteins are major components of a cell, which account for about 50 wt% of the dry weight of the cell, and play important roles in crucial life phenomena.[1,18] 20 Kinds of amino acids, each of which has a unique side chain, are the building blocks of proteins.[19] Amino acid side chains have various properties involved in size, shape, charge, hydrophilicity/hydrophobicity, chemical reactivity, and interactions such as hydrogen bonding, electrostatic interaction, Van der Waals force, and hydrophobic interaction.

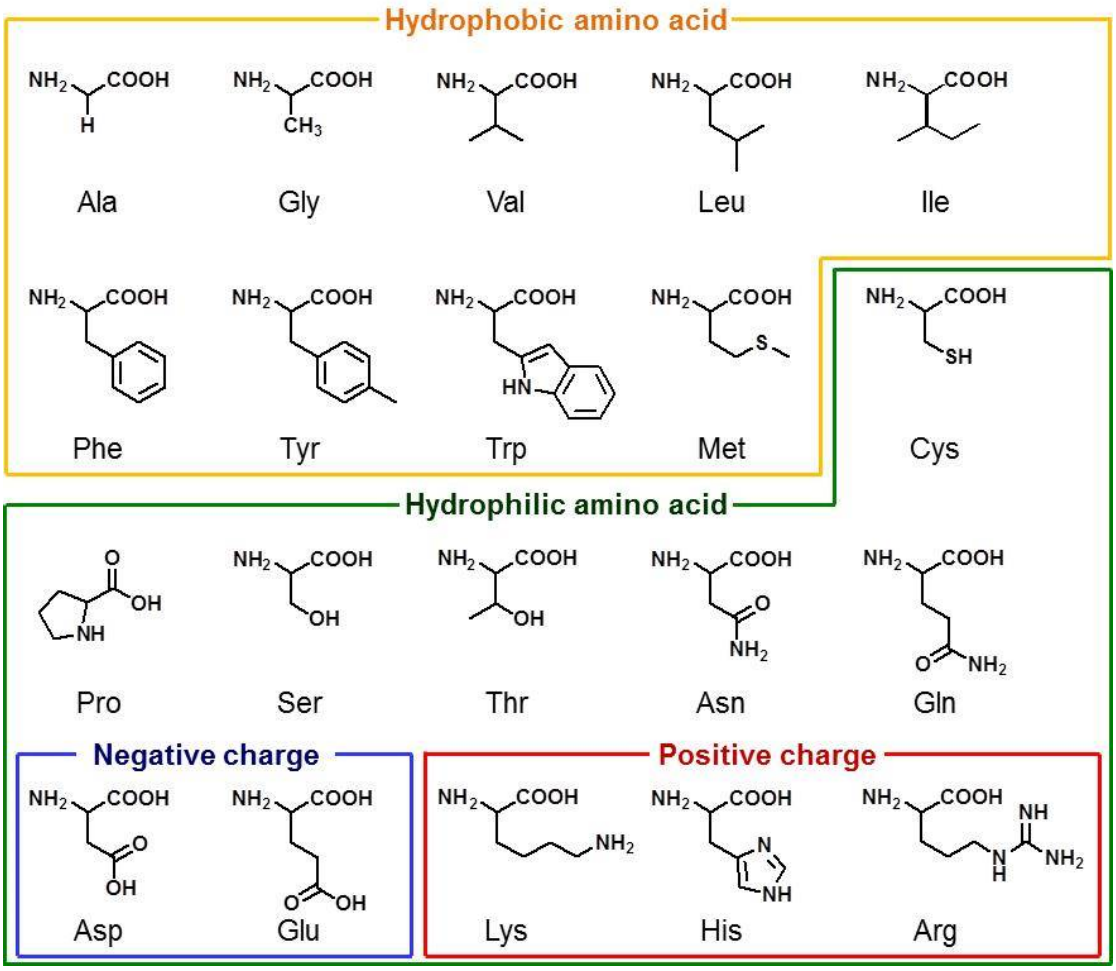

Figure 1-2. Classification of 20 kinds of amino acids.

Differences in the amino acid side chains strongly influence stability and functions of the proteins.[20-23] Within a protein, many amino acids are linked together by peptide bond. The amino acid sequence of a polypeptide chain (primary structure) is critical to a three-dimensional structure of the protein. Linear polypeptide chains can spontaneously fold into three-dimensional structures in an aqueous solution at physiological temperature. Hydrophobic amino acids are buried inside the protein core due to entropy-driven hydrophobic interaction between the hydrophobic amino acids, followed by stabilizing the protein structure. Hydrophilic amino acids reside preferentially on outside of the proteins, which determine solubility of the protein in aqueous solutions.

Polypeptide chains have the secondary structure based on the backbone dihedral angles that are defined as ϕ and ψ.[24,25] Known as α-helix, β-sheet and β-turn, these stable folding are main elements of the secondary structure of proteins. The α-helix is stabilized by hydrogen bonds between the backbone carbonyl and amino groups. In α-helix structure, the carbonyl oxygens make hydrogen bonds to the amino hydrogens located four residues earlier along the polypeptide sequence.[26-28]. β-Sheet structure is formed by association of two or more β-strand structures that run alongside each other and are linked in regular manner by hydrogen bonds between the backbone carbonyl and amino groups.[29,30]

A tertiary structure of proteins is an ensemble of α-helix, β-sheet, turn and loop structures in a polypeptide chain using a variety of intramolecular interactions caused by both hydrophilic and hydrophobic amino acids[31-35] In most cases, a protein is the macromolecule involving multiple polypeptide chains or subunits. The three-dimensional structure of a protein based on intermolecular bonding has been called quaternary structure.

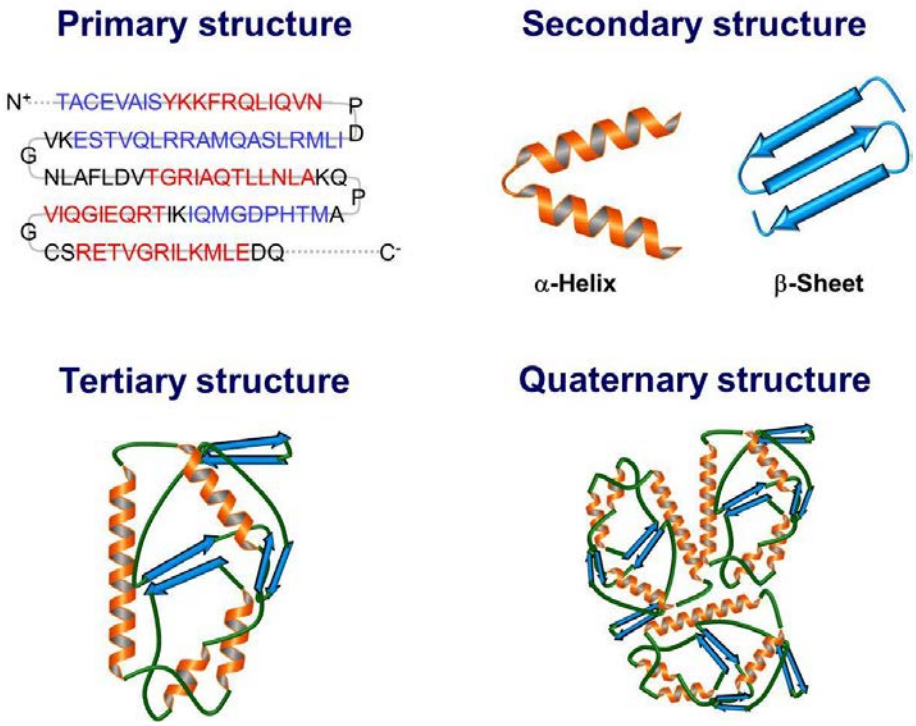

Figure 1-3. Levels of protein structure.

Protein stability, which is governed by various interactions in proteins[22,36] is defined as net loss of Gibbs free energy (*ΔG*) including both enthalpy and entropy following the equation 1-1.

$$\Delta G = \Delta H - T\Delta S \qquad (1\text{-}1)$$

where, *ΔH* is a change in the enthalpy, *ΔS* is a change in the entropy, *T* is the temperature. A decrease of Gibbs free energy that means a reaction is favorable occurs by a decrease enthalpy with bond formation which is an exothermic reaction, by an increase entropy of the protein and solvent environment, and by the balance between enthalpy and entropy changes.

All chemical bonds have some flexibility and rotate at a temperature above absolute zero. Because most of the forces that stabilize native states of proteins are non-covalent bonds, there is enough thermal energy to break and reform of weak

interactions at physiological temperature.[37-40] Therefore, proteins have good flexibility in comparison with other molecules having only covalent bonds. The protein structures continuously fluctuate in the range from a few hundredths of an angstrom for a simple atomic vibration to many angstromes for the movement of a whole segment of a protein structure. These fluctuations have enough magnitude to allow small molecule to penetrate into the protein. The atomic fluctuations are indispensable for protein functions such as molecular recognition and catalysis because they enable the protein to bind with a specific molecule and to adjust its structure to the shape of the substrate in accordance with the progress of a reaction.

1.2.2 Protein functions

Proteins have many biochemical functions such as molecular recognition, catalysis, molecular switching, and as structural matrix of cells. The molecular recognition based on their binding is the most fundamental biochemical function of proteins. Such specific functions of proteins depend on their binding capacity for ligand molecules. Proteins specifically bind with ligand molecules including small molecules and macromolecules. Such specific bindings are attributed to complementary binding sites in the proteins, which are formed as a consequence of the three-dimensional structure of the proteins.[41-45] Packing defect of polypeptide side chains creates clefts of various sizes on its surface or internal cavities. Such clefts and cavities are important elements for the proteins to specifically bind ligands. Environments around clefts and cavities are quite different from the other portions. For example, environments of the clefts and the cavities that have many hydrophobic residues resemble nonpolar organic solvents. As a result, the hydrophobic clefts and cavities can bind highly hydrophobic ligands such as lipids. If most of their residues have a positive charge or a negative charge, there are very strong local electrostatic field that enable protein to bind with highly charged ligands.

Enzymes promote and catalyze the chemical reaction in the living cell. Due to their complicated structures, enzymes have distinct features regarding (i) reaction rate, (ii) reaction condition, (iii) specificity and (iv) regulation in compare with inorganic catalysts. (i): The catalytic efficiency of the enzymes is remarkable: reaction rate of enzyme is several orders of magnitude faster than that of inorganic catalyst. (ii): The enzyme-catalyzed reactions proceed under condition of mild physiological temperature, atmospheric pressure and nearly neutral pH. In contrast, reactions with inorganic catalyst often require severe conditions such as high temperature, high pressure and extreme of pH. (iii): Enzymes can recognize slight differences of molecular structure and act on only one substrate. (iv): The reaction rate of some enzymes can be regulated

(activation or inhibition) in the presence of other molecules. More details about this regulation are described in *Chapter 1.2.3 Regulation of Protein Functions*.

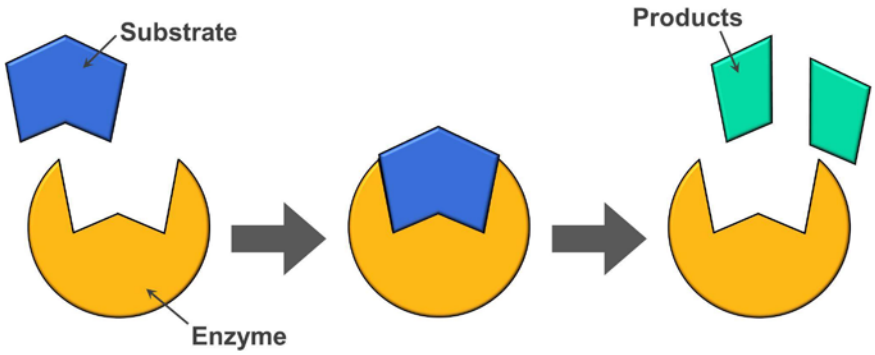

Figure 1-4. Schematic illustration for catalytic reaction of an enzyme.

1.2.3 Regulation of protein functions

The fact that the three-dimensional structure of proteins determines their functions is a basic principle of biology. Usually, proteins regulate their functions according to the change of their three-dimensional structure.[46-51] If the activity of the proteins remains unchanged anywhere in the cell, there is fear that the proteins express an unnecessary function. The proteins undergo conformational change to their active forms to switch their activity in accordance with the environments.

Effector molecules as ligands induce conformational transition of the proteins to their inactive or active forms, and regulate their activity. Usually, the effector molecules act as inhibitors that compete with the substrate in binding.[52] Enzymatic reaction products that are also competitive inhibitor adjust the catalytic activity of enzyme when they are excessively produced. In cases of the allosteric proteins, such effector molecules and reaction products bind to distant sites remote from active sits of the proteins, and inhibit (negative cooperativity) or activate (positive cooperativity) enzymatic activity. In the positive cooperativity, the binding capacity of an allosteric protein, which has multiple subunits, for a first effector molecule is weak. However, conformational transition of the allosteric protein occurs by its binding with the first effector molecule, followed by increasing the binding capacity of the second subunit for a second effector molecule. In turn, this cooperative binding can chain to even more subunits. Due to their unique phenomena, allosteric proteins exhibiting cooperative binding were often used to regulate metabolic pathways. For example, the hemoglobin composed of four subunits efficiently transports oxygen due to its oxygen binding with positive cooperativity.

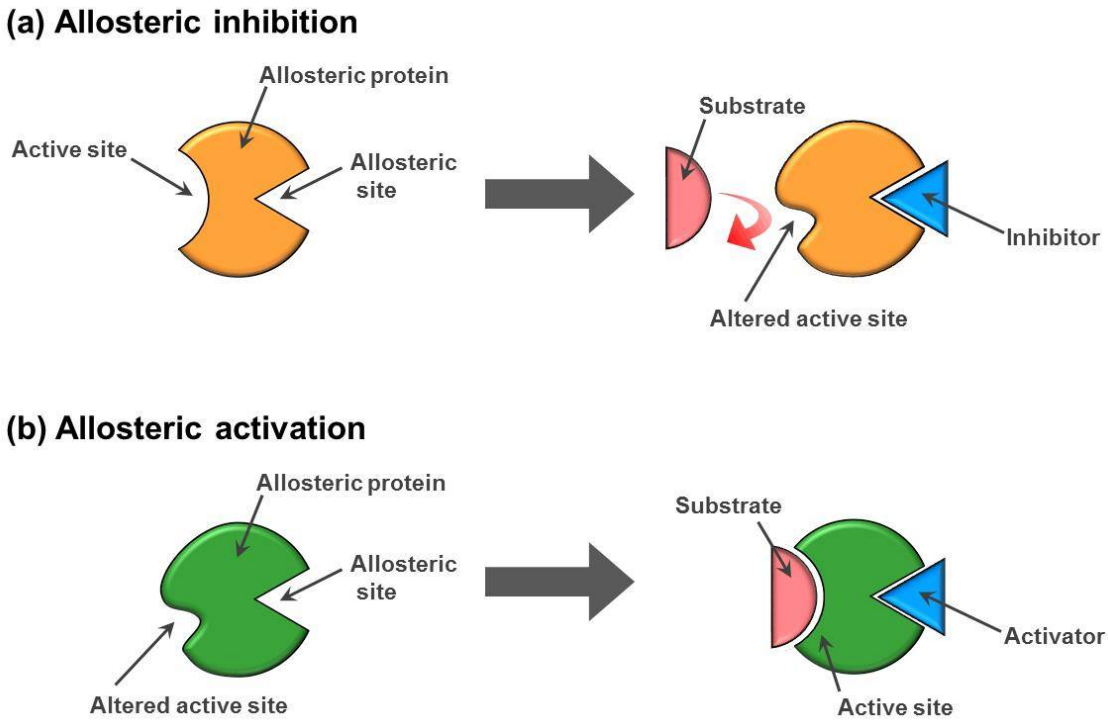

Figure 1-5. Schematic illustration for allosteric inhibition (a) and allosteric activation (b) behavior of an allosteric protein in response to its substrate.

1.3 Intelligent hydrogels

1.3.1 Stimuli-responsive hydrogels

Polymeric hydrogels are composed of physically or chemically cross-linked three-dimensional hydrophilic polymer networks and solvents. Hydrogels have been used as a jelly and an agar for several centuries. Because the hydrogels have various fascinating properties such as swelling properties, permeation properties, adsorbing properties and biocompatibility, they have also been utilized as contact lenses, disposable diaper and biomaterials.[53-55] Since the first report about volume phase transition of the hydrogel by Tanaka,[56,57] basic researches and applications of the hydrogels have been accelerated all over the world. A variety of stimuli-responsive hydrogels that undergo change in their volume in response to environmental stimuli such as temperature,[6-8] pH[9,10] and electric field,[58,59] which are often called intelligent hydrogels, have been reported. Such intelligent hydrogels have been increasingly studied as smart materials for biomedical, environmental and energy applications to diagnosis, drug delivery systems (DDS), artificial muscle, micro total analysis system (μTAS) and cell cultures.[60-65] Thermo- and pH-responsive hydrogels have been developed as representative intelligent hydrogels. pH-responsive hydrogels that are usually prepared using polyelectrolytes with carboxy and amino groups undergo changes in volume due to changes in osmotic pressure by association and dissociation of charged groups.[66-70] The polymer chains of thermo-responsive hydrogels have a lower critical solution temperature (LCST), at which polymers exhibited drastic hydrophilicity/hydrophobicity changes in an aqueous solution.[71-75] As a result, poly(*N*-isopropyl acrylamide) (PNIPAAm) hydrogel shrinks drastically with rising temperature above LCST around 32 °C.

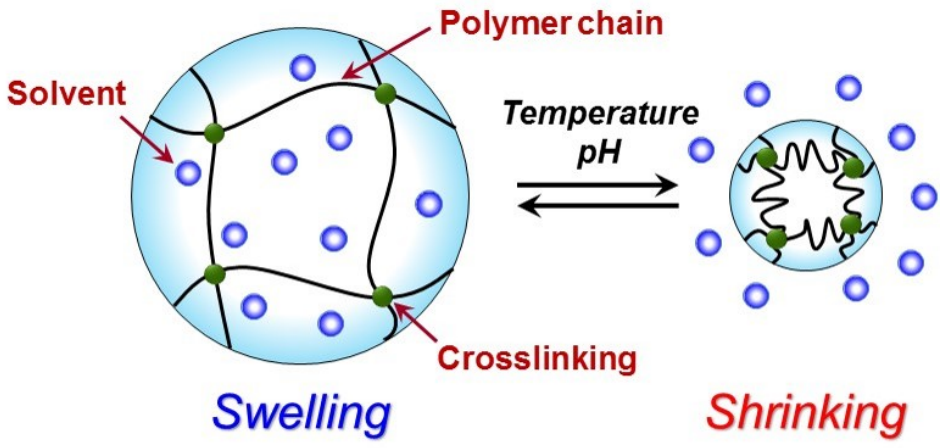

Figure 1-6. Drastic changes in volume of a stimuli-responsive hydrogel in response to environmental changes.

In general, the swelling/shrinking behavior of polymer hydrogels is governed by three free energy terms,[76-78] i.e., the changes in the free energy of mixing (Π_{mix}), elastic deformation (Π_{el}) and electrostatic interactions (Π_{ion}):

$$\Pi = \Pi_{mix} + \Pi_{el} + \Pi_{ion}$$
$$= -\frac{NkT}{v}\left[\phi + ln(1-\phi) + \frac{\Delta F}{2kT}\phi^2\right] + \nu kT\left[\frac{\phi}{2\phi_0} - \left(\frac{\phi}{\phi_0}\right)^{1/3}\right] + f\nu kT\left(\frac{\phi}{\phi_0}\right) \quad (1\text{-}2)$$

where Π is the osmotic pressure of a hydrogel, N is the Avogadro's number, k is the Boltzmann constant, T is the absolute temperature, v is the molar volume of the solvent, ϕ is the volume fraction of the network in the swollen hydrogel, ΔF is the free energy of interaction between polymer and solvent, ν is the concentration of constituent chains at gel formation, ϕ_0 is the volume fraction of the network after the hydrogel preparation, f is the effective charge density of the network. The osmotic pressure (Π) of a hydrogel

determines whether the hydrogel tends to swell or to shrink. Namely, the three factors, i.e., interactions between polymer and solvent (ΔF), a number of cross-linking (ν), and charge density of the network (f) influence the swelling/shrinking behavior of a hydrogel. The thermo- and pH-responsive hydrogels exhibit stimuli-responsiveness based on the changes of Π_{mix} and Π_{ion}, respectively. On the other hand, few intelligent hydrogels undergo changes in volume depending on their cross-linking densities related to Π_{el}.

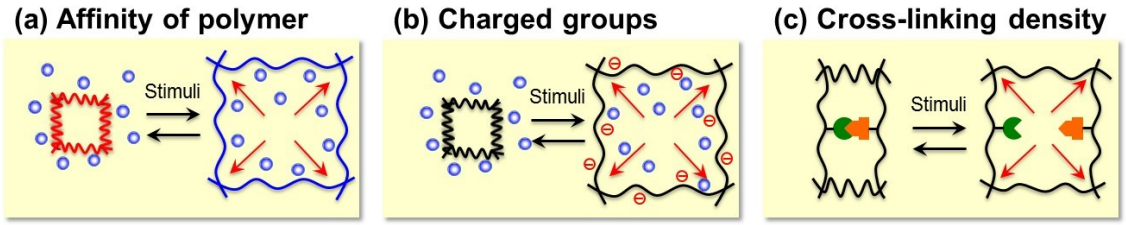

Figure 1-7. Schematic illustration for stimuli-responsiveness of intelligent hydrogels based on (a) the interaction between polymer and solvent, (b) the charge density of network, and (c) a number of cross-linking density.

1.3.3 Molecule-responsive hydrogel

Specific molecular recognition of biomolecules such as antibody-antigen, DNA-protein and sugar-lectin complexes plays important roles in the biological activity. Since the expression level of biomarkers is a critical parameter to monitor body conditions and detection of diseases, various biomarker-based diagnosis systems such as enzyme-linked immunosorbent assay (ELISA) and quantitative polymerase chain reaction (PCR) have been developed using biomolecular interactions. Molecular stimuli-responsive hydrogels (molecule-responsive hydrogel) that undergo a change in volume in response to the presence of biomarkers through specific molecular recognition have great possibilities for novel diagnosis systems.[79-81] However, there are few studies on the molecule-responsive hydrogels because of the difficulty in combination between the molecular recognition function and responsive swelling/shrinking behavior of the hydrogels.

Focusing on Π_{el} of the equation 1-2, molecule-responsive hydrogels have been designed using molecular complexes as dynamic cross-links in hydrogel network. The dissociation or association of molecular complexes as dynamic cross-links in the molecule-responsive hydrogels results in changes in their cross-linking density, followed by swelling or shrinking of their volume. Based on the strategy, the

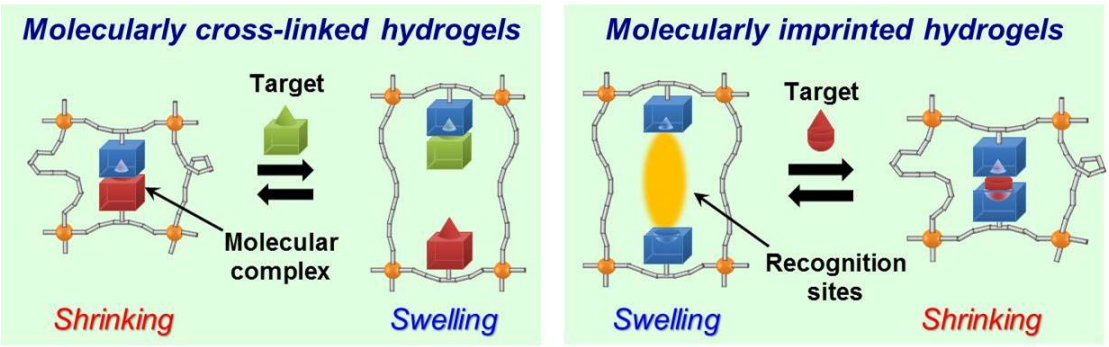

Figure 1-8. Schematic illustration for the molecularly cross-linked hydrogels (a) and the molecularly imprinted hydrogels (b).

molecule-responsive hydrogels are classified to two types, i.e. molecularly cross-linked hydrogel and molecularly imprinted hydrogel.[15,82]

The molecularly cross-linked hydrogels that have dissociable molecular complexes as dynamic cross-links can swell in the presence of a target molecule. Examples of molecularly cross-linked hydrogels include antigen-responsive hydrogels[83-87] and glucose-responsive hydrogels.[88-94] Such hydrogels involving antigen-antibody and sugar-lectin complexes as dynamic cross-links undergo reversible changes in volume in the presence of a target molecule with higher activity.

In contrast, the molecularly imprinted hydrogels with recognition sites for a target molecule can shrink in the presence of the target molecule. Molecular imprinting is a useful technique for designing synthetic hosts having molecular recognition sites. In standard molecular imprinting methods, after ligand monomers with functional groups interact with a template molecule by noncovalent interactions, they are copolymerized with a large amount of cross-linkers to form networks. The molecular recognition cavities are creating by splitting off the template molecule from the resultant polymer network.[95-101] On the other hand, the molecularly imprinted hydrogels are prepared using the molecular complexes between ligands and a target molecule and a minute amount of cross-linker by molecular imprinting method.[102,103] For example, when BPA-imprinted hydrogels using β-cyclodextrin (CD) as ligands were exposed to endocrine disrupter bisphenol A (BPA) as a target molecule, they exhibited a great shrinkage because their cross-linking density increased by the complex formation between a BPA molecule and two CD ligands.[16,104,105] As other molecularly imprinted hydrogels, tumor marker α-fetoprotein (AFP)-imprinted hydrogels with antibody (anti-AFP) and concanavalin A (ConA) ligands shrank in response to the presence of target AFP.[17,106] Thus, a variety of molecule-responsive hydrogels have been increasingly studied using molecular complexes as dynamic cross-links because of their potential applications as smart soft materials.[107-122]

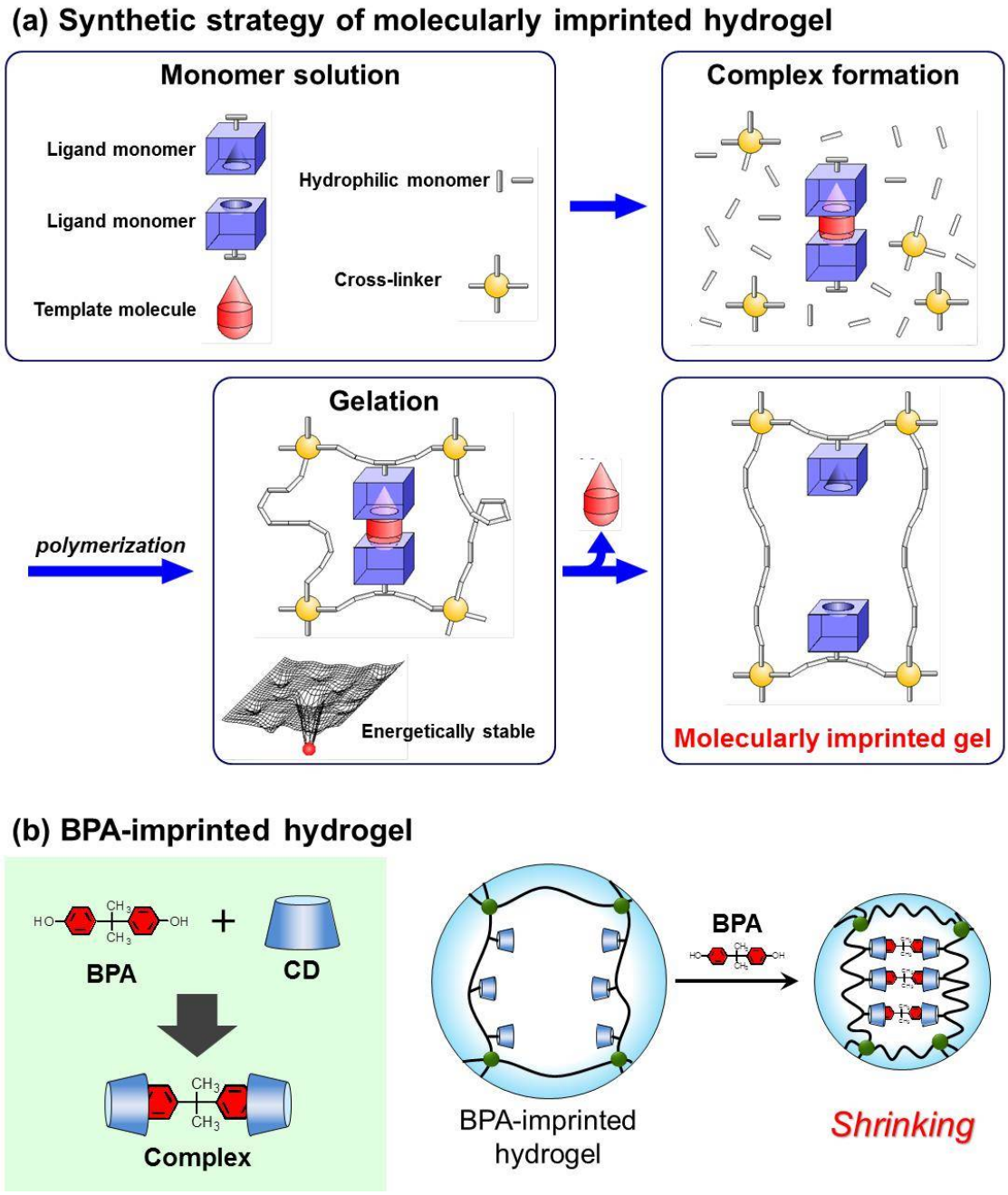

Figure 1-9. (a) Synthetic strategy of hydrogels with molecular recognition sites by molecular imprinting. (b) Schematic illustration for BPA-imprinted hydrogel.

1.4 Overview of this thesis

Figure 1-10 shows overview of this thesis.

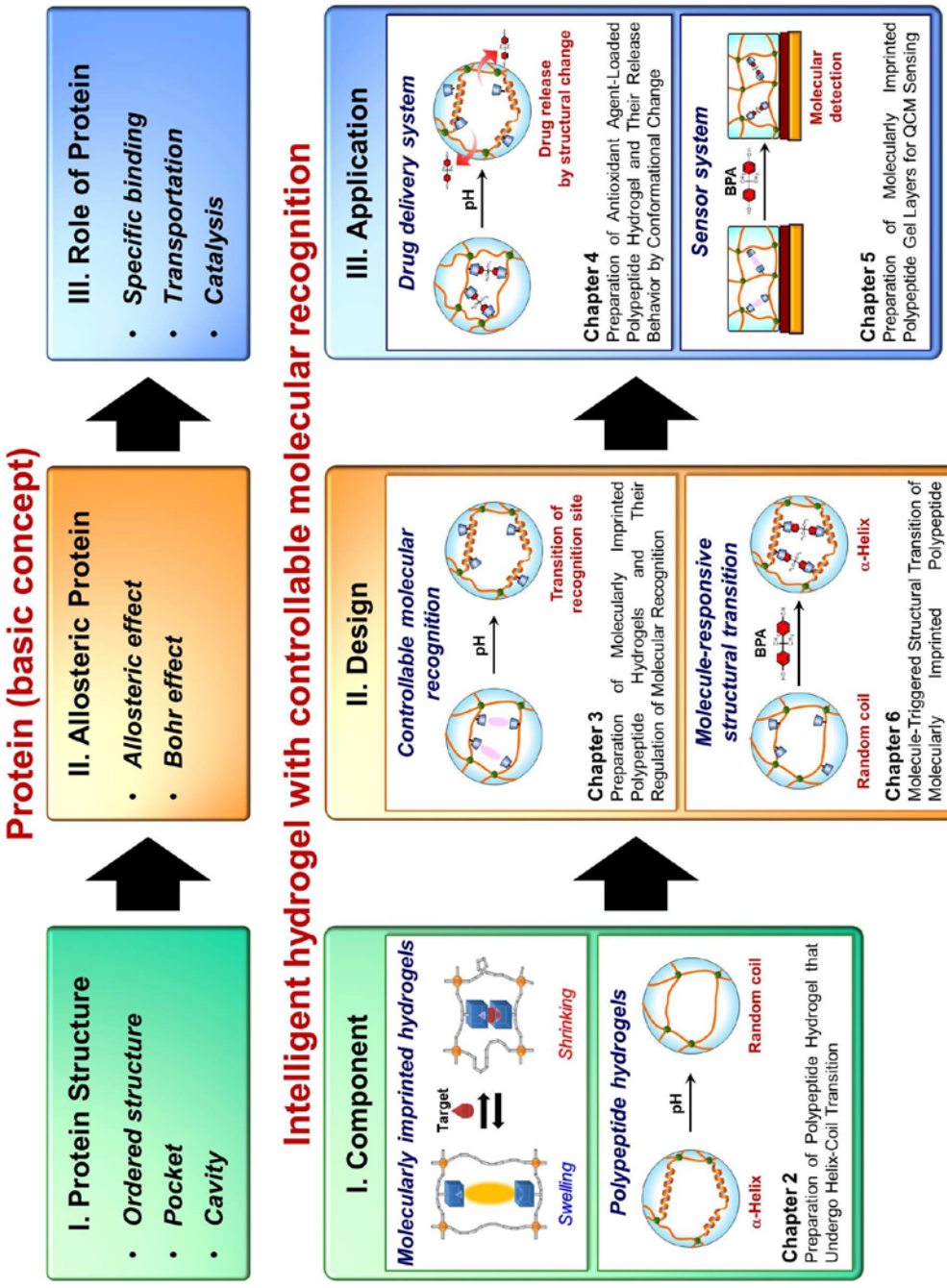

Figure 1-10. Overview of this thesis

This thesis is composed of seven chapters.

Chapter 1 is a general introduction describing protein-inspired intelligent hydrogels with controllable molecular recognition sites. In the first section, structures and functions of proteins are summarized as fundamentals to achieve their controllable molecular recognition. In the second section, the fundamentals of intelligent hydrogels such as stimuli-responsive hydrogels and molecule-responsive hydrogels are introduced.

Chapter 2 provides the preparation of polypeptide hydrogels that undergo structural transition of their polymeric main chains. Poly(L-lysine) (PLL) was used as a main chain of polypeptide hydrogel. The preparation of PLL hydrogel by chemical cross-linking of PLL is described. PLL hydrogels showed pH-responsive swelling and structural change behaviors.

Chapter 3 describes the design of the molecularly imprinted hydrogels with controllable molecular recognition ability. In the preparation of the molecularly imprinted hydrogels, CD and BPA were selected as ligands and a target molecule, respectively. BPA-imprinted CD-introduced PLL (CD-PLL) hydrogels were prepared by molecular imprinting method. The binding capacity of BPA-imprinted CD-PLL hydrogels can be regulated by structural transition of PLL chains in response to a change in pH. Furthermore, release behavior of BPA from the BPA-loaded CD-PLL by the structural transition was also estimated.

Chapter 4 offers antioxidant agents-loaded polypeptide hydrogels. Poly(L-glutamic acid) (PGA) that undergoes structural transition under an acidic condition was used as a main chain of molecularly imprinted hydrogels. Resveratrol (RSV), which is one of the antioxidant agents, was loaded within CD-introduced PGA (CD-PGA) hydrogels by

pseudo molecular imprinting method. The RSV release behavior from RSV-loaded CD-PGA hydrogels, which was triggered by pH-responsive structural transition of PGA chains, was shown in this chapter.

Chapter 5 presents molecularly imprinted gel layers that detected target molecules with high sensitivity and selectivity. BPA-imprinted CD-PLL gel layers were prepared on polyterthiophene-modified quartz crystal microbalance (QCM) sensor chips. BPA recognition behavior was estimated with QCM technique.

Chapter 6 is concerned with a molecule-responsive structural transition behavior of molecularly imprinted polypeptide hydrogels. BPA-imprinted hydrogels that memorize an original conformation induced by target BPA were designed by molecular imprinting method using polypeptide as a main chain. The structural transition behavior in response to target BPA was evaluated with circular dichroism.

Chapter 7 is the conclusion of this thesis. The features of the molecularly imprinted hydrogels with controllable molecular recognition sites are summarized, and their applications are proposed.

1.5 References

1. G. A. Petsko, D. Ringe, “Protein Structure and Functions” Oxford Univ. Press, 2008.
2. J. Monod, J. Wyman, J.-P. Changeux, *J. Mol. Biol.*, **12**, 88-118, 1965.
3. G. Braunitzer, K. Hilse, V. Rudloff, N. Hilschmann, *Advances in Protein Chem.*, **19**, 1-46,1964.
4. E. Antonini, *Physiol. Rev.*, **45**, 123-170, 1965.
5. J. B. Steen, “Comparative physiology of respiratory mechanisms”, Academic Press Inc (London), 1971.
6. T. Amiya, Y. Horikawa, Y. Hirose, Y. Li, T. Tanaka, *J. Chem. Phys.*, **86**, 2375-2379, 1987.
7. G. Chen, A. S. Hoffman, *Nature*, **373**, 49-52, 1995.
8. R. Yoshida, K. Uchida, Y. Kaneko, K. Sakai, A. Kikuchi, Y. Sakurai, T. Okano, *Nature*, **374**, 240-242, 1995.
9. T. Tanaka, D. Fillmore, S-T. Sun, I. Nishio, G. Swislow, A. Shah, *Phys. Rev. Lett.*, **45**, 1636-1639, 1980.
10. M. Annaka, T. Tanaka, *Nature*, **355**, 430-432, 1992.
11. K. Ishihara, M. Kobayashi, N. Ishimaru, I. Shinohara, *Polym. J.*, **16**, 625-631, 1984.
12. K. Ishihara, K. Matsui, *J. Polym. Sci., Polym. Lett. Ed.*, **24**, 413-417, 1986.
13. K. Kataoka, H. Miyazaki, M. Bunya, T. Okano, Y. Sakurai, *J. Am. Chem. Soc.*, **120**, 12694-12695, 1998.
14. Z-R. Lu, P. Kopečková, J. Kopeček, *Macromol. Biosci*., **3**, 296-300, 2003.
15. T. Miyata, *Polymer J.*, **42**, 277-289, 2010.
16. A. Kawamura, T. Kiguchi, T. Nishihata, T. Uragami, T. Miyata, *Chem. Commun.*, **50**, 11101-11103, 2014.
17. T. Miyata, M. Jige, T. Nakaminami, T. Uragami, *Proc. Natl. Acad. Sci. USA*, **103**, 1190-1193, 2006.
18. B. Alberts, Q, Johnson, J. Lewis, M. Raff, K. Roberts, P. Walter, “Molecular Biology of the Cell 4th ed. Chapter 3”, Garland, New York, 2002.
19. T. E. Creighton, “Proteins: Structure and Molecular Properties 2nd ed.”, Freeman, New York, 1993.
20. R. Jaenicke, *J. Biotechnol.*, **79**, 193-203, 2000.

21. K. A. Sharp, S. W. Englander, *Trends Biochem. Sci.*, **19**, 526-529, 1994.
22. S. K. Burley, G. A. Petsko, *Adv. Prot. Chem.*, **39**, 125-189, 1988.
23. J. D. Dunitz, *Chem. Biol.*, **2**, 709-712, 1995.
24. R. B. Martin, *Met. Ions Biol. Syst.*, **38**, 1-23, 2001.
25. L. Pauling, "The Nature of the Chemical Bond and the Structure of Molecules and Crystals 3rd ed. Chapter 8" Cornell Univ. Press, Ithaca, New York, 1960.
26. W. G. Hol, *Prog. Biophys. Mol. Biol.*, **45**, 149-195, 1985.
27. L. C. Pauling, R. B. Corey, H. R. Branson, *Proc. Natl. Acad. Sci. USA*, **37**, 205-211, 1951.
28. J. E. Scott, *Trends Biochem. Sci.*, **12**, 318-321, 1987.
29. S. H. Gellman, *Curr. Opin. Chem. Biol.*, **2**, 717-725, 1998.
30. L. Pauling, R. B. Corey, *Proc. Natl. Acad. Sci. USA*, **37**, 729-740, 1951.
31. D. J. Barlow, J. M. Thornton, *J. Mol. Biol.*, **201**, 601-619, 1988.
32. M. Eilers, S. C. Shekar, T. Shieh, S. O. Smith, P. J. Fleming, *Proc. Natl. Acad. Sci. USA*, **97**, 5796-5801, 2000.
33. A. M. Lesk, C. Chothia, *Biophys. J.*, **32**, 35-47, 1980.
34. G. D. Rose, S. Roy, *Proc. Natl. Acad. Sci. USA*, **77**, 4643-4647, 1980.
35. D. Walther, F. Eisenhaber, P. Argos, *J. Mol.Biol.*, **255**, 536-553, 1996.
36. K. A. Dill, S. Bromberg, "Molecular Driving Forces: Statistical Thermodynamics in Chemistry and Biology" Garland Science, New York and London, 2003.
37. J. L. Arrondo, F. M. Goni, *Prog. Biophys. Mol. Biol.*, **72**, 367-405, 1999.
38. V. Daggett, *Curr. Opin. Struct. Biol.*, **10**, 160-164, 2000.
39. R. Ishima, D. A. Torchia, *Nat. Struct. Biol.*, **7**, 740-743, 2000.
40. M. Karplus, G. A. Petsko, *Nature*, **347**, 631-639, 1990.
41. J. Badger, I. Minor, M. A. Oliveira, T. J. Smith, M.G. Rossmann, *Protein*, **6**, 1-19, 1989.
42. L. A. Highbarger, J. A. Gerlt, G. L. Kenyon, *Biochemistry*, **35**, 41-46, 1996.
43. D. Ringe, *Curr. Opin. Struct. Biol.*, **5**, 825-829, 1995.
44. G. G. Hammes, *Biochemistry*, **41**, 8221-8228 2002.
45. D. E. Koshland, G. Némethy, D. Filmer, *Biochemistry*, **5**, 365-385, 1966.
46. D. S. Goodsell, *Trends Biochem. Sci.*, **16**, 203-206, 1991.
47. R. B. Jensen, L Shapiro, *Trends Cell Biol.*, **10**, 483-488, 2000.
48. D. Kornitzer, A. Ciechanover, *J. Cell Physiol.*, **182**, 1-11, 2000.

49. M. F. Perutz, *Q. Rev. Biophys.*, **22**, 139-237, 1989.
50. T. K. Sato, M. Overduin, S. D. Emr, *Science*, **294**, 1881-1885, 2001.
51. J. J. Wyrick, R. A. Young, *Curr. Opin. Genet. Dev.*, **12**, 130-136, 2002.
52. D. E. Koshland, K. Hamadani, *J. Biol. Chem.*, **277**, 46841-46844, 2002.
53. N. A. Peppas, "Hydrogels in Medicine and Pharmacy", CRC, Boca Raton, 1987.
54. D. DeRossi, K. Kajiwara, Y. Osada, A. Yamauchi, "Polymer Gels, Fundamentals and Biomedical Applications", Plenum, New York, 1991.
55. T. Miyata, "Stimuli-Responsive Polymers and Gels, *Supramolecular Design for Biological Applications*" (ed. N. Yui.), CRC Press, 191, 2002.
56. T. Tanaka, *Phys. Rev. Lett.*, **40**, 820,-823 1978.
57. Y. Hirokawa, T. Tanaka, *J. Chem. Phys.*, **81**, 6379-6380, 1984.
58. T. Tanaka, I. Nishio, S-T. Sun, S. Ueno-Nishio, *Science*, **218**, 467-469, 1982.
59. Y. Osada, H. Okuzaki, H. Hori, *Nature*, **355**, 242-244, 1992.
60. T. Tanaka, *Sci. Am.*, **244**, 124-136, 1981.
61. K. Dusek, Responsive Gels: Volume Transitions I, Adv. Polym. Sci., **109**, Springer, Berlin, 1993.
62. K. Dusek, Responsive Gels: Volume Transitions II, Adv. Polym. Sci., **110**, Springer, Berlin, 1993.
63. T. Okano, "Biorelated Polymers and Gels", Academic Press, Boston, 1998.
64. A. S. Hoffman, *Macromol. Symp.*, **98**, 645-664, 1995.
65. D. T. Eddington, D. J. Beebe, *Adv. Drug Deliv. Rev.*, **56**, 199-210, 2004.
66. R. A. Siegel, *Adv. Polym. Sci.* **109**, 233-267, 1993.
67. C. S. Brazel, N. A. Peppas, *Macromolecules*, **28**, 8016-8020, 1995.
68. L-C. Dong, A. S. Hoffman, *J. Controlled Release*, **15**, 141-152, 1991.
69. T. Miyata, K. Nakamae, A. S. Hoffman, Y. Kanzaki, *Macromol. Chem. Phys.*, **195**, 1111-1120, 1994.
70. K. Nakamae, T. Nizuka, T. Miyata, M. Furukawa, T. Nishio, K. Kato, T. Inoue, A. S. Hoffman, Y. Kanzaki, *J. Biomater. Sci. Polym. Ed.*, **9**, 43-53, 1997.
71. A. S. Hoffman, *J. Controlled Release*, **6**, 297-305, 1987.
72. T. Okano, *Adv. Polym. Sci.*, **110**,179-197, 1993.
73. L-C. Dong, A. S. Hoffman, *J. Controlled Release*, **13**, 21-31, 1990.
74. T. Okano, Y. H. Bae, H. Jacobs, S. W. Kim, *J. Controlled Release*, **11**, 255-265, 1990.

75. N. Matsuda, T. Shimizu, M. Yamato, T. Okano, *Adv. Mater.*, **19**, 3089-3099, 2007.
76. V. V. Vasilevskaya, A. R. Khokhlov, *Macromolecules*, **25**, 384-390, 1992.
77. A. R. Khokhlov, E. Y. Kramarenko, *Macromol. Theory Simul.*, **2**, 169-177, 1993.
78. T. Miyata, "Gels and Interpenetrating Polymer Networks, Supramolecular Design for Biological Applications", (ed. N. Yui.), Chapter 6, CRC Press, 95-136, 2002.
79. T. Miyata, T. Uragami, K. Nakamae, *Adv. Drug Deliv. Rev.*, **54**, 79-98, 2002.
80. T. Miyata, T. Uragami, "Biomolecule-responsive hydrogels. In Biomedical Applications of Hydrogels Handbook" (eds. R. M. Ottenbrite, K. Park, T. Okano), Springer, New York, 65, 2010.
81. T. Miyata, T. Uragami, "Biological Stimuli-Responsive Hydrogels, Polymeric Biomaterials", (ed. S. Dumitriu), Chapter 36, Marcel Dekker, Inc., 959-974, 2002.
82. K. Matsumoto, T. Miyata, *Kobunshi Ronbunshu*, 71, 125-142, 2014.
83. T. Miyata, N. Asami, T. Uragami, *Nature*, **399**, 766-769, 1999.
84. T. Miyata, N. Asami, T. Uragami, *Macromolecules*, **32**, 2082-2084, 1999.
85. T. Miyata, N. Asami, T. Uragami, *J. Polym. Sci. Polym. Phys.*, **47**, 2144-2157, 2009.
86. T. Miyata, N. Asami, Y. Okita, T. Uragami, *Polym. J.*, **42**, 834-837, 2010.
87. J. Kim, N. Singh, L. A. Lyon, *Angew. Chem. Int. Ed.*, **45**, 1446-1449, 2006.
88. K. Nakamae, T. Miyata, A. Jikihara, A. S. Hoffman, *J. Biomater. Sci., Polym. Ed.*, **6**, 79-90, 1994.
89. T. Miyata, A. Jikihara, K. Nakamae, A. S. Hoffman, *Macromol. Chem. Phys.*, **197**, 1135-1146, 1996.
90. T. Miyata, A. Jikihara, K. Nakamae, A. S. Hoffman, *J. Biomater. Sci. Polym. Ed.*, **15**, 1085-1098, 2004.
91. S. J. Lee, K. Park, *J. Mol. Recognit.*, **9**, 549-557, 1996.
92. A. A. Obaidat, K. Park, *Pharm. Res.*, **13**, 989-995, 1996.
93. A. A. Obaidat, K. Park, *Biomaterials*, **18**, 801-806, 1997.
94. A. Kawamura, Y. Hata, T. Miyata, T. Uragami, *Colloid Surf. B*, **99**, 74-81, 2012.
95. G. Wulff, A. Sarhan, K. Zabrocki, *Tetrahedron Lett.*, **14**, 4329-4332, 1973.
96. B. Sellergren, M. Lepistoe, K. Mosbach, *J. Am. Chem. Soc.*, **110**, 5853-5860, 1988.
97. K. Mosbach, *Trends Biochem. Sci.*, **19**, 9-14, 1994.
98. K. J. Shea, *Trends. Polym. Sci.*, **2**, 166-173, 1994.

99. G. Wulff, *Angew. Chem. Int. Ed.*, **34**, 1812-1832, 1995.
100. M. Byrne, K. Park, N. A. Peppas, *Adv. Drug Deliv. Rev.*, **54**, 149-161, 2002.
101. N. M. Bergmann, N. A. Peppas, *Prog. Polym. Sci.*, **33**, 271-288, 2008.
102. M. Watanabe, T. Akahoshi, Y. Tabata, D. Nakayama, *J. Am. Chem. Soc.*, **120**, 5577-5578, 1998.
103. T. Oya, T. Enoki, A. U. Grosberg, S. Masamune, T. Sakiyama, Y. Takeoka, K. Tanaka, G. Wang, Y. Yilmaz, M. S. Feld, R. Dasari, T. Tanaka, *Science*, **286**, 1543-1545, 1999.
104. Y. Shiraki, K. Tsuruta, J. Morimoto, C, Ohba, A. Kawamura, R. Yoshida, R. Kawano, T. Uragami, T. Miyata, *Macromol. Rapid. Commun.*, **36**, 515-519, 2015.
105. A. Kawamura, T. Katoh, T. Uragami, T. Miyata, *Polym. J.*, **47**, 206-211, 2015.
106. T. Miyata, T. Hayashi, Y. Kuriu, T. Uragami, *J. Mol. Recognit.*, **25**, 336-343, 2012.
107. Y. Kuriu, M. Ishikawa, A. Kawamura, T. Uragami, T. Miyata, *Chem. Lett.*, **41**, 1660-1662, 2012.
108. Y. Kuriu, A. Kawamura, T. Uragami, T. Miyata, *Chem. Lett.*, **43**, 825-827, 2014.
109. R. Naraprawatphong, G. Kawanka, M. Hayashi, A. Kawamura, T. Miyata, *Mol. Impr.*, **4**, 21-30, 2016.
110. W. Bai, N. A. Gariano, D. A. Spivak, *J. Am. Chem. Soc.*, **135**, 6977-6984, 2013.
111. N. Yamaguchi, L. Zhang, B-S. Chae, C. S. Palla, E. M. Furst, K. L. Kiick, *J. Am. Chem. Soc.*, **129**, 3040-3041, 2007.
112. M. P. Lutolf, G. P. Raeber, A. H. Zisch, N. Tirelli, J. A. Hubbell, *Adv. Mater.*, **15**, 888-892, 2003.
113. M. P. Lutolf, J. L. Lauer-Fields, H. G. Schmoekel, A. T. Metters, F. E. Weber, G. B. Fields, J. A. Hubbell, *Proc. Natl. Acad. Sci. USA*, **100**, 5413-5418, 2003.
114. R. V. Ulijn, *J. Mater. Chem.*, **16**, 2217-2225, 2006.
115. P. D. Thornton, R. J. Mart, R. V. Ulijn, *Adv. Mater.*, **19**, 1252-1256, 2007.
116. P. D. Thornton, G. McConnell, R. V. Ulijn, *Chem. Commun.*, 5913-5915, 2005.
117. D. C. Lin, B. Yurke, N. A. Langrana, *J. Biomech. Eng.*, **126**, 104-110, 2004.
118. B. Wei, I. Cheng, K. Q. Luo, Y. Mi, *Angew. Chem. Int. Ed.*, **47**, 331-333, 2008.
119. H. Yang, H. Liu, H. Kang, W. Tan, *J. Am. Chem. Soc.*, **130**, 6320-6321, 2008.
120. J. D. Ehrick, S. K. Deo, T. W. Browning, L. G. Bachas, M. J. Madou, S. Daunert, *Nat. Mater.*, **4**, 298-302, 2005.
121. W. Yuan, J. Yang, P. Kopečková, J. Kopeček, *J. Am. Chem. Soc.*, **130**,

15760-15761, 2008.

122. Y. Murakami, M. Maeda, *Biomacromolecules*, **6**, 2927-2929, 2005.

Chapter 2

Preparation of Polypeptide Hydrogels that Undergo Helix-Coil Transition

2.1 Introduction

Polypeptides have inherent secondary structures such as α-helix, β-sheet, and random coil structure, which are determined by their amino acid sequence. As the secondary structures of polypeptides depend on environmental changes, polypeptides exhibit structural transition by changes in pH, temperature, and so on. For example, PLL that has amino groups in pendant chains forms a random coil structure below pH 11 because the amino groups with pKa of 10.7 are positively charged. With increasing pH above 11, the PLL chain changes to an inherent α-helix structure owing to neutral amino groups. Thus, some polypeptides such as PLL undergo structural transitions, i.e., secondary structural transitions, from α-helix to random coil in response to a change in pH and ionic strength in aqueous solutions.[1, 2] In addition, as PLL is a representative cationic polymer that strongly interacts with plasmid DNA and negatively charged proteins, it has been extensively studied for biomedical applications to gene therapy carriers,[3-5] scaffolds for tissue engineering,[6-8] and so on.[9]

Stimuli-responsive hydrogels have recently received much attention as smart biomaterials10 because of their swelling/shrinking properties in response to external physical and chemical stimuli such as pH,[11-14] temperature,[15,16] electric field,[17,18] and target molecules.[19-22] For example, polyelectrolyte hydrogels based on acrylic acids exhibit pH-responsive volume changes due to changes in osmotic pressure by pH-dependent dissociation of carboxy groups. Such pH-dependent dissociation of acidic or basic groups induces conformational changes in polyelectrolyte polymers. In contrast to polypeptides with secondary structures, however, the conformational changes of normal polyelectrolyte polymers are not conformational transition but structural transitions from expanded to collapsed states.

In this study, pH-responsive hydrogels that underwent changes in volume and secondary structures between the α-helix and random coil structure in response to pH changes were prepared by chemical cross-linking of PLL. In the hydrogels, PLL chains

behaved as not only polyelectrolytes with amino groups but also polypeptides that undergo structural transition from α-helix to random coil. This chapter focuses on the relationship between structural transition of PLL chains in hydrogel networks and their pH-responsive swelling/shrinking properties.

2.2 Experimental

2.2.1 Materials

PLL hydrobromide (12,000 MWCO) and ethylene glycol diglycidyl ether (EGDE) were purchased from Peptide Ins. Co. Ltd (Osaka, Japan) and Tokyo Chemical Ind. Co. Ltd (Tokyo, Japan), respectively. All aqueous solutions were prepared with ultra-pure water (Milli-Q, 18.2 MΩ cm). The other solvents and reagents were of analytical grade, were obtained from commercial sources and were used without further purification.

2.2.2 Preparation of PLL hydrogel

PLL hydrogels were prepared as follows (Scheme 2-1); PLL (100 mg) was dissolved in 500 μL of Na_2HPO_4/NaOH buffer solution (50 mM, pH 12, 0.5 M NaCl). The PLL solution was kept for 24 hours at room temperature so that PLL chains could form α-helix structure. EGDE (8.32 mg) as a cross-linker was mixed with the PLL solution at room temperature.[23,24] The mixed solution was injected into a glass mold whose thickness was adjusted by silicon spacers (ϕ = 5 mm, thickness = 2 mm) and kept for 24 hours at 35 °C for cross-linking PLL with EGDE (Figure 2-1). The resultant PLL hydrogels were thoroughly rinsed with a Na_2HPO_4/NaOH buffer solution at pH 12.

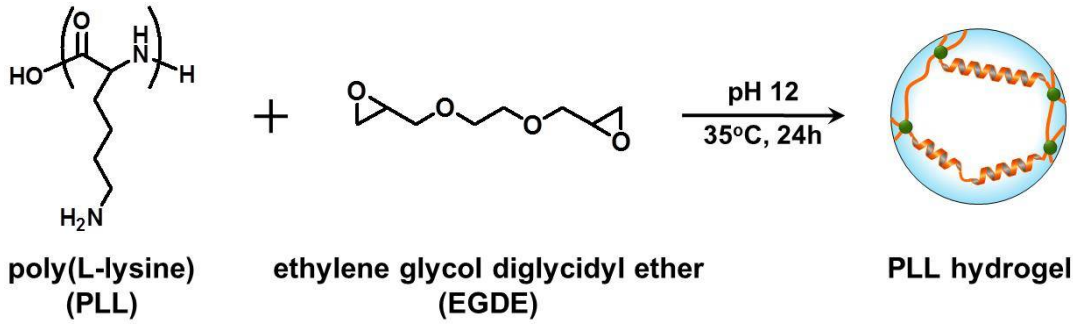

Scheme 2-1. Preparation scheme of the PLL hydrogel by cross-linking PLL with EGDE.

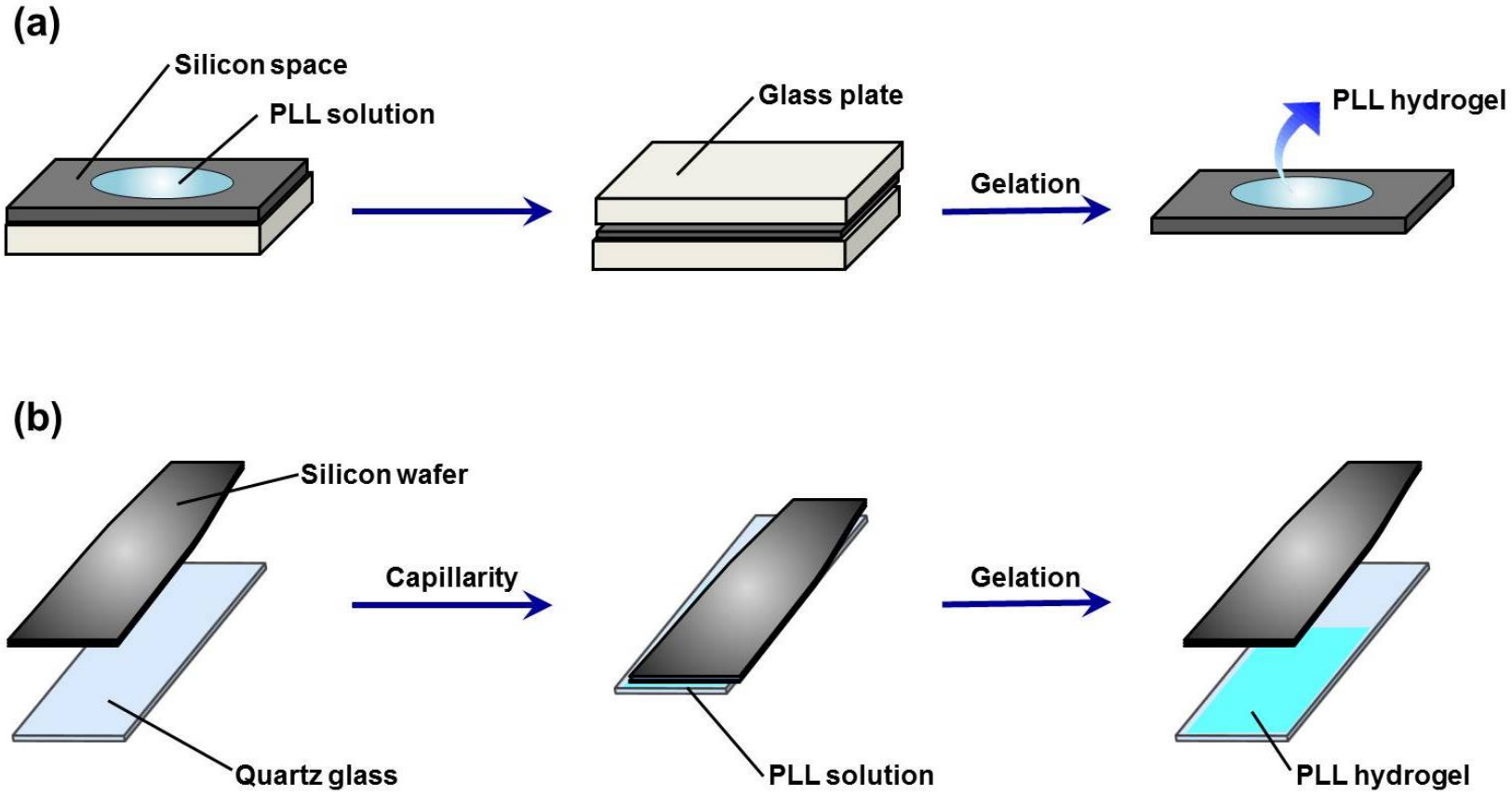

Scheme 2-1. Preparation procedures of the PLL hydrogel for swelling ratio measurement (a) and for circular dichroism measurement (b).

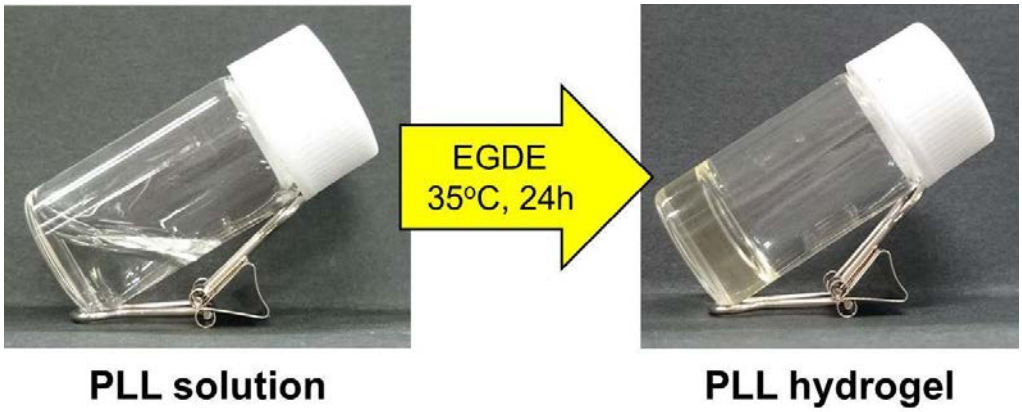

Figure 2-2. Photo images of the PLL solution (200 mg/mL) and the PLL hydrogel cross-linked with EGDE.

2.2.3 Measurements of swelling ratio changes

To measure swelling ratios of the PLL hydrogels, buffer solutions given the required pH were prepared as follows; Five kinds of acidic and basic solutions, 50 mM aqueous solution of acetic acid (CH_3COOH), sodium acetate (CH_3COONa), sodium dihydrogenphosphate (NaH_2PO_4), disodium hydrogenphosphate (Na_2HPO_4) and sodium hydroxide (NaOH) were prepared to adjust the pH of buffer solutions in a range from 3.5 to 12.0. CH_3COOH/CH_3COONa, NaH_2PO_4/Na_2HPO_4 and Na_2HPO_4/NaOH buffer solution have useful pH ranges of 3.5-5.0, 6.0-8.0 and 9.0-12.0, respectively. To prepare buffer solutions with various pHs, the resulting acidic or basic solutions were mixed to adjust pH of the buffer solutions using a pH meter (Horiba F-53). In addition, ionic strength of the buffer solutions was adjusted by 0.5 M NaCl. The PLL hydrogels were immersed in CH_3COOH/CH_3COONa, NaH_2PO_4/Na_2HPO_4 and Na_2HPO_4/NaOH buffer solutions with various pHs after the swelling of the PLL hydrogels attained equilibrium in a Na_2HPO_4/NaOH buffer solution at pH 12. The swelling ratios of the PLL hydrogels (V/V_0) were determined from their diameters in the CH_3COOH/CH_3COONa, NaH_2PO_4/Na_2HPO_4 and Na_2HPO_4/NaOH buffer solutions with various pHs using the equation (2-1). The diameters of the PLL hydrogels were measured with a microscope

(BX51, Olympus, Tokyo, Japan) equipped with a digital camera (DP-21, Olympus, Tokyo, Japan).

$$\text{Swelling ratio} = \frac{V}{V_0} = \left(\frac{d}{d_0}\right)^3 \qquad (2\text{-}1)$$

where d and d_0 are diameters of the PLL hydrogels in a buffer solution with each pH and pH 12, respectively.

2.2.4 Circular dichroism

The circular dichroism spectrum of the PLL hydrogels was measured using a circular dichroism spectrometer (J-1500, JASCO, JAPAN). The PLL hydrogels for circular dichroism measurements were prepared using molds composed of a quartz glass and silicon wafer. After the hydrogel formation, the silicon wafer was peeled off from the surface of the resulting PLL hydrogel. The PLL hydrogels on a quartz glass were placed in the 1 mm quartz sandwich cell for circular dichroism measurements. The PLL hydrogels and the PLL linear polymers in buffer solutions with various pHs were subjected to scanning from 250 nm to 200 nm at 0.1 nm data pitch at the rate of 100 nm/min with background subtracted. The HT value of the results was suppressed below 600 V within the range between 201 nm and 250 nm. The electric voltage spectrum of the PLL hydrogel in a buffer solution at pH 12 is shown in Figure 2-3. To reveal the relationship between pH and the structure of PLL chains, the relative α-helix content of the PLL hydrogel was determined from the ellipticity at 222 nm using equation 2-2.

$$\text{Relative } \alpha\text{-helix content} = \frac{\theta_{222}{}^{pH} - \theta_{222}{}^{pH7}}{\theta_{222}{}^{pH12} - \theta_{222}{}^{pH7}} \times 100 \qquad (2\text{-}2)$$

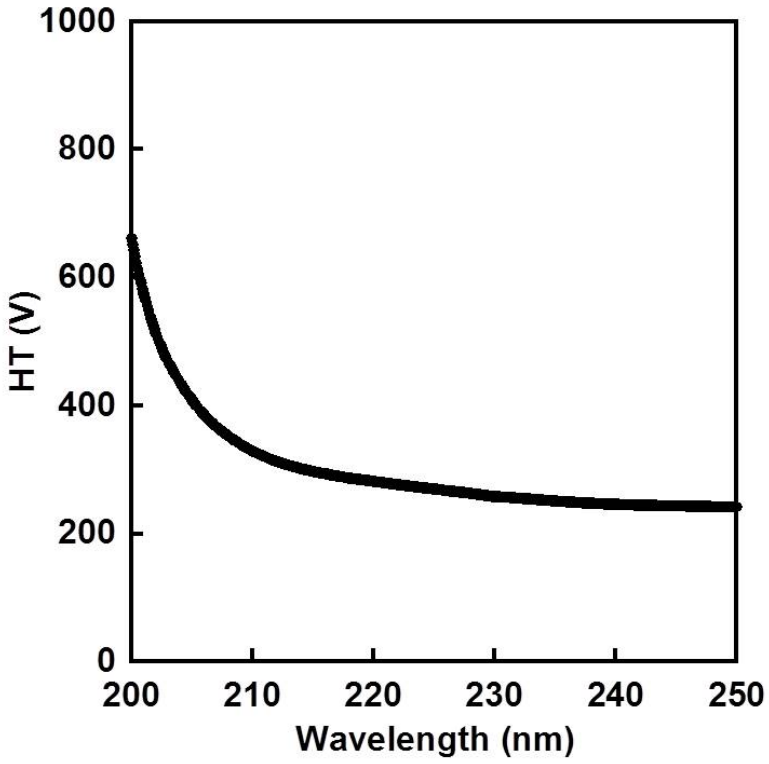

Figure 2-3. Electric voltage spectrum of the PLL hydrogel in a buffer solution at pH 12.

2.3 Results and Discussion

2.3.1 pH-Responsive swelling ratio change of PLL hydrogel

The pH-responsive behavior of the PLL hydrogels was investigated in a buffer solution with various pHs because the PLL chains have many amino groups that are dissociated as a function of pH. The swelling ratio of the PLL hydrogels (V/V_0) was determined from their diameters in a CH_3COOH/CH_3COONa, NaH_2PO_4/Na_2HPO_4, or Na_2HPO_4/NaOH buffer solution at various pHs, (d/d_0),[3] which were measured with an optical microscope. Ionic strength of all buffer solutions was adjusted at 0.5 M by NaCl due to the strong effects on swelling ratios of polyelectrolyte hydrogels. After the swelling of PLL hydrogels attained equilibrium in a buffer solution at pH 12, changes in their swelling ratio were measured in a buffer solution with various pHs. The relationship between pH and swelling ratio of the PLL hydrogel is shown in Figure 2-4. Here, the swelling ratio of the PLL hydrogels in a buffer solution at each pH was normalized by that at pH 12. The swelling ratio of the PLL hydrogel decreased gradually with increasing pH of a buffer solution. The reversibility of swelling ratio changes of the PLL hydrogel was investigated between pH 7 and pH 12. After the PLL hydrogel attained equilibrium swelling ratio in a buffer solution at pH 7, it was immersed in a buffer solution at pH 12. Then the swelling ratio of the PLL hydrogel decreased again (Figure 2-5). The pH-responsive behavior of the PLL hydrogel is attributed to a change in the degree of dissociation of amino groups in the PLL network. In a buffer solution with pH lower than pKa (= 10.7) of PLL, the amino groups of PLL are protonated, followed by increasing the number of fixed ions within the hydrogel networks. The protonation of amino groups results in increasing osmotic pressure inside the hydrogel by incorporation of counter anion within the network. As a result, the PLL hydrogel swells in a solution with acidic and neutral pHs, and shrinks in a solution with basic pHs because the osmotic pressure inside the hydrogel is directly influenced by

protonation of the amino groups.

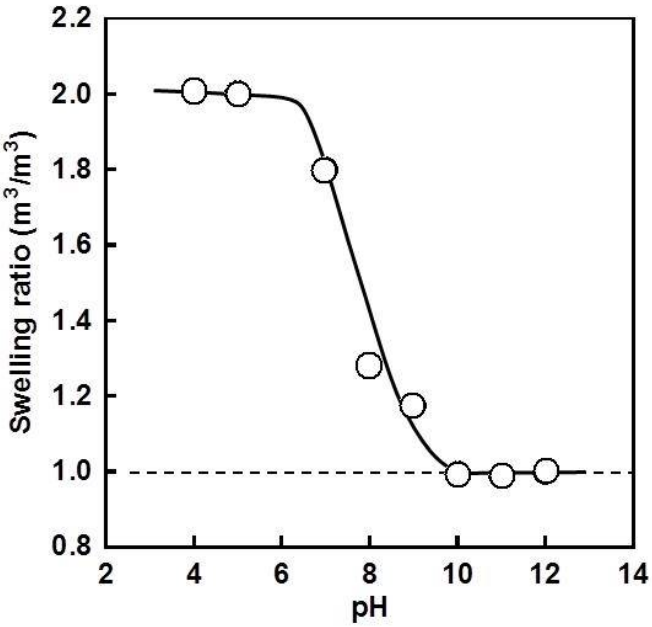

Figure 2-4. Relationship between pH and swelling ratio of the PLL hydrogel in a buffer solution with various pHs.

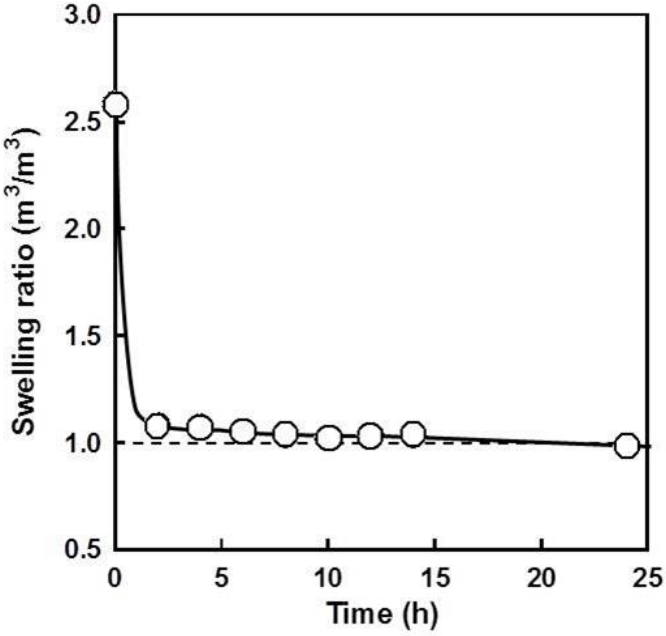

Figure 2-5. Swelling ratio changes of the PLL hydrogel in a buffer solution at pH 12 (the pH of buffer solution was changed from pH 7 to 12).

2.3.2 pH-Responsive structural transition of PLL hydrogel

A PLL linear polymer forms the α-helix at pH above 11 but undergoes a structural transition to random coil structure at pH below 11. The structural transition of the PLL linear polymer from α-helix to random coil is attributed to the repulsion between positively charged amino groups generated by the protonation at pH below 11. In this study, to focus on the structural transition of PLL chains as a function of pH, author prepared the PLL hydrogels by cross-linking PLL chains with α-helix structure at pH 12. After the resulting PLL hydrogels were immersed in a NaH_2PO_4/Na_2HPO_4 or Na_2HPO_4/NaOH buffer solution with various pHs for 24 h, the secondary structures of PLL hydrogels swollen in the buffer solution were investigated by circular dichroism spectroscopy. The PLL linear polymer was dissolved in a NaH_2PO_4/Na_2HPO_4 or Na_2HPO_4/NaOH buffer solution to be 50 μg L^{-1} in a quartz cell of 1 cm path length. The thin PLL hydrogel films were prepared on the 1mm quartz sandwich cell by the method described above.[25] The circular dichroism spectra of an aqueous PLL linear polymer solution and a thin PLL hydrogel film were measured using a JASCO J-1500 spectrometer (Japan Spectroscopy Co., Ltd.). Figure 2-6 shows the ellipticity of the PLL hydrogel swollen in a buffer solution with various pHs. The PLL hydrogel in a buffer solution with pH 12 demonstrated circular dichroism spectra with negative peaks at 208 and 222 nm, which were characteristic of an α-helix structure.[2] When pH of the buffer solution decreased, the PLL chains of hydrogel underwent structural transitions to random coil, which were characterized by positive peak at 215 nm. In addition, the PLL hydrogel underwent reversible changes in structural transition between α-helix and random coil (Figure 2-7). These indicate that the PLL hydrogel undergoes reversible changes in both volume and conformation in response to pH changes.

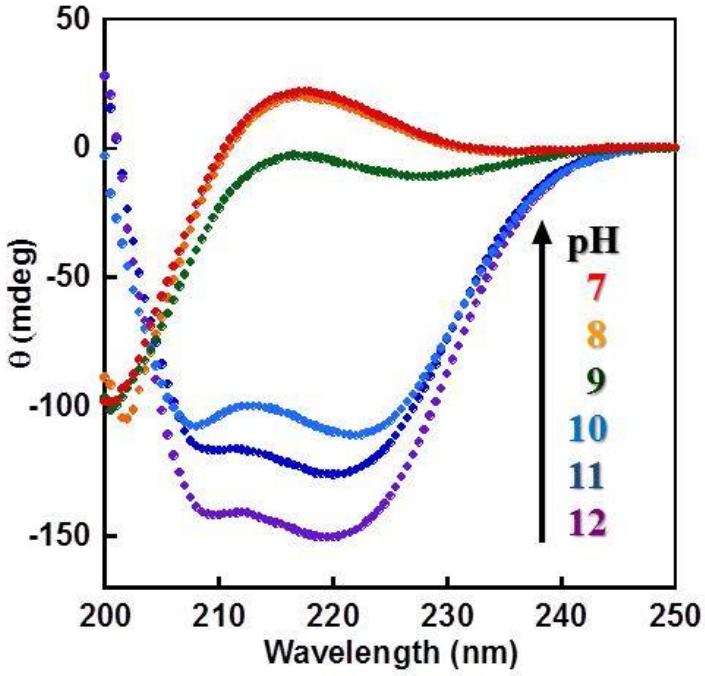

Figure 2-6. Circular dichroism spectra of the PLL hydrogels as a function of pH.

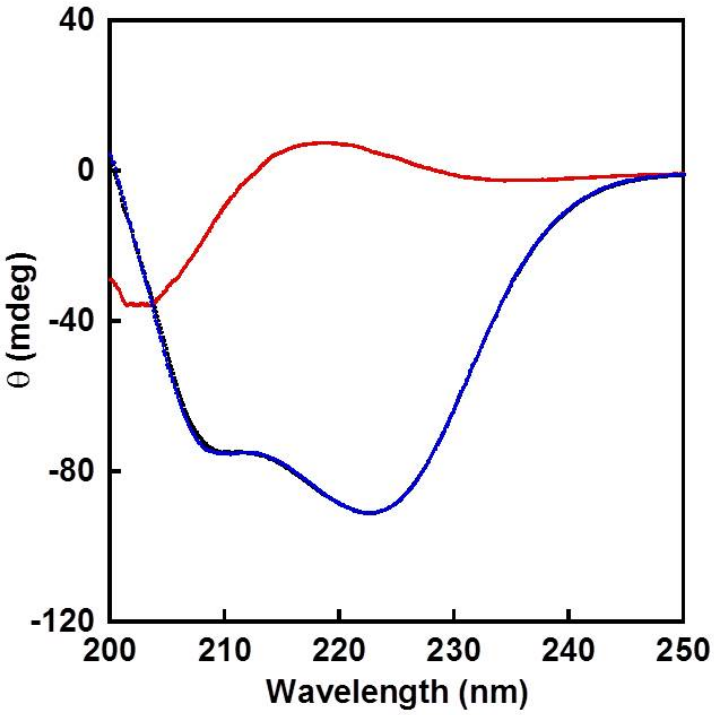

Figure 2-7. Reversibility of structural transition of the PLL hydrogel at pH 12 (●) and pH 7 (●); the second cycle at pH 12 (●).

Figure 2-8 shows the effect of pH on relative α-helix content of the PLL linear polymer and hydrogel in a buffer solution. The PLL linear polymer formed α-helix at pH above 12 but the α-helix content decreased dramatically with decreasing pH below 11. On the other hand, the PLL hydrogel had high α-helix content at pH above 10 and decreased α-helix content dramatically with decreasing pH below 9. It should be noted that the PLL linear polymer underwent a structural transition around pH 11 but the structural transition of the PLL hydrogel took place around pH 9. In addition, pKa of the PLL hydrogel, which was determined by neutralization titration, was approximately pH 11, similarly to the pKa of the PLL linear polymer. These mean that the PLL hydrogel can maintain the α-helix structure in a wider pH range than the PLL linear polymer. Chemical cross-linking can stabilize the α-helix structure of the PLL chains because it inhibits a structural transition from the α-helix to random coil structure.[26] The important point for the stabilization of the α-helix structure is chemical cross-linking of the PLL chains under the condition that they form an α-helix structure at pH above 12. These results are closely correlated with the memorization of hydrogel networks; they can memorize their initial structure during network formation.

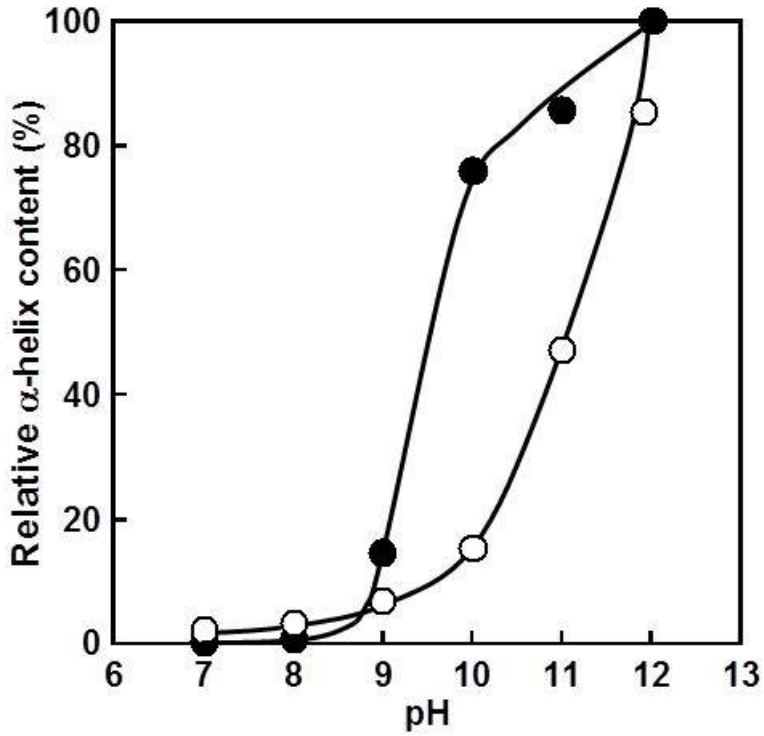

Figure 2-8. Relationship between pH and relative α-helix content of the aqueous PLL solution (○) and the PLL hydrogels (●) at various pHs.

2.4 Conclusions

In summary, by chemical cross-linking of the PLL that exhibits helix-coil transition, we prepared a PLL hydrogel that underwent changes in volume and conformation in response to pH changes. In addition, the chemical cross-linking enabled effective stabilization of the α-helix structure of the PLL chains, which was directly correlated with the pH-responsive change in swelling ratio of the PLL hydrogel.

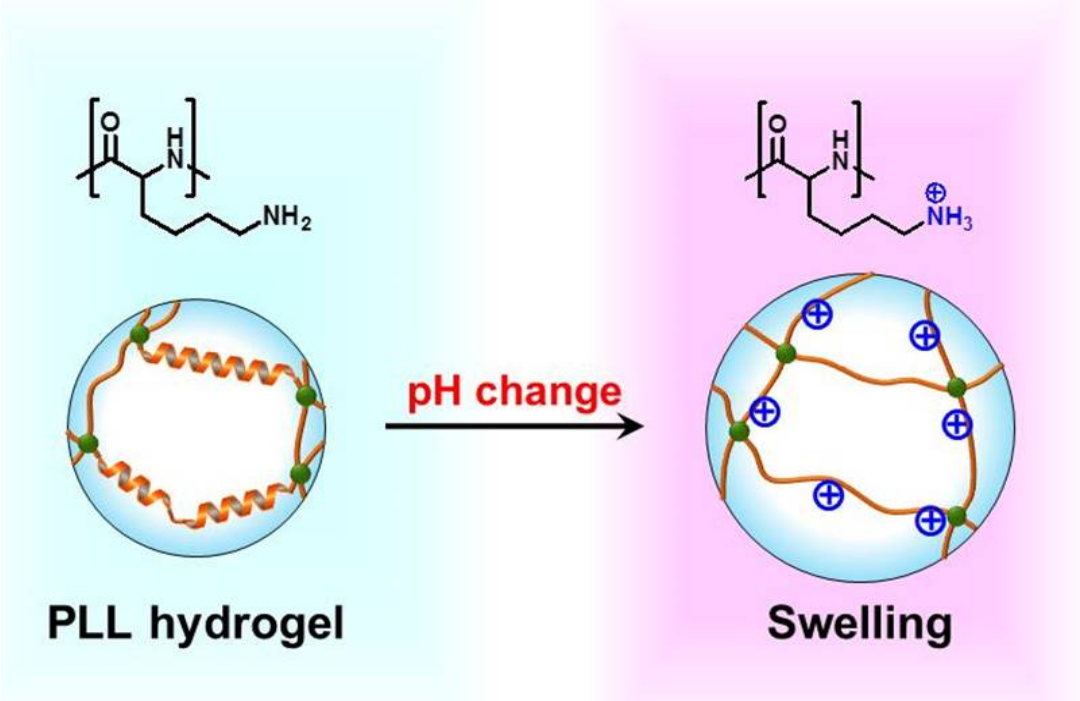

Figure 2-9. Schematic illustration of pH-responsive behavior of the PLL hydrogel at neutral or basic pHs.

2.5 References

1. D. Fischer, Y. Li, B. Ahlemeyer, J. Krieglstein, T. Kissel, *Biomaterials*, **24**, 1121-1131, 2003.
2. P. Midoux, M. Monsigny, *Bioconjugate Chem.*, **10**, 406-411, 1999.
3. R. Townend, T. F. Kumosinski, S. N. Timasheff, G. D. Fasman, B. Davidson, *Biochem. Biophys. Res. Commun.*, **23**, 163-169, 1966.
4. N. Greenfield, G. D. Fasman, *Biochemistry*, **8**, 4108-4116, 1969.
5. G. L. Kenausis, J. Vo1ro1s, D. L. Elbert, N. Huang, R. Hofer, L. Ruiz-Taylor, M. Textor, J. A. Hubbell, N. D. Spencer, *J. Phys. Chem. B*, **104**, 3298-3309, 2000.
6. B. R. Kranz, E. Thiel, S. Thierfelder, *Blood*, **73**, 1942-1950, 1989.
7. S. VandeVondele, J. Voros, J. A. Hubbell, *Biotech. Bioeng.*, **82**, 784-790, 2003.
8. J-W. Nah, L. Yu, S. Han, C.-H. Ahn, S. W. Kim, *J. Control. Rel.*, **78**, 273-284, 2002.
9. K. Ariga, Y. Yamauchi, G. Rydzek, Q. Ji, Y. Yonamine, K. C.-W. Wu, J. P. Hill, *Chem. Lett.*, **43**, 36-68, 2014.
10. A. S. Hoffman, *Adv. Drug Deliv. Rev.*, **54**, 3-12, 2002.
11. T. Amiya, Y. Horikawa, Y. Hirose, Y. Li, T. Tanaka, *J. Chem. Phys.*, **86**, 2375-2379, 1987.
12. G. Chen, A. S. Hoffman, *Nature*, **373**, 49-52, 1995.
13. R. Yoshida, K. Uchida, T. Kaneko, K. Sakai, A. Kikuchi, Y. Sakurai, T. Okano, *Nature*, **374**, 240-242, 1995.
14. T. Miyata, K. Nakamae, A. S. Hoffman, Y. Kanzaki, Macromol. *Chem. Phys.*, **195**, 1111-1120, 1994.
15. T. Tanaka, D. Fillmore, S-T. Sun, I. Nishio, G. Swislow, A. Shah, *Phys. Rev. Lett.*, **45**, 1636-1639, 1980.
16. M. Annaka, T. Tanaka, *Nature*, **355**, 430-432, 1992.
17. T. Tanaka, I. Nishio, S-T. Sun, S. Ueno-Nishio, *Science*, **218**, 467-469, 1982.
18. Y. Osada, H. Okuzaki, H. Hori, *Nature*, **355**, 242-244, 1992.
19. T. Miyata, A. Jikihara, K. Nakamae, A. S. Hoffman, *Macromol. Chem. Phys.*, **197**, 1135-1146, 1996.
20. T. Miyata, N. Asami, T. Uragami, *Nature*, **399**, 766-769, 1999.

21. T. Miyata, M. Jige, T. Nakaminami, T. Uragami, *Proc. Natl. Acad. Sci. USA*, **103**, 1190-1193, 2006.
22. A. Kawamura, T. Kiguchi, T. Nishihata, T. Uragami, T. Miyata, *Chem. Commun.*, **50**, 11101-11103, 2014.
23. S. Taira, Y. Du, M. Kodaka, *Biotech. Bioeng.*, **93**, 396-400, 2006.
24. E. Kokufuta, H. Suzuki, R. Yoshida, K. Yamada, M. Hirata, F. Kaneko, *Langmuir*, **14**, 788-795, 1998.
25. K. Maeda, H. Mochizuki, K. Osato, E. Yashima, *Macromolecules*, **44**, 3217-3226, 2011.
26. A. Harada, S. Ichimura, E. Yuba, K. Kono, *Soft Matter*, **7**, 4629-4635, 2011.

Chapter 3

Preparation of Molecularly Imprinted Polypeptide Hydrogels and Their Regulation of Molecular Recognition

3.1 Introduction

Hydrogels are physically or chemically cross-linked hydrophilic polymer networks that are swollen in an aqueous solution. Fundamental studies on hydrogels and their applications as smart materials have been accelerated by the discovery of the volume phase transition of ionic hydrogels by Tanaka,[1,2] As a result of this discovery, stimuli-responsive hydrogels have received much attention as novel soft materials because they undergo swelling/shrinking changes in response to external physical and chemical stimuli such as temperature,[3-5] pH[6,7] and electric field.[8,9] For example, hydrogels containing acrylic acid exhibit a pH-responsive behavior due to changes in osmotic pressure by the dissociation of carboxy groups.[10-12] Stimuli-responsive hydrogels have been extensively studied as smart biomaterials for biomedical applications and in diagnosis, DDS and cell cultures. The stimuli-responsive behavior of hydrogels that was previously reported was based on drastic changes in the affinity of their polymer chains to water or in the osmotic pressure induced by their electrolyte groups. As the fact that swelling/shrinking behavior of hydrogels is strongly influenced by the number of cross-links, Miyata et al. have proposed a novel strategy for preparing biologically stimuli-responsive hydrogels;[13-19] our strategy uses biomolecular complexes as dynamic cross-links in hydrogel networks. Based on this strategy, we have designed a variety of biologically stimuli-responsive hydrogels that undergo a change in volume in response to a target biomolecule; these are referred to as biomolecule-responsive hydrogels.

Molecular imprinting is an attractive technique for designing synthetic hosts with molecular cavities for molecular recognition. In standard molecular imprinting, after ligand monomers with a functional group such as carboxy or amino groups are prearranged around template molecules by noncovalent interactions, they are copolymerized with a large amount of cross-linkers to form polymer networks. Then, molecular recognition cavities are created by the extraction of template molecules from

the resultant hydrogel. Thus molecularly imprinted polymers with specific recognition sites for a target molecule were easily designed by molecular imprinting. Unlike standard molecular imprinting, we have prepared molecularly imprinted hydrogels using molecular complexes as dynamic cross-links and a minute amount of cross-linker, which undergo changes in the volume in response to a target molecule. Such molecularly imprinted hydrogels with specific ligands can shrink gradually in response to a target molecule because their cross-linking density increases due to the complex formation between the ligands and the target molecule. For example, using a minute amount of cross-linkers and CDs, which form inclusion complexes with a variety of guest molecules such as phenol derivatives, as ligands, molecularly imprinted hydrogels were prepared with molecular recognition sites for a target BPA, which can functions as an endocrine disruptor.[20] The resulting BPA-imprinted hydrogels exhibited a significant shrinkage in response to BPA because their cross-linking density increased due to the complex formation between a BPA molecule and two CD ligands. Thus target molecule-responsive hydrogels that shrink in response to a target molecule can be strategically designed by molecular imprinting using molecular complex cross-links and a minute amount of cross-linker. Such molecularly imprinted hydrogels as dynamic materials can provide a variety of useful applications for molecular sensors and separation technology. In the previous studies on molecularly imprinted hydrogels using molecular complex ligands and a minute amount of cross-linkers, author used hydrophilic polymers such as polyacrylamide, which forms random conformations, as main chains for the formation of hydrogel networks. The use of main chains that form well-defined conformations in molecular imprinting enables us to design molecularly imprinted hydrogels that exhibit unique responsive behaviors and have controllable recognition sites for a target molecule.

Proteins have an ordered structure that enables its excellent functions such as molecular recognition and catalytic actions. Some proteins regulate their molecular

recognition ability by conformational changes of their highly ordered structure, which is well-known as allosteric regulation. Polypeptides have inherent secondary structures such as α-helix, β-sheet and random coil structures, which are determined by their amino acid sequence. As the secondary structures strongly depend on environmental changes, polypeptides exhibit a structural transition by changes in pH, temperature and so on. For example, PLL that has amino groups in its side chain undergoes structural transition between the α-helix and random coil structures in response to a change in pH and ionic strength in an aqueous solution.[21,22] In a previous paper, we reported the preparation of polypeptide hydrogels by chemical cross-linking of PLL as a main chain.[23] The PLL hydrogel underwent changes in volume and conformation in response to a change in pH due to protonation of the amino groups of the PLL chains. Interestingly, the previous study on the pH-responsive structural transition of the PLL hydrogel also revealed that cross-linking PLL chains stabilizes their α-helix structure in a wider pH range than that of the PLL linear polymer. Thus, author can prepare responsive hydrogels with highly ordered network structures using a polypeptide as a main chain and regulate their structures using environmental stimuli, such as pH.

In this study, author designed molecularly imprinted polypeptide hydrogels that regulated the binding capacity for a target molecule by the structural transition from the random coil to α-helix structure in response to a pH change, mimicking the allosteric regulations behavior of proteins. The molecularly imprinted polypeptide hydrogels with dynamic molecular recognition sites were strategically prepared by the chemical cross-linking of CD-introduced PLL (CD-PLL) with poly(ethylene glycol) diglycidyl ether (PEGDE) in the presence of BPA as a template molecule. The BPA-imprinted CD-PLL hydrogel with a random coil structure shrank in response to target BPA because the cross-linking density of hydrogel networks increased due to the complex formation between two CD molecules and a target BPA. However, a change of pH induced a conformational change of the molecular recognition sites due to a structural

transition from a random coil to an α-helix. As a result, the binding capacity of the BPA-imprinted CD-PLL hydrogel was sharply regulated by the conformational change of the molecular recognition sites induced by the structural transition of PLL chains. The unique property through which the binding capacity of the molecular recognition sites within the hydrogel network can be regulated similar to allosteric regulations suggests a high capability of the BPA-imprinted CD-PLL hydrogels as smart carriers for self-regulated DDSs. Author also loaded BPA as a model drug into the CD-PLL hydrogel networks by molecular imprinting and investigated its release behavior in response to a pH change. In a buffer solution with neutral pH, the release of BPA from the BPA-loaded CD-PLL hydrogel with a random coil structure was effectively suppressed by the formation of stable CD-BPA-CD complexes. In a buffer solution with basic pH, however, BPA was smoothly released from the BPA-loaded CD-PLL hydrogel with a α-helix structure because a conformational change of the molecular recognition sites induced by the structural transition of the PLL chains lowered the stability of the CD-BPA-CD complexes. This paper focuses on the regulation of the binding capacity of dynamic molecular recognition sites within the BPA-imprinted CD-PLL hydrogel, which is a novel smart material with a controllable molecular recognition ability, similar to proteins that exhibit allosteric regulations.

3.2 Experimental

3.2.1 Materials

PLL hydrobromide (12,000 MWCO) was purchased from Peptide Ins. Co. Ltd. (Osaka, Japan). PEGDE (Mw = 6,000) was purchased from Sigma-Aldrich Co. LLC. All aqueous solutions were prepared with ultra-pure water (Milli-Q, 18.2 MΩ cm). The other solvents and reagents of analytical grade were obtained from commercial sources and were used without further purification.

3.2.2 Synthesis of Mono-6-carboxy-6-deoxy-β-CD (carboxy-CD)

The carboxy-CD was synthesized in five steps (Scheme 3-1).

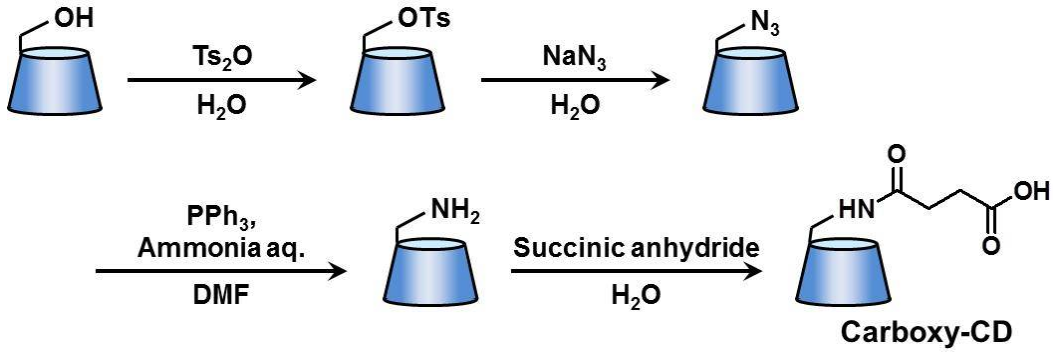

Scheme 3-1. Synthesis route of the carboxy-CD.

(1) Synthesis of p-toluenesulfonic anhydride (Ts_2O)

p-Toluenesulfonyl chloride (20.0 g, 104.9 mmol) and *p*-toluenesulfonic acid monohydrate (10.0 g, 52.6 mmol) were dissolved in dichloromethane (125 mL). The reaction mixture was stirred overnight and the unreacted *p*-toluenesulfonyl chloride was subsequently removed by filtration. The filtrate was dried and the residue was recrystallized from isopropyl ether to yield Ts_2O as a white solid (11.7 g, 71.1 % yield).

(2) Synthesis of mono-6-O-monotosyl-6-deoxy-β-cyclodextrin (TsO-CD)

CD (11.5 g, 10.1 mmol) and Ts_2O (4.9 g, 15.8 mmol) were dispersed in ultra-pure water (100 mL) and the resulting suspension was stirred for 2 hours. NaOH solution (0.1 g/mL, 50 mL) was added to the reaction mixture and, after 10 min, the unreacted Ts_2O was removed by filtration. The filtrate was neutralized by HCl addition to afford TsO-CD, which was collected after cooling overnight at 4 °C (5.3 g, 39.9 % yield). ^{1}H NMR (400 MHz, DMSO-d_6 δ): 7.75 (d, *J* = 8.0 Hz, 2 H; Ar H), 7.44 (d, *J* = 8.0 Hz, 2 H; Ar H), 5.86–5.66 (m, 13 H; OH of CD), 4.84–4.19 (m, 14 H; CH of CD), 4.59–4.19 (m, 7 H; O_6H of CD), 3.36–3.48 (m, overlaps with HOD), 2.09 (s, 3 H; CH_3 Ar).

(3) Synthesis of mono-6-deoxy-6-azide-β-cyclodextrin (N_3-CD)

TsO-CD (5.3 g, 4.1 mmol) and sodium azide (NaN_3, 3.4 g, 52.3 mmol) were dispersed in ultra-pure water (25 mL) and allowed to react under stirring for 5 h at 80 °C. The mixture was poured into acetone to precipitate N_3-CD, which was subsequently dried *in vacuo* (4.6 g, 96.8 % yield). ^{1}H NMR (400 MHz, DMSO-d_6 δ): 5.74 (br, 14 H; OH), 4.88–4.54 (m, 14 H; CH of CD), 3.85–3.29 (m, overlaps with HOD).

(4) Synthesis of mono-6-deoxy-6-amino-β-cyclodextrin (NH_2-CD)

N_3-CD (4.6 g, 4.0 mmol), triphenylphosphine (2.3 g, 8.8 mmol), and 28% ammonia solution (15.4 mL) were dissolved in DMF (77.0 mL) and the reaction was allowed to proceed for 4 h.[31,44] The reaction mixture was poured into acetone to precipitate NH_2-CD as a white powder, which was further dried *in vacuo* (4.4 g, 97.4 % yield).

(5) Synthesis of mono-6-deoxy-6-carboxy-β-cyclodextrin (carboxy-CD)

NH_2-CD (4.0 g, 3.52 mmol) was dispersed in 30 mL of ultra-pure water. Succinic anhydride (0.352 g, 4.2 mmol) was added to the solution. The solution was stirred at 60 °C and was allowed to react for 6 h.[45-47] After the prescribed time, the solution was poured into acetone (300 mL). The supernatant was removed via filtration, and the precipitate was concentrated under reduced pressure to yield carboxy-CD (2.9 g, 66.4% yield).

3.2.3 Introduction of CD to PLL

Carboxy-CD (0.5 g, 0.40 mmol) was dissolved in 150 mL of ultra-pure water. 1-Ethyl-3-(3-(dimethylamino)-propyl)carbodiimide (EDC) (156 mg, 0.8 mmol) and *N*-hydroxysuccinimide (93 mg, 0.8 mmol) were added to the aqueous solution containing carboxy-CD and allowed to react for 1 hour at room temperature. PLL (0.84 g, 4.0 mmol primary amines), which was dissolved in 50 mL of ultra-pure water, was added to the aqueous solution containing an activated carboxy-CD. The reaction proceeded for 4 hours at room temperature (Scheme 1). Then, the reaction mixture was poured into a seamless cellulose tubing (molecular weight cut off: 3,500) and was dialyzed against ultra-pure water for purification. The resultant CD-PLL was obtained by freeze-drying. The content of CD introduced to PLL was determined from ^{1}H NMR proton integration. CD-PLL was dissolved in D_2O, and ^{1}H NMR was recorded on a JEOL JNM-AL 400 spectrometer using sodium 3-(trimethylsilyl)propionate-2,2,3,3-d_4 as the internal standard.

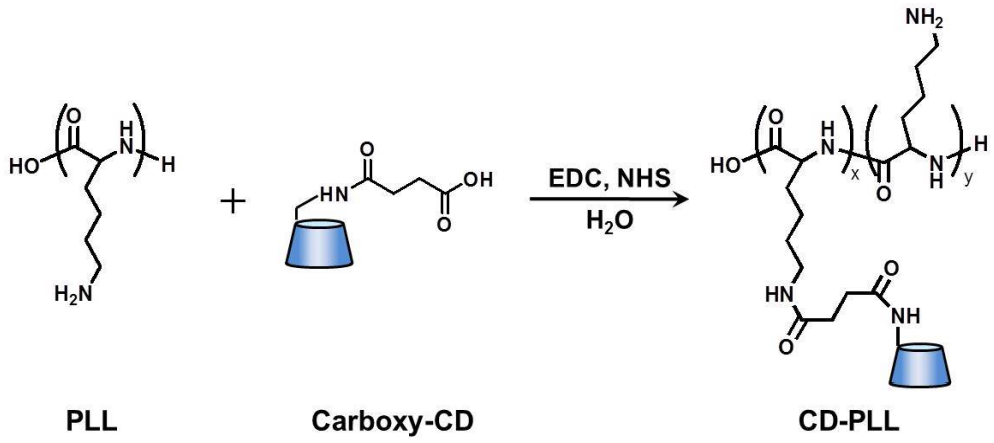

Scheme 3-2. Reaction scheme for the synthesis of CD-PLL.

3.2.4 Preparation of BPA-imprinted and BPA-loaded CD-PLL hydrogels

The BPA-imprinted CD-PLL hydrogels were prepared by the method shown in Scheme 2. CD-PLL (100 mg) was dissolved in 500 μL of NaH_2PO_4/Na_2HPO_4 buffer solution (50 mM, pH 7, 0.5 M NaCl). The CD-PLL solution was kept for 24 hours at room temperature to enable the PLL chains to form the random coil structure. After complex formation between CD and BPA, CD-PLL was cross-linked with PEGDE (10 mol% for amino groups of PLL chains) in the NaH_2PO_4/Na_2HPO_4 buffer solution for 24 hours at 35 °C in the presence of BPA template.[23,28,29] BPA-imprinted CD-PLL hydrogels were obtained by extraction of the BPA template from the resultant hydrogels by immersing the hydrogels in a NaH_2PO_4/Na_2HPO_4 buffer solution/acetone (70/30) mixture. Here, molds composed of glasses or a quartz glass/silicon wafer, the thickness of which was adjusted with silicon spacers, were used to prepare hydrogels for circular dichroism and swelling ratio measurements.

The BPA-loaded CD-PLL hydrogels were prepared, as follows, by *pseudo* molecular imprinting, which includes no process for extracting the BPA template. Similar to method used to prepare the BPA-imprinted CD-PLL hydrogels, after complex formation between CD and BPA, CD-PLL was cross-linked with PEGDE (10 mol% for amino groups of PLL chains) in the presence of the BPA template at pH 7. The BPA-loaded CD-PLL hydrogels were obtained by immersion in NaH_2PO_4/Na_2HPO_4 buffer solution to remove unreacted chemicals. An important difference in the preparative method between the BPA-loaded and BPA-imprinted CD-PLL hydrogels was the absence of an extraction process of the BPA template from the resultant hydrogel networks.

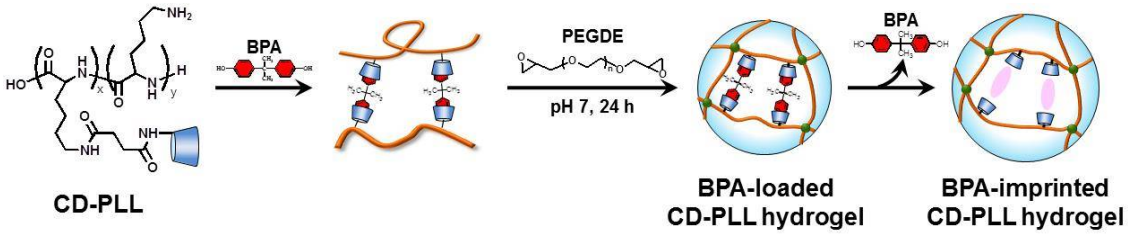

Scheme 3-3. Preparation scheme of the BPA-imprinted CD-PLL hydrogel by molecular imprinting.

3.2.5 FT-IR measurement

The chemical structures of the BPA-imprinted CD-PLL hydrogel were examined by the KBr method with a Fourier transform infrared spectrophotometer (FT-IR, Perkin Elmer, Waltham, MA, USA) after drying the hydrogel at 70 °C. All the spectra represent an average of 32 scans taken in the wave number range of 4000-600 cm^{-1}.

3.2.6 Circular dichroism

The circular dichroism spectrum of the BPA-imprinted CD-PLL hydrogels was measured using a circular dichroism spectrometer reported in Chapter 2. The hydrogels for circular dichroism measurements were prepared using molds composed of a quartz glass and silicon wafer. After the hydrogel formation, the silicon wafer was peeled off from the surface of the resulting BPA-imprinted CD-PLL hydrogel. The BPA-imprinted CD-PLL hydrogel on a quartz glass was placed in a quartz sandwich cell of 1 mm for the circular dichroism measurements. The BPA-imprinted CD-PLL hydrogels in buffer solutions with various pHs were subjected to scanning from 250 nm to 200 nm at a 0.1 nm data pitch at the rate of 100 nm/min with the background subtracted. To investigate the relationship between pH and the structure of the PLL chains, the relative α-helix content of the PLL hydrogel was determined from the ellipticity at 222 nm using equation (2-2).

3.2.7 Measurement of BPA adsorption into hydrogels

The BPA adsorption into the CD-PLL hydrogel was investigated by measuring the BPA concentration after the immersion of the hydrogel in NaH_2PO_4/Na_2HPO_4 and Na_2HPO_4/NaOH buffer solutions (50 mM, 0.5 M NaCl) containing BPA at a concentration of 80 mg/L as follows: The absorbances of NaH_2PO_4/Na_2HPO_4 and Na_2HPO_4/NaOH buffer solutions (50 mM, 0.5 M NaCl) containing BPA at pH 7 and 12 were measured in the wavelength range of 250-350 nm using a UV-vis spectrometer (UV-1550, Shimadzu, Kyoto, Japan) against a blank containing the buffer solution at each pH. The characteristic absorbance peaks were at 276 and 296 nm. The BPA concentration in the buffer solution was calculated against the calibration curve of the standard BPA solution. For each sample, the measurement was performed in duplicate. The amounts of BPA adsorbed into the hydrogels were determined using equation (3-1):

$$Adsorption = \frac{V(M - aA)}{W_g} \qquad (3\text{-}1)$$

where V is the volume of a buffer solution containing BPA (L), M is the initial BPA concentration (mg/L), a is the slope of the standard curve of the BPA solution, W_g is the weight of the dried gel (g), and A is the absorbance of the supernatant of the BPA solution.

3.2.8 Measurement of molecularly stimuli-responsive swelling ratio changes

The BPA-imprinted CD-PLL hydrogels were prepared in tablet form using glass molds with silicon spacers (ϕ = 5 mm, thickness = 2 mm). The BPA-imprinted CD-PLL hydrogels were kept immersed in 16 mL of NaH_2PO_4/Na_2HPO_4 (pH 7) or Na_2HPO_4/NaOH (pH 12) buffer solutions until equilibrium was reached at 25 °C. Afterwards, the hydrogels were transferred and kept immersed in each buffer solution containing BPA (80 mg/L) at 25 °C. The ionic strength of all buffer solutions was adjusted at 0.5 M by NaCl because it strongly affects the swelling ratios of polyelectrolyte hydrogels. The swelling ratio of the BPA-imprinted CD-PLL hydrogels (V/V_0) was determined from their diameters in NaH_2PO_4/Na_2HPO_4 (pH 7) or Na_2HPO_4/NaOH (pH 12) buffer solutions by equation (2-1). The diameters of the hydrogels swollen in a buffer solution (d_0) and a buffer solution containing BPA (d) were measured with a microscope (BX51, Olympus, Tokyo, Japan) equipped with a digital camera (DP-21, Olympus, Tokyo, Japan).

3.2.9 Measurements of pH-responsive swelling ratio changes

The BPA-imprinted CD-PLL hydrogels were kept immersed in 16 mL of NaH_2PO_4/Na_2HPO_4 buffer solution (pH 7) until equilibrium was reached at 25 °C. Subsequently, the hydrogels were transferred and kept immersed in CH_3COOH/CH_3COONa (pH 4 and 5), NaH_2PO_4/Na_2HPO_4 (pH 7 and 8) or Na_2HPO_4/NaOH (pH 9, 10, 11 and 12) buffer solutions at 25 °C. The ionic strength of all buffer solutions was adjusted at 0.5 M. The swelling ratio of the BPA-imprinted CD-PLL hydrogels (V/V_0) was determined from their diameters in CH_3COOH/CH_3COONa, NaH_2PO_4/Na_2HPO_4 and Na_2HPO_4/NaOH buffer solutions with various pHs using the equation (2-1). The diameters of the hydrogels swollen in a buffer solution at pH 7 (d_0) and with each pH (d) were measured with a microscope equipped with a digital camera .

3.2.10 Release of BPA from CD-PLL hydrogels

The BPA-loaded CD-PLL hydrogel was rinsed, and it attained equilibrium in a NaH_2PO_4/Na_2HPO_4 buffer solution at pH 7 at 25 °C. Then, the hydrogels were transferred and kept immersed in NaH_2PO_4/Na_2HPO_4 (pH 7 and 8) or Na_2HPO_4/NaOH (pH 9, 10, 11 and 12) buffer solutions at 25 °C. The amount of BPA released from the hydrogel was determined by measuring the BPA concentration after the immersion of the hydrogel in each buffer solution, as follows: The absorbances of the NaH_2PO_4/Na_2HPO_4 and Na_2HPO_4/NaOH buffer solutions containing BPA at different time intervals were measured in the wavelength range of 250-350 nm using a UV-vis spectrometer against a blank containing the buffer solution at each pH. The BPA concentration in the buffer solution was calculated against the calibration curve of the standard BPA solution.

3.3 Results and Discussion

3.3.1 Synthesis results of carboxy-CD

Carboxy-CD was synthesized according to the reaction shown in Scheme 3-1. The chemical structure of TsO-CD, N_3-CD and carboxy-CD were confirmed using ^{1}H NMR as shown in Figure 3-1, Figure 3-2 and Figure 3-3, respectively.

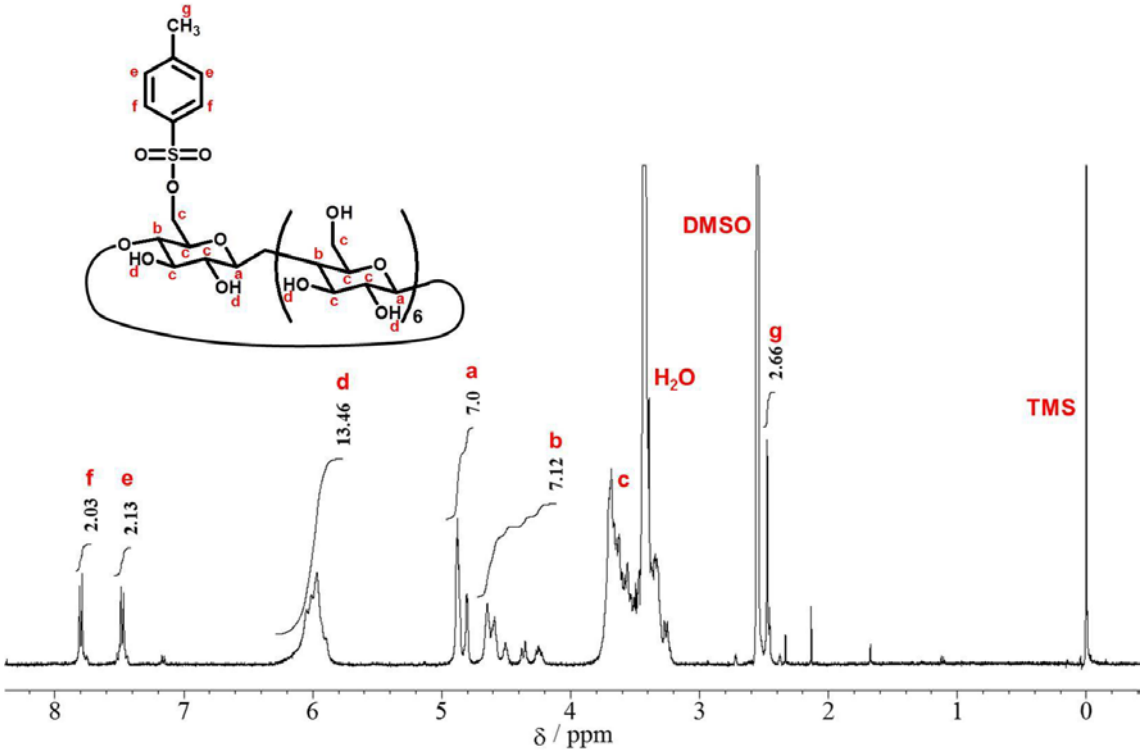

Figure 3-1. ^{1}H NMR spectrum of TsO-CD (400 MHz, DMSO-d_6).

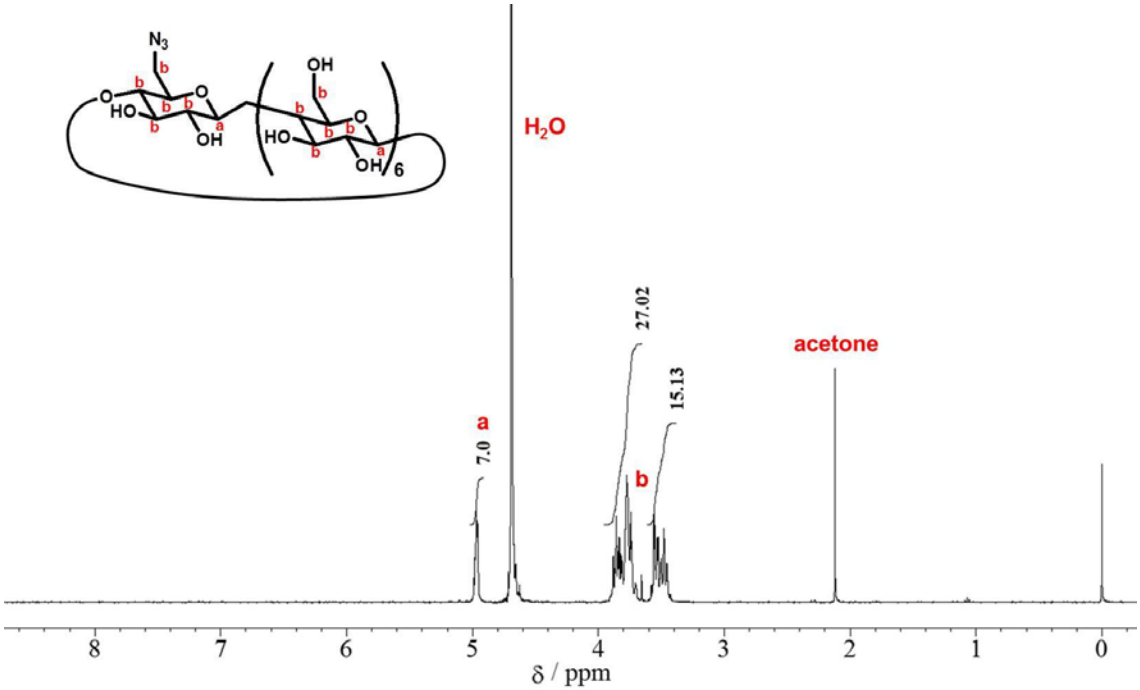

Figure 3-2. ^{1}H NMR spectrum of N_3-CD (400 MHz, D_2O).

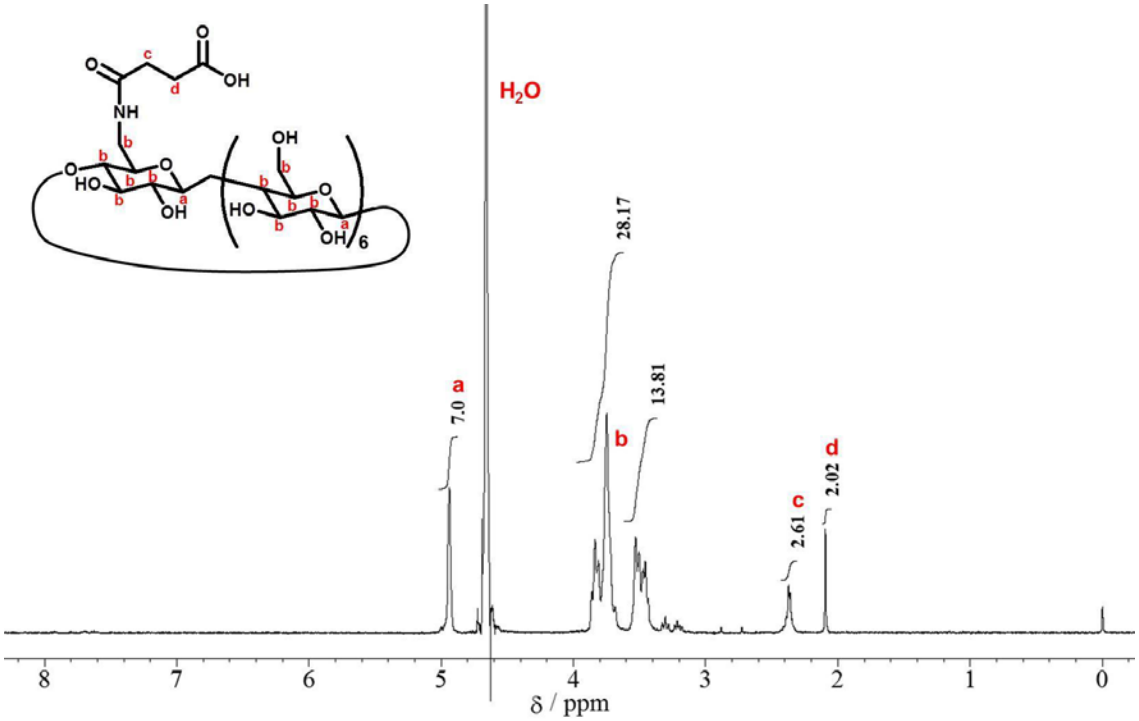

Figure 3-3. ^{1}H NMR spectrum of carboxy-CD (400 MHz, D_2O).

3.3.2 Characterization of BPA-imprinted CD-PLL hydrogel

Molecular imprinting enables us to easily create molecular recognition sites within polymeric materials. Standard molecular imprinting uses synthetic polymers with random conformations to form matrix polymer networks. On the other hand, proteins have well-designed structures with unique conformations such as α-helix and β-sheet structures. The conformational changes of well-designed polypeptide chains play an important role in allosteric regulations that change the molecular recognition of and the binding capacity for a target molecule. To design dynamic materials with controllable molecular recognition sites by mimicking allosteric regulations, we combined the structural transition of polypeptides with molecular imprinting. In this study, CD and PLL were used as the ligand and main chain in molecular imprinting, respectively. After the synthesis of a monosubstituted CD derivative possessing a carboxy group, it was reacted with PLL using EDC and NHS to obtain CD-PLL. The average degree of substitution of the resulting CD-PLL was found to be 0.10 (i.e., an average of one CD per ten lysine units) by ^{1}H NMR analysis (Figure 3-4).

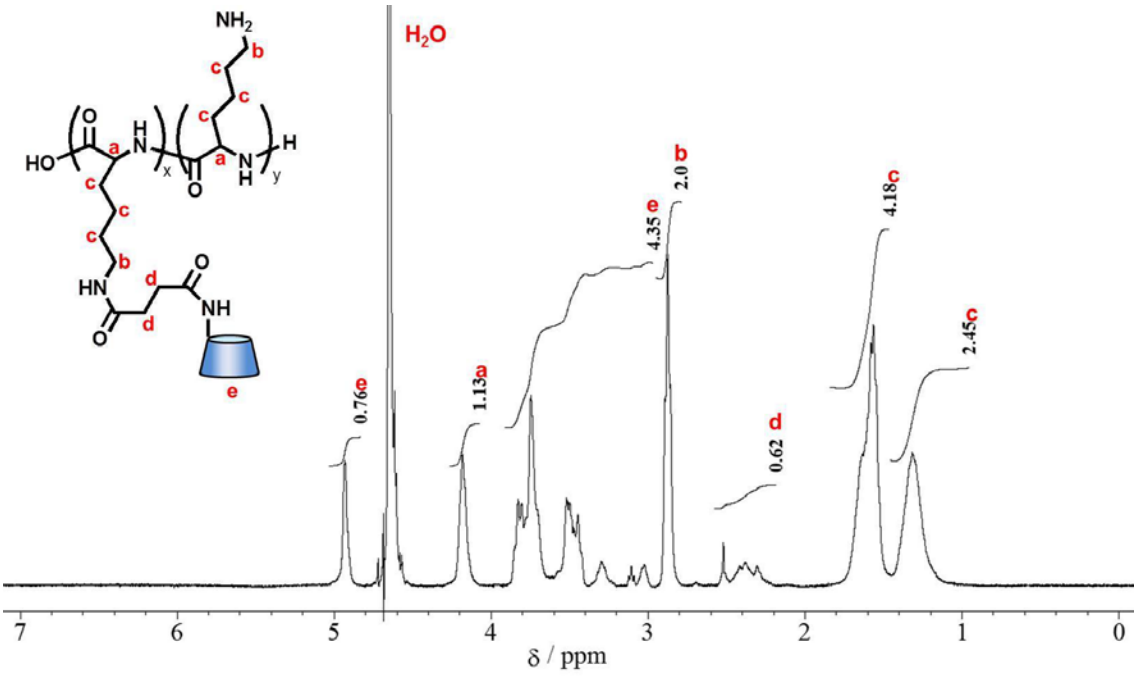

Figure 3-4. ^{1}H NMR spectrum of CD-PLL (400 MHz, D_2O).

Figure 3-5 shows the FT-IR spectra of the PLL hydrogel, CD and the BPA-imprinted CD-PLL hydrogel. The FT-IR spectrum of the BPA-imprinted CD-PLL hydrogel displays peaks at 1150 cm^{-1}, which are assigned to the antisymmetric glycosidic vibration, and peaks at 1030 and 1080 cm^{-1}, which are assigned to the coupled stretching vibration. The broad band at 3400 cm^{-1} arises from O-H vibrations. There were strong absorption bands at 1540 cm^{-1} and 1650 cm^{-1} corresponding to the amide I and amide II of PLL. These FT-IR bands for the BPA-imprinted CD-PLL hydrogel indicate the presence of ligand CDs in the PLL hydrogel networks. From these results, we concluded that the BPA-imprinted CD-PLL hydrogel was successfully synthesized by the chemical cross-linking of CD-PLL using BPA as a template in molecular imprinting.

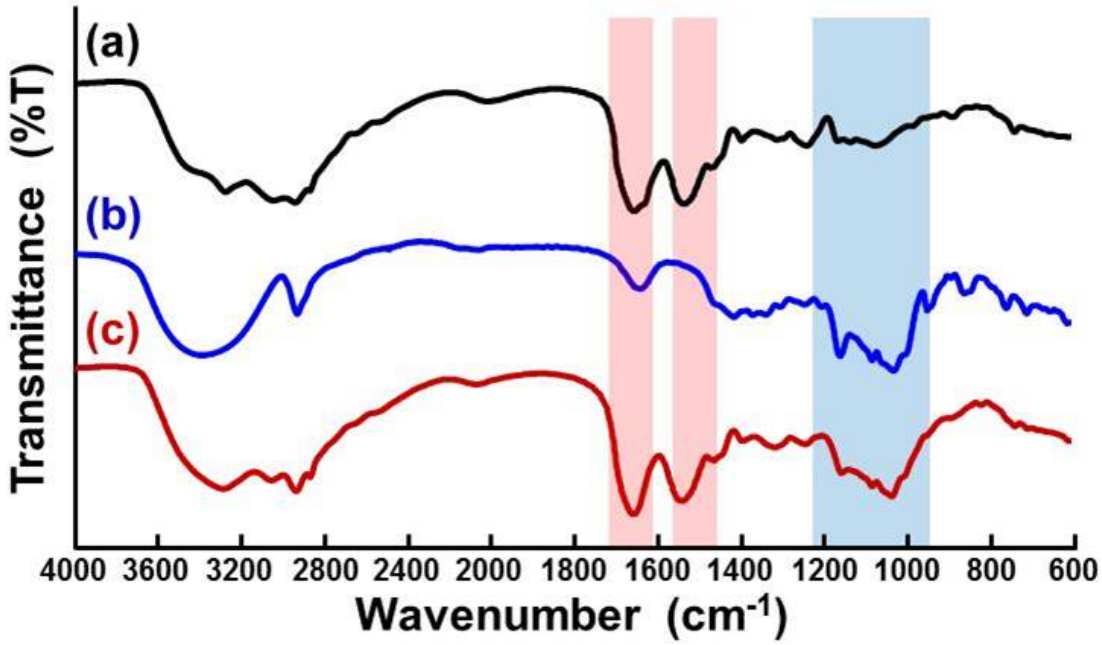

Figure 3-5. FT-IR spectra of (a) PLL hydrogel, (b) CD and (c) BPA-imprinted CD-PLL hydrogel.

3.3.3 pH-Responsive conformational change of BPA-imprinted CD-PLL hydrogel

To create dynamic molecular recognition sites with binding capacities that can be regulated by the structural transition of PLL chains as a function of pH, we prepared the BPA-imprinted CD-PLL hydrogels by cross-linking of the PLL chains with random coil structures at pH 7. After the resulting BPA-imprinted CD-PLL hydrogels were immersed in a NaH_2PO_4/Na_2HPO_4 or Na_2HPO_4/NaOH buffer solution with various pHs for 24 hours, the secondary structures of the hydrogels swollen in the buffer solution were investigated with circular dichroism spectroscopy. The BPA-imprinted CD-PLL hydrogel films were prepared within the 0.1 cm quartz sandwich cells by the method described above.[30] Figure 3-6a shows the ellipticities of the BPA-imprinted CD-PLL hydrogel swollen in a buffer solution with various pHs. In a buffer solution with pH 7, the circular dichroism spectra of the BPA-imprinted CD-PLL hydrogel showed a positive peak at 215 nm, which is characteristic of a random coil structure.[4] In the spectra of the BPA-imprinted CD-PLL hydrogel in buffer solutions with more than pH 9, negative peaks appeared at 208 nm and 222 nm, which are assigned to the α-helix structure. The circular dichroism spectra revealed that the CD-PLL chains of the hydrogel underwent a structural transition from the random coil to α-helix when the pH of a buffer solution increased.

Figure 3-6b shows the effect of pH on the relative α-helix content of the BPA-imprinted CD-PLL hydrogel in the buffer solution with various pHs. In buffer solutions below pH 9, the BPA-imprinted CD-PLL hydrogel had a low α-helix content, which means that the hydrogel was composed of PLL main chains with random coils. However, the relative α-helix content increased dramatically with increasing pH in buffer solutions above pH 9. These results suggest that the PLL main chains of the BPA-imprinted CD-PLL hydrogel undergo a structural transition from the random coil to an α-helix at approximately pH 9. The amino groups of PLL are positively charged

by the protonation above pH 9, which inhibits the formation of the α-helix due to hydrogen bonding. Therefore, the structural transition is attributed to a drastic decrease in the repulsion between positively charged amino groups. Our previous paper reported that the relative α-helix structure of the PLL chains is stabilized by chemical cross-linking. The PLL linear polymer undergoes a structural transition from the random coil to an α-helix at pH 11, but the CD-PLL chains of the BPA-imprinted CD-PLL hydrogel undergoes this transition at pH 9, which is similar to the PLL hydrogel. This means that the α-helix structure of the BPA-imprinted CD-PLL hydrogel is stabilized by chemical cross-linking with PEGDE although bulky CDs are introduced to PLL. Thus, the CD-PLL networks form a secondary structure that underwent a structural transition between the random coil and α-helix in response to a change in pH.

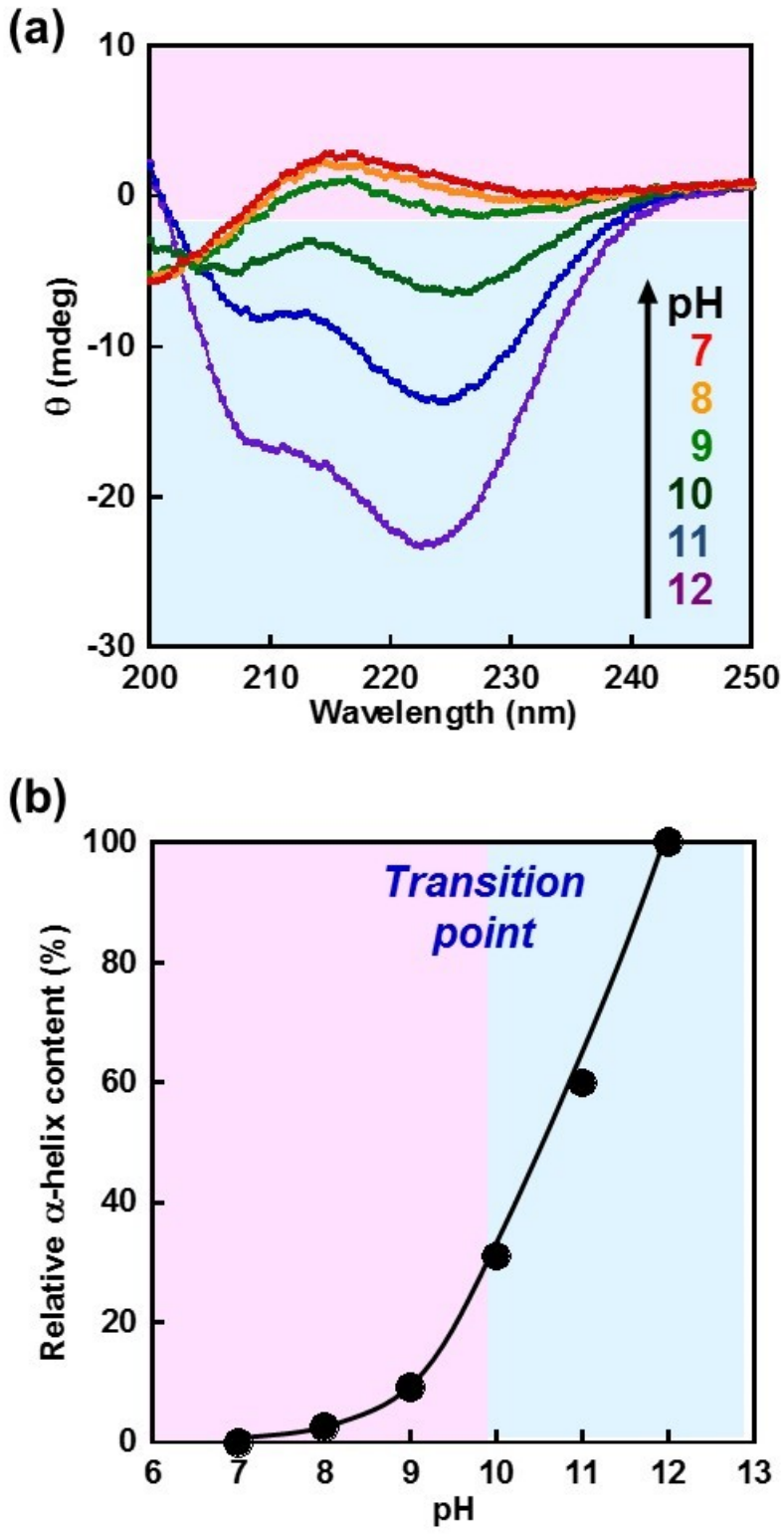

Figure 3-6. (a) Circular dichroism spectra of the BPA-imprinted CD-PLL hydrogels as a function of pH. (b) Relationship between pH and the relative α-helix content of the BPA-imprinted CD-PLL hydrogels in a buffer solution with various pHs.

3.3.4 Molecule-responsive swelling ratio changes of BPA-imprinted CD-PLL hydrogel

The molecularly stimuli-responsive behavior of the BPA-imprinted CD-PLL hydrogel was investigated in a buffer solution containing BPA at pH 7 and 12. Figure 3 shows the swelling ratio changes of the BPA-imprinted CD-PLL hydrogel in response to BPA. In a buffer solution with pH 12, the BPA-imprinted CD-PLL hydrogel exhibited little change in volume in the presence of BPA. At pH 7, however, the swelling ratio of the hydrogel decreased significantly in response to BPA. The BPA-responsive shrinkage is attributed to the formation of CD-BPA-CD complexes that act as cross-links. Thus, the BPA-responsive shrinking of the BPA-imprinted CD-PLL hydrogel was strongly influenced by pH, which is an important factor to induce the structural transition of PLL chains.

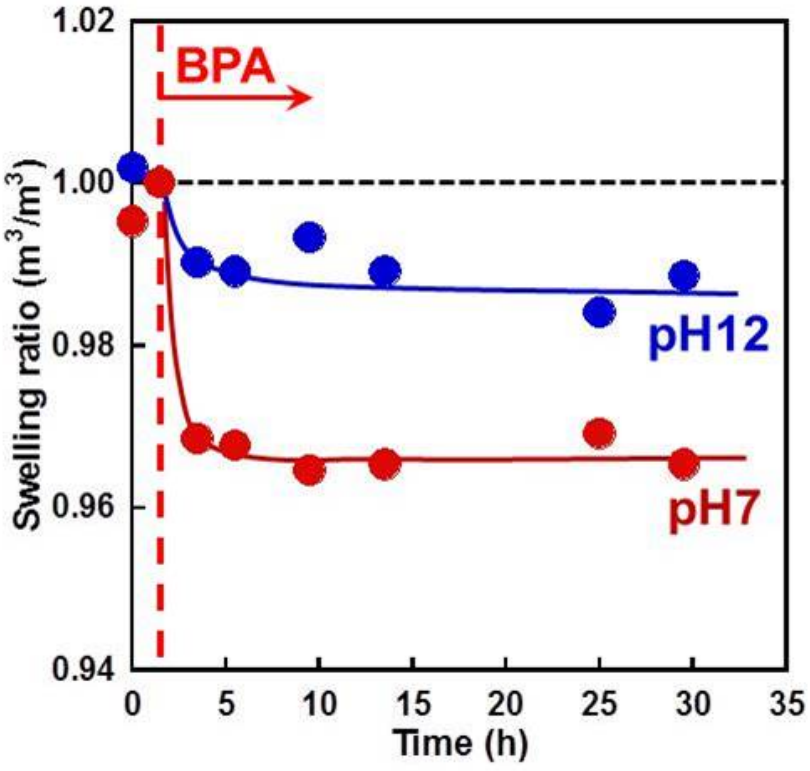

Figure 3-7. Swelling ratio changes of the BPA-imprinted CD-PLL gels in a buffer solution with BPA at pH 7 (●) and pH 12 (●).

We also investigated the molecular recognition behavior of the BPA-imprinted CD-PLL hydrogels by measuring the change in the swelling ratio in a buffer solution containing 4-*tert*-butylphenol (*t*-BP). Similar to BPA, *t*-BP possesses one phenolic group that forms an inclusion complex with CD. In contrast to BPA, which forms a 2:1 complex with two CD molecules, *t*-BP forms a 1:1 inclusion complex with one CD molecule. Figure 3-8 shows the swelling ratio changes of the BPA-imprinted CD-PLL hydrogel in a buffer solution containing BPA or *t*-BP after it attained equilibrium swelling in a buffer solution with pH 7. The presence of BPA resulted in a responsive shrinkage of the BPA-imprinted CD-PLL hydrogel. In contrast, the BPA-imprinted CD-PLL hydrogel underwent no change in volume in the presence of *t*-BP. Because a *t*-BP molecule forms a 1:1 inclusion complex with a ligand CD molecule, the resultant *t*-BP-CD complex cannot act as a cross-link for the hydrogel network.

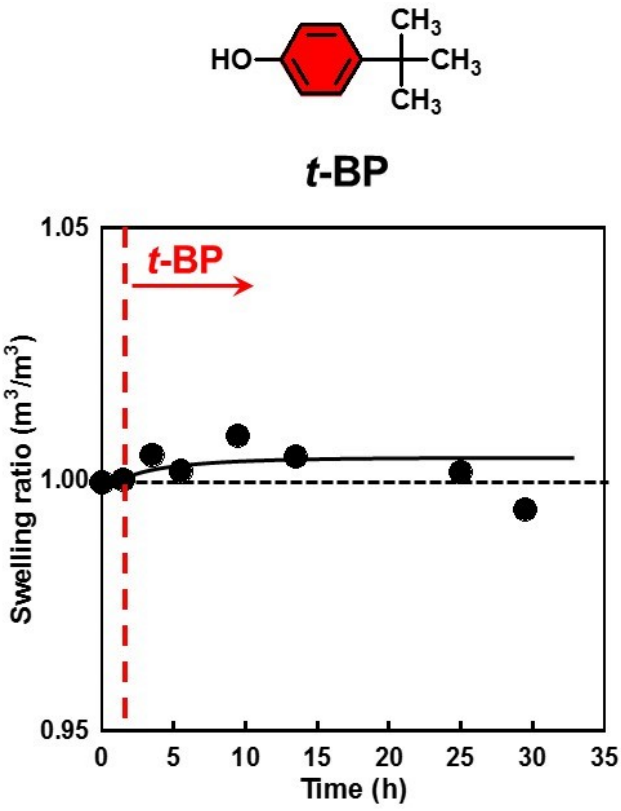

Figure 3-8. Swelling ratio changes of the BPA-imprinted CD-PLL gels in a buffer solution with *t*-BP at pH 7.

These results reveal that the BPA-responsive shrinkage of the BPA-imprinted CD-PLL hydrogel is induced by the action of the CD-BPA-CD complexes as cross-links within the hydrogel network. The BPA-responsive shrinkage of the BPA-imprinted CD-PLL hydrogel at pH 12 was lower than that at pH7. The shape of BPA as a target molecule was memorized within the CD-PLL networks with random coil structures in a buffer solution with pH 7 by molecular imprinting. In a buffer solution with pH 12, however, the CD-PLL polymer chains undergo a structural transition from the random coil to α-helix, followed by rearrangements of the ligand CDs (Figure 4). The rearrangements of the ligand CDs cause a lower possibility of the formation of sandwich-like CD-BPA-CD complexes because the molecular recognition sites created by molecular imprinting are conformationally changed. This may be the reason why the CD-PLL hydrogel exhibited a lower BPA-responsive shrinkage at pH 12. These results imply that the conformationally changeable structure of the PLL network can regulate the molecular binding capacity of the BPA-imprinted hydrogel. Next, we investigated the BPA adsorption behavior of the BPA-imprinted CD-PLL hydrogel.

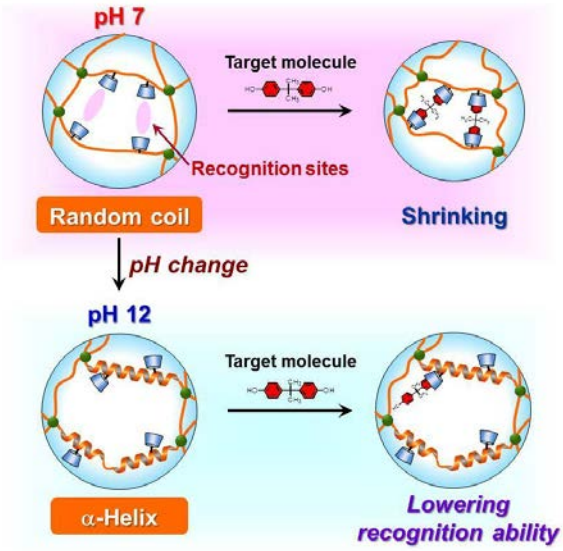

Figure 3-9. Schematic illustration for the BPA-responsive behavior of the BPA-imprinted CD-PLL hydrogel at neutral or basic pHs.

3.3.5 BPA adsorption behavior of BPA-imprinted CD-PLL hydrogel

To determine the relationship between the structural transition and binding capacity of the CD-PLL hydrogel networks, we measured the amount of BPA adsorbed into the hydrogel at pH 7 and 12. Figure 3-10 illustrates the adsorption behavior of BPA into the BPA-imprinted CD-PLL hydrogel at pH 7 and 12. When the BPA-imprinted CD-PLL hydrogel was immersed in a buffer solution containing BPA, BPA adsorption into the hydrogel increased gradually and attained equilibrium after approximately 30 h. The amount of BPA adsorbed into the hydrogel at pH 7 was larger than that at pH 12. Therefore, author concludes that the binding capacity of the BPA-imprinted CD-PLL hydrogel can be regulated by pH changes.

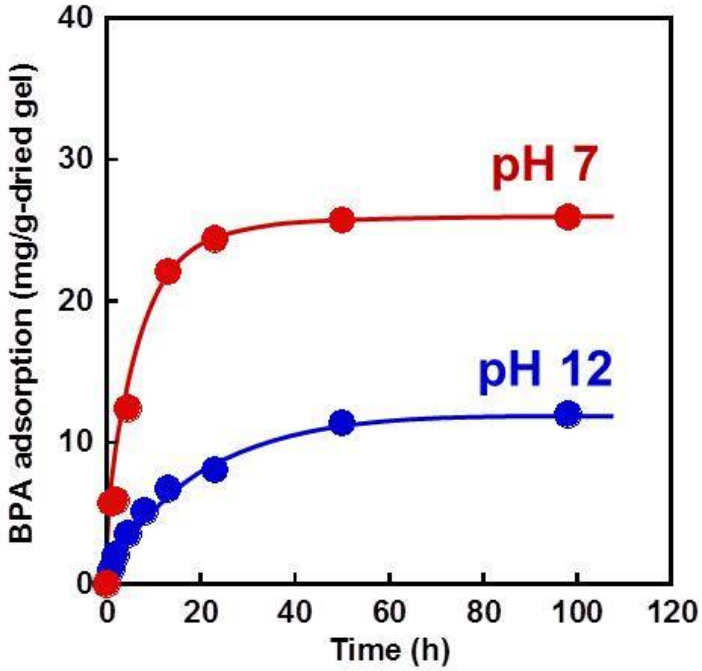

Figure 3-10. Amount of BPA adsorbed into BPA-imprinted CD-PLL gel at pH 7 (●) and pH 12 (●).

The pH dependence of the binding capacity can be attributed to three important factors: the pH dependence of the affinity of CD for BPA, the interaction between the PLL chain and BPA, and the conformational change of the molecular recognition sites. First, we investigated the affinity constant of CD for BPA at pH 7 and 12 by measuring the absorbance of aqueous mixtures of CD and BPA at a wavelength of 280 nm. When BPA forms an inclusion complex with CD, the absorbance of an aqueous BPA solution at 280 nm, which is assigned to two aromatic groups of BPA, is shifted to a lower wavelength. Therefore, we can determine the apparent affinity constant of CD for BPA by measuring the shift of the wavelength in response to a change in the molar ratio of CD to BPA. From the absorbance shift of the mixture of CD and BPA (Figure 3-11), the apparent affinity constants of CD for BPA at pH 7 and 12 were determined as 1.33×10^3 M^{-1} and 0.92×10^3 M^{-1}, respectively. The affinity constant of CD for BPA at pH 7 was a little stronger than that at pH 12. However, the difference in the affinity constant of CD for BPA between pH 7 and 12 is too small to explain why the amount of BPA adsorbed into the BPA-imprinted CD-PLL at pH 7 was larger than that at pH 12.

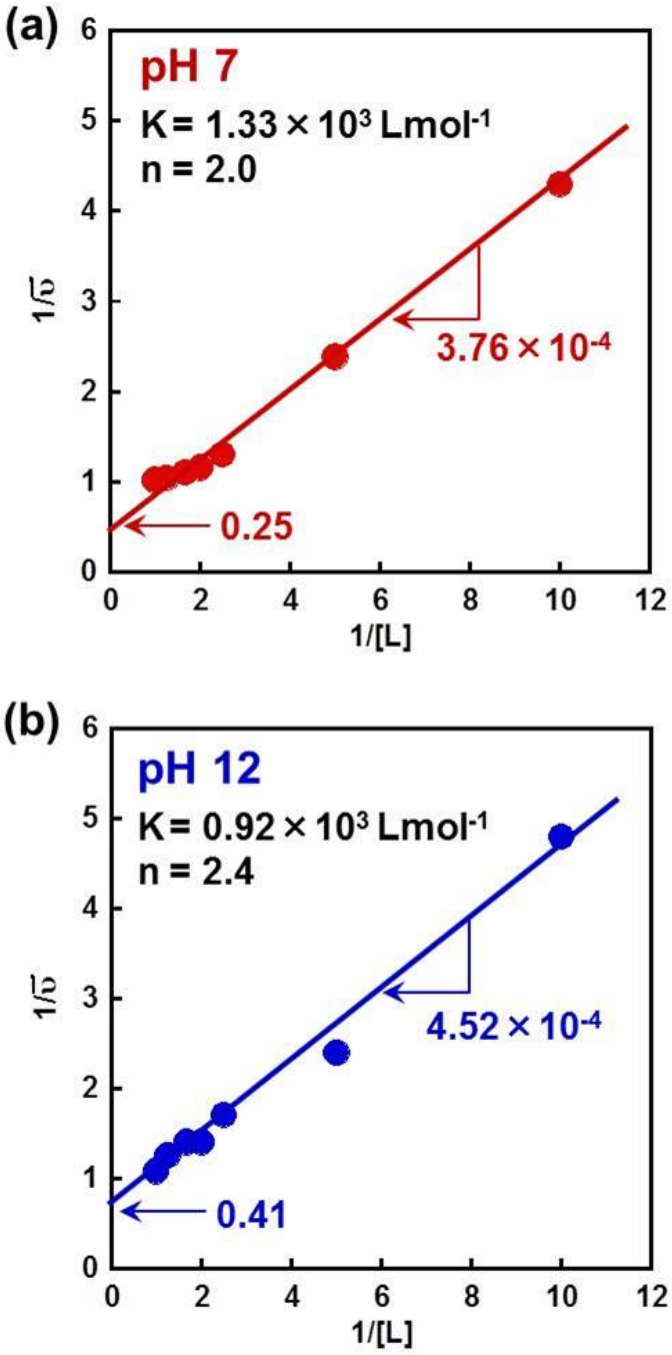

Figure 3-11. Klotz-plot analysis of CD binding to BPA in a buffer solution at (a) pH 7 and (b) pH 12.

Next, to investigate the interaction between the PLL chain and BPA, we measured the BPA adsorption into a PLL hydrogel that has no CDs as ligands (Figure 3-12). A very small amount of BPA was adsorbed into the PLL hydrogel compared with the BPA-imprinted CD-PLL hydrogel. This means that the interaction between BPA and the PLL chain is not an important factor that governs BPA adsorption into the BPA-imprinted CD-PLL hydrogel at pH 7. Therefore, we can explain why the amount of BPA adsorbed into the BPA-imprinted CD-PLL hydrogel at pH 7 was larger than that at pH 12 as follows.

As the BPA-imprinted CD-PLL hydrogel was prepared by molecular imprinting at pH 7, the molecular recognition sites for BPA were created within PLL networks with a random coil structure. This means that the ligand CDs linked with the random coil-structured PLL networks were arranged at optimal positions to enable the formation of sandwich-like CD-BPA-CD complexes with the target BPA. At pH 12, however, the PLL chains of the hydrogel underwent a structural transition from the random coil to α-helix structure, as shown in Figure 3-6. As a result, the cavity structures of the molecular recognition sites formed by molecular imprinting changed due to a structural transition of the PLL chains from random coil to α-helix structures, followed by a drastic change in the positions of ligand CDs. The conformational change in the molecular recognition sites at pH 12 led to a decrease in their binding capacity because the drastic change in the positions of ligand CDs inhibited the formation of the sandwich-like CD-BPA-CD complexes. Therefore, the binding capacity of the BPA-imprinted CD-PLL hydrogel can be regulated by pH because the pH-responsive structural transition from the random coil to α-helix induces a conformational change of its molecular recognition sites, which is similar to the allosteric regulation of proteins. The controllable binding capacity of the molecular recognition sites formed within polypeptide networks provides a useful tool for achieving a sensitive pH-responsive binding and release of a specific molecule such as a drug.

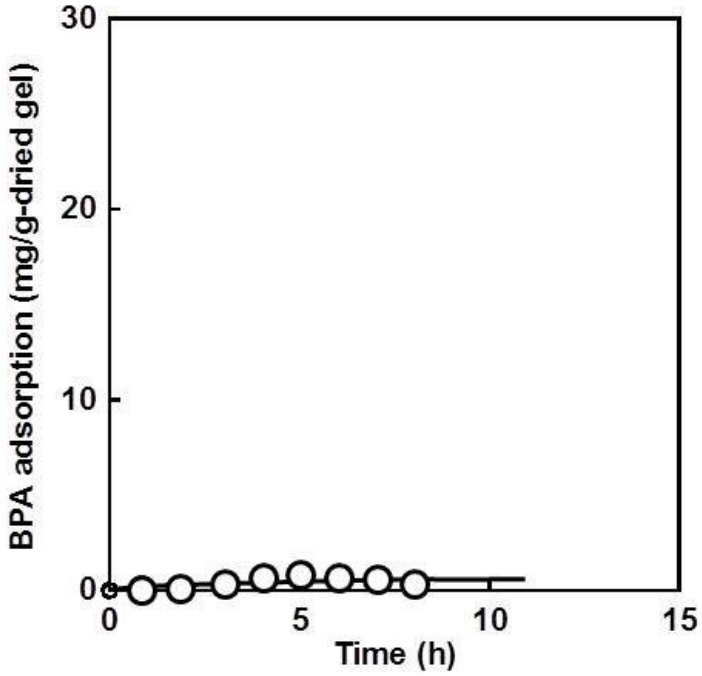

Figure 3-12. Amount of BPA adsorbed into the PLL gel at pH 7.

3.3.6 Molecular release triggered by structural transition of PLL

The previous section described how the BPA-imprinted CD-PLL hydrogel with controllable binding sites can be strategically designed by molecular imprinting that uses CDs as the ligands and polypeptides as the main chains. This leads to our underlying hypothesis that a conformational change of the CD-PLL hydrogel triggers the release of a specific molecule, such as a drug that is loaded within the hydrogel network by molecular imprinting. The specific molecule needs to have multi-binding sites for CDs so that the conformational change of the molecular recognition sites with the arranged CDs can induce a decrease in their binding capacity by preventing the target molecule from forming multiple bonds with the CDs. The BPA used in this study is a representative target molecule with two binding sites for CDs, which may be used as a model drug, such as docetaxel (DTX). In particular, DTX that is a successful agent currently in use for the chemotherapy of cancer forms a complex with two CD molecules.[31] The release behavior of BPA from the CD-PLL hydrogel by the pH-responsive conformational change of PLL chains is described in this section.

To construct novel pH-responsive molecular release systems, CDs as ligands for BPA were introduced into PLL, which undergoes a conformational change in response to a pH change. After the resulting CD-PLL formed a CD-BPA-CD complex with BPA in a buffer solution with pH 7, at which the PLL chains form a random coil structure, the BPA-loaded CD-PLL hydrogel with CDs was prepared by cross-linking CD-PLL with PEGDE. An important process for the BPA-loaded CD-PLL hydrogel is the complex formation between CD-PLL with a random coil structure and BPA before chemical cross-linking for the network formation. This method follows the same process as molecular imprinting without the extraction of the template molecule from the networks, i.e., *pseudo* molecular imprinting. Such *pseudo* molecular imprinting enables the arrangement of CD ligands at optimal positions for the formation of CD-BPA-CD complexes with the BPA template. As can be easily observed from the

previous section, the optimal arrangement of the CD ligands by molecular imprinting stabilizes the CD-BPA-CD complexes within the BPA-loaded CD-PLL hydrogel with a random coil structure.

The release profiles of BPA from the BPA-loaded CD-PLL and PLL hydrogels at various pHs are shown in Figure 3-13. The release of BPA from the BPA-loaded CD-PLL hydrogel was suppressed in a buffer solution with neutral pHs. Under basic conditions above pH 10, however, BPA was effectively released from the BPA-loaded CD-PLL hydrogel. These results indicate that the release behavior of BPA from the BPA-loaded CD-PLL hydrogel was strongly influenced by pH. In addition, to investigate the BPA release behavior by diffusion from a BPA-loaded PLL hydrogel without CDs as a ligand, we prepared BPA-loaded PLL hydrogels by cross-linking PLL chains with a random coil structure in the presence of free BPA. Figure 3-13b demonstrates that BPA was quickly released from the BPA-loaded PLL hydrogel without CD ligands at both pH 7 and pH 12. The PLL hydrogel was unable to prevent the loaded BPA from leaking out in a buffer solution with pH 7 and pH 12. No difference was observed in the amount of BPA released from the BPA-loaded PLL hydrogel between pH 7 and 12. Therefore, we concluded that the pH-dependent BPA release behavior of the BPA-loaded CD-PLL hydrogel was not attributed to the effect of pH on the solubility and diffusivity of BPA. In general, the release behavior of a solute from a hydrogel strongly depends on its swelling ratio because the diffusion coefficient is closely correlated with the network size. Therefore, we investigated the swelling ratio of the BPA-loaded CD-PLL hydrogel when it was immersed in a buffer solution with various pHs.

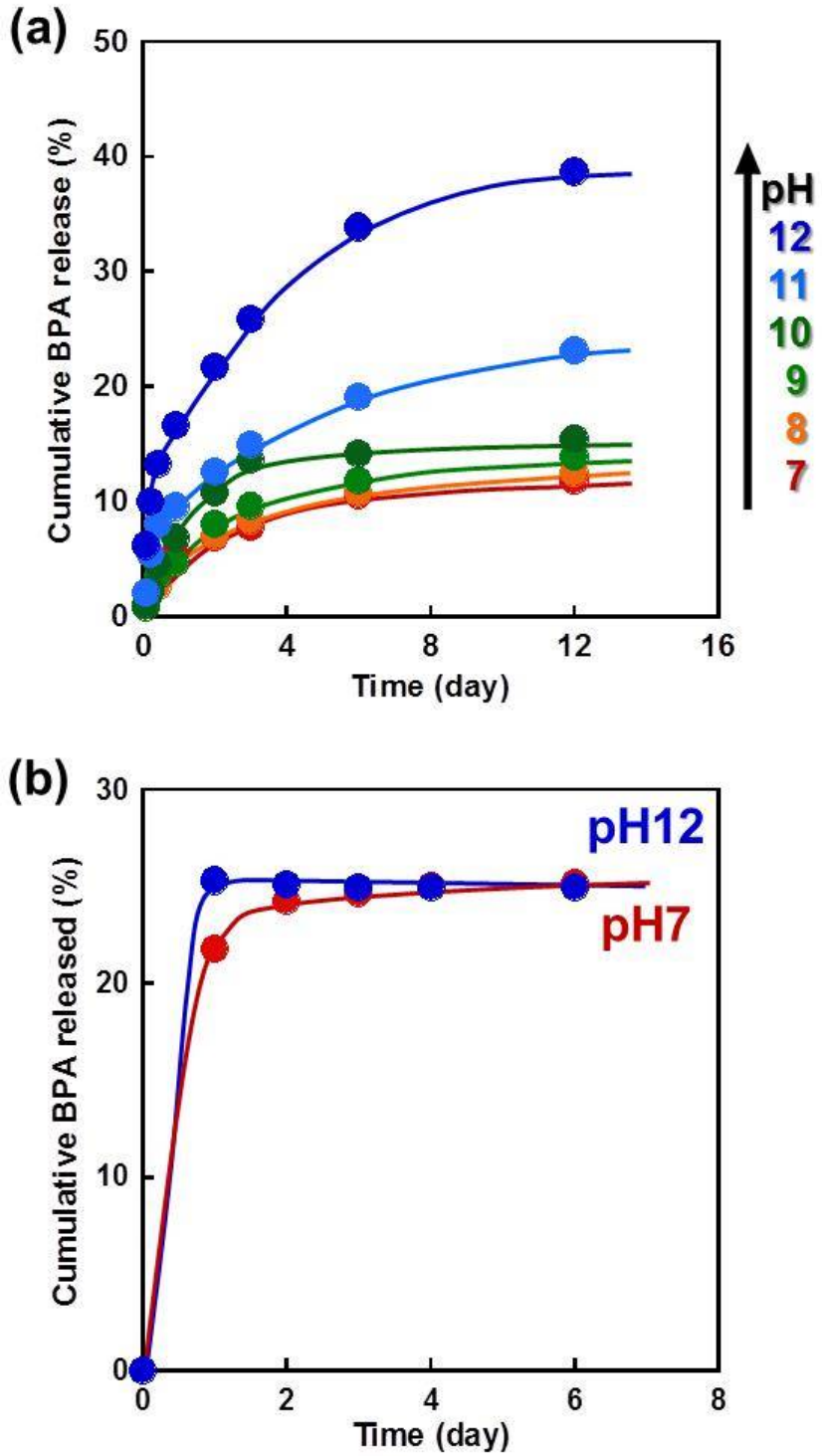

Figure 3-13. (a) Release profiles of the BPA from BPA-loaded CD-PLL hydrogel at pH 7 (●), pH 8 (●), pH 9 (●), pH 10 (●), pH 11 (●) and pH 12 (●). (b) Release profiles of BPA from the BPA-loaded PLL hydrogel at pH 7 (●) and pH 12 (●).

Figure 3-14 shows the effect of pH on the swelling ratio of the BPA-loaded CD-PLL hydrogel and the relative amount of BPA released from the hydrogel in a buffer solution with various pHs. The relative amount of BPA released from the hydrogel is the ratio of BPA released for 24 hours to the total BPA loaded within the hydrogel. Above pH 6, the swelling ratio of the CD-PLL hydrogel decreased drastically with increasing pH of the buffer solution. In a buffer solution with a pH less than pH 6, the protonation of the amino groups of CD-PLL chains leads to an increase in the osmotic pressure of the hydrogel, followed by the swelling of the hydrogel network. However, the CD-PLL hydrogel exhibits great shrinkage in a buffer solution with a pH of more than pH 6 because the amino groups were deprotonated. In contrast to the pH-dependence of the swelling ratio, the relative amount of BPA released from the BPA-loaded CD-PLL hydrogel was reduced at pHs less than pH 9 but increased at pHs more than pH 10. It should be noted that the BPA-loaded CD-PLL hydrogels released BPA effectively in spite of their shrinkage with increasing pH. This means that the enhancement in the BPA release at pHs more than pH 10 was not based on the diffusivity of BPA in the hydrogel networks. As shown in Figure 2, the α-helix content of the BPA-imprinted CD-PLL hydrogel increased sharply with increasing pH at pHs more than pH 10, which indicates the structural transition of PLL chains from the random coil to α-helix. It should be noted that the pH-dependence of the α-helix content of the CD-PLL hydrogel was consistent with that of the BPA release. Therefore, the enhanced BPA release at pHs more than pH 10 can be explained by a conformational change of the CD-PLL hydrogel network, as follows.

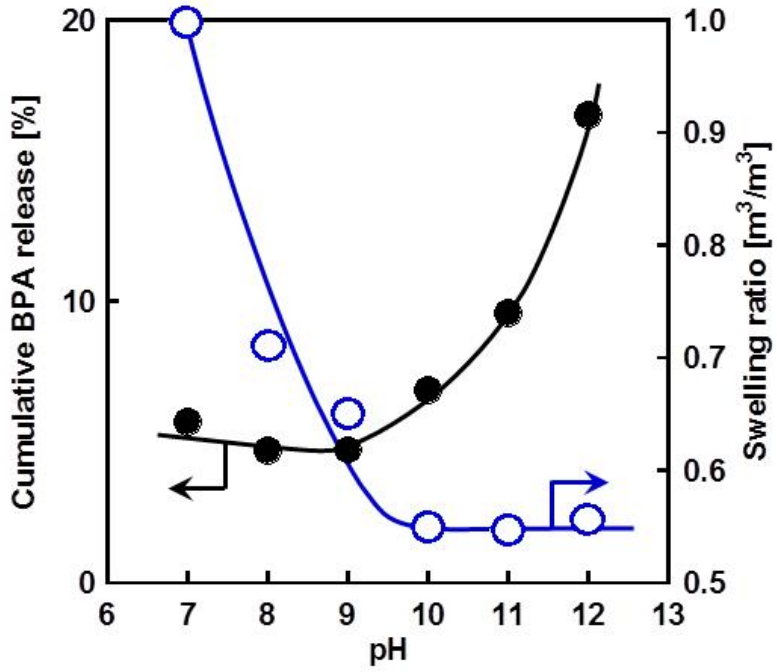

Figure 3-14. Effect of pH on the amount of BPA released from the BPA-loaded CD-PLL hydrogel (●) and swelling ratio of the BPA-imprinted CD-PLL hydrogel (○).

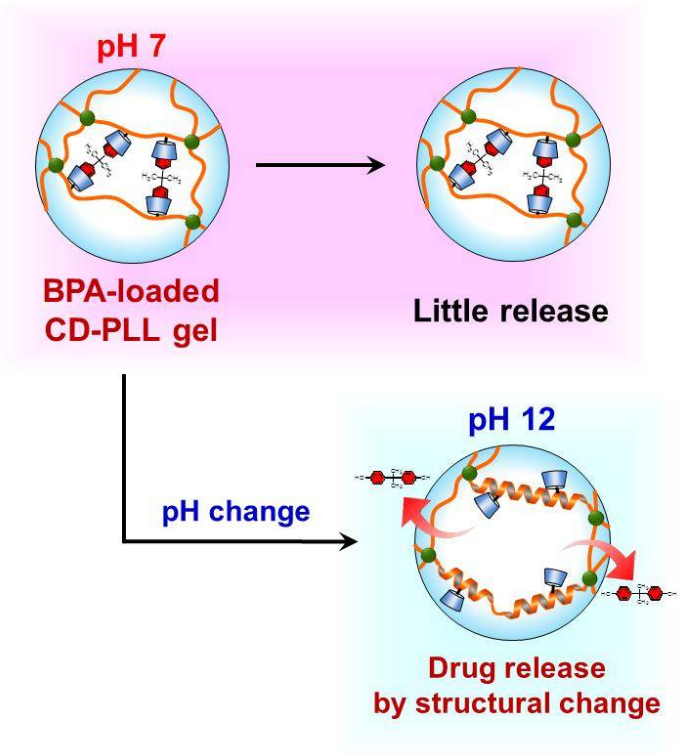

Figure 3-15. Schematic illustration for the BPA release behavior of the BPA-loaded CD-PLL hydrogels in at neutral or basic pH.

In the BPA-loaded CD-PLL hydrogel prepared by *pseudo* molecular imprinting without the process for extracting the BPA template, CD ligands are arranged at optimal positions to form CD-BPA-CD complexes with BPA. Importantly, the CD-PLL network has a random coil structure when the CD-PLL chains are chemically crosslinked at pH 7. The stabilization of the CD-BPA-CD complexes by *pseudo* molecular imprinting prevents BPA from being released from the CD-PLL hydrogel network with a random coil structure at pHs less than pH 10. At pHs more than pH 10, however, the stability of the CD-BPA-CD complexes become low because a structural transition of the CD-PLL hydrogel network from a random coil to α-helix induces a conformational change of the molecular recognition sites with well-arranged CD ligands for BPA. Therefore, the CD-PLL hydrogel network with random coil structures can retain BPA without leaking at pHs less than pH 10, but the hydrogel network with α-helix structure effectively releases it by lowering the stability of the CD-BPA-CD complexes in spite of its shrinkage at pHs more than pH 10. These conclusions are well supported by the pH-dependence of BPA adsorption into the BPA-imprinted CD-PLL hydrogel, which was described in the previous section. These results suggest that molecularly imprinted hydrogels with polypeptide chains can regulate molecular binding and release in response to a small change in pH. Such a regulation of the molecular binding and release by conformational changes is similar to the allosteric regulation of proteins. The use of both molecular imprinting and the conformational change of polypeptides enables the hydrogel networks to regulate molecular binding and release, which are not governed by the diffusivity within the swollen or shrunken networks. Although the novel strategy of combining molecular imprinting with conformational changes of polypeptides still requires further research into possible applications, both methods are likely to become relatively important for self-regulated DDSs in the future.

3.4 Conclusions

BPA-imprinted CD-PLL hydrogels, which can be prepared from PLL with random coil structures by molecular imprinting using complex formation, have molecular recognition sites for specific molecules. The swelling ratio of the resulting BPA-imprinted CD-PLL hydrogel with a random coil structure decreased significantly in response to BPA at neutral pH. Upon a structural transition of PLL from the random coil to α-helix at basic pHs, however, the molecular recognition sites created by molecular imprinting are conformationally changed. As a result, the binding capacity of the BPA-imprinted CD-PLL hydrogel can be regulated by a pH-responsive structural transition of the PLL chains, similar to the allosteric effect. Furthermore, the BPA-loaded CD-PLL hydrogels that were prepared by *pseudo* molecular imprinting can also regulate the BPA release in response to a small change in pH because a pH change induced a reduction in the stability of CD-BPA-CD complexes within the hydrogel networks. The underlying concepts in our results will assist others in preparing new materials for drug delivery, including the translation to other polymers and drug compositions. Thus, we designed a BPA-imprinted CD-PLL hydrogel as a protein-mimicking smart hydrogel that regulates molecular binding and release for specific molecules by conformational changes.

3.5 References

1. T. Tanaka, *Phys. Rev. Lett.*, **40**, 820-823, 1978.
2. Y. Hirokawa, T. Tanaka, *J. Chem. Phys.*, **81**, 6379-6380, 1984.
3. T. Amiya, Y. Horikawa, Y. Hirose, Y. Li, T. Tanaka, *J. Chem. Phys.*, **86**, 2375-2379, 1987.
4. G. Chen, A. S. Hoffman, *Nature*, **373**, 49-52, 1995.
5. R. Yoshida, K. Uchida, T. Kaneko, K. Sakai, A. Kikuchi, Y. Sakurai, T. Okano, *Nature*, **374**, 240-242, 1995.
6. T. Tanaka, D. Fillmore, S-T. Sun, I. Nishio, G. Swislow, A. Shah, *Phys. Rev. Lett.*, **45**, 1636-1639, 1980.
7. M. Annaka, T. Tanaka, *Nature*, **335**, 430-432, 1992.
8. T. Tanaka, I. Nishio, S-T. Sun, S. Ueno-Nishio, *Science*, **218**, 467-469, 1982.
9. Y. Osada, H. Okuzaki, H. Hori, *Nature*, **355**, 242-244, 1992.
10. C. S. Brazel, N. A. Peppas, *Macromolecules*, **28**, 8016-8020, 1995.
11. T. Miyata, K. Nakamae, A. S. Hoffman, Y. Kanzaki, *Macromol. Chem. Phys.*, **195**, 1111-1120, 1994.
12. K. Nakamae, T. Nizuka, T. Miyata, M. Furukawa, T. Nishio, K. Kato, T. Inoue, A. S. Hoffman, Y. Kanzaki, *J. Biomater. Sci. Polym. Ed.*, **9**, 43-53, 1997.
13. T. Miyata, *Polym. J.*, **42**, 277-289, 2010.
14. T. Miyata, N. Asami, T. Uragami, *J. Polym. Sci. Part B: Polym. Phys.*, **47**, 2144-2157, 2009.
15. T. Miyata, M. Jige, T. Nakaminami, T. Uragami, *Proc. Natl. Acad. Sci. U.S.A.*, **103**, 1190-1193, 2006.
16. T. Miyata, N. Asami, T. Uragami, *Nature*, **399**, 766-769, 1999.
17. T. Miyata, N. Asami, T. Uragami, *Macromolecules*, **32**, 2082-2084, 1999.
18. T. Miyata, A. Jikihara, K. Nakamae, A.S. Hoffman, *Macromol. Chem. Phys.*, **197**, 1135-1146, 1996.
19. T. Miyata, A. Jikihara, K. Nakamae, A. Hoffman, *J. Biomater. Sci. Polym. Ed.*, **15**, 1085-1098, 2004.
20. A. Kawamura, T. Kiguchi, T. Nishihata, T. Uragami, T. Miyata, *Chem. Commun.*, **50**, 11101-11103, 2014.
21. R. Townend, T. F. Kumosinski, S. N. Timasheff, G. D. Fasman, B. Davidson,

Biochem. Biophys. Res. Commun., **23**, 163-169, 1966.

22. N. Greenfield, G. D. Fasman, *Biochemistry*, **8**, 4108-4116, 1969.
23. K. Matsumoto, A. Kawamura, T. Miyata, *Chem. Lett.*, **44**, 1284-1286, 2015.
24. N. Zhong, H. S. Byun, R. Bittman, *Tetrahedron Lett.*, **42**, 1839-1841, 2001.
25. M. Prabaharan, J. F. Mano, *Macromol. Biosci.*, **5**, 965-973, 2005.
26. T. Girek, W. Ciesielski, *J. Incl. Phenom. Macrocycl. Chem.*, **69**, 439-444, 2011.
27. F. Adrian,T. Budtova, E. Tarabukina, M. Pinteala, S. Mariana, C. Peptu, V. Harabagiu, B. C. Simionescu, *J. Incl. Phenom. Macrocycl. Chem.*, **64**, 83-94, 2009.
28. S. Taira, Y. Du, M. Kodaka, *Biotech. Bioeng.*, **93**, 396-400, 2006.
29. E. Kkokufuta, H. Suzuki, R. Yoshida, K. Yamada, M. Hirata, F. Kaneko, *Langmuir*, **14**, 788-795, 1998.
30. K. Maeda, H. Mochizuki, K. Osato, E. Yashima, *Macromolecules*, **44**, 3217-3226, 2011.
31. S. Mazzaferro, K. Bouchemal, J. F. Gallard, B. I. Iorga, M. Cheron, C. Gueutin, C. Steinmesse, G. Ponchel, *Int, J. Pharm.*, **416**, 171-180, 2011.

Chapter 4

Preparation of Antioxidant Agent-Loaded Polypeptide Hydrogel and Their Release Behavior by Conformational Change

4.1 Introduction

Oxygen has a key role in metabolism to produce metabolism energy in a biological context. A few presents of oxygen in the body divert to reactive oxygen species (ROS), including superoxide anion (O_2^-), hydrogen peroxide (H_2O_2) and hydroxyl radical (HO·), that shows bactericidal action and signal transduction.[1,2] However, ROS levels dramatically increase by alcohol drinking, tobacco smoking, bad diet and environmental stress. The excessive ROS denature and damage proteins, lipids and DNAs. As a result, ROS has been implicated in various disease such as diabetes, myocardial infarction, carcinogenesis and aging.[3-7] Antioxidants can reduce the ROS levels and have been reported as effective compounds for the treatment of cancer, heart disease, cerebral infraction, congenital abnormalities and cataract.[8-13]

Resveratrol (RSV) is one of the antioxidant, which is included in several foods such as grapes, peanuts and red wines.[14] A number of studies have focused on its biological anti-platelet aggregation effect, anti-atherogenic property, estrogen-like growth promoting effect, growth inhibiting activity and immunomodulation.[15-19] More recently, RSV has also drawn considerable attention as effective anticancer drugs. RSV inhibits cancer initiation, promotion and progression, followed by prevention and reduction of cancer risk.[20] RSV also be able to induce apoptosis in cancer through transactivation of p53 activity and expression of p53 protein.[21] In addition, RSV has an ability to sensitize a synergistic cytotoxic activity in drug-resistant tumor cells, when RSV is used in combination with cytotoxic drugs such as DTX and doxorubicin.[22] Then, RSV is a useful agent for the use in cancer chemoprevention and chemotherapy.

During chemotherapy, the concept of DDS is becoming popular to enhance the drug efficacy and to minimize the toxic side effects of drug. Various DDS carriers such as micelle, liposome, hydrogel and so on, have been developed as slow delivery, target delivery and stimuli-responsive release.[23-25] However, the initial burst release of the drugs from these carriers often causes side effects due to the overdose of the released

drugs. Therefore, the methods to reduce the burst release and to control the drug release with an effective concentration over several weeks become the key points in designing promising DDS carriers.

As mentioned in earlier chapters, the molecular imprinting method can form recognition sites within the matrix. Author has loaded molecules into the molecularly imprinted CD-PLL hydrogels. The molecule-loaded CD-PLL hydrogels slowly released the molecules over two weeks. Furthermore, the model drug molecule release behavior was regulated by structural transition of the PLL networks in response to a change in pH. These drug release systems using the molecularly imprinted CD-PLL hydrogels with controllable molecular recognition sites provide unique models of DDS applications. However, the basic pH for structural transition of the PLL is not useful in controlling DDS carriers under physiological conditions.

It is well known that poly(L-glutamic acid) (PGA) undergoes a structural transition between an α-helix and random coil structure around slightly acidic pH, because the dissociated carboxy groups in its side chains destabilize the α-helix structure.[26] Human body has some slightly acidic regions such as stomach, organelle and cancer. Thus, the structural transition of PGA around slightly acidic pH has potential for biomedical applications. In the work presented here, we report a novel drug release behavior of RSV-loaded CD-introduced PGA (CD-PGA) hydrogels, based on the fact that a RSV molecule forms an inclusion complex with two CD molecules.[27] The RSV-loaded CD-PGA hydrogels not only suppressed releasing of RSV from the hydrogels due to stabilization of the CD-RSV-CD complex, but also accelerated its release due to a conformational change of the molecular recognition sites by the structural transition of PGA chains. Additionally, forming an inclusion complex with CD resulted in a significant enhancement in the solubility of RSV which is little soluble in aqueous media.

4.2 Experimental

4.2.1 Materials

PGA sodium salt (12,000 MWCO) and *O,O'*-bis(3-aminopropyl)polyethylene glycol (PEG-diamine) were purchased from Peptide Ins. Co. Ltd (Osaka, Japan) and NOF Co. Ltd (Tokyo, Japan), respectively. All aqueous solutions were prepared with ultra-pure water (Milli-Q, 18.2 MΩ cm). The other solvents and reagents were of analytical grade, were obtained from commercial sources and were used without further purification.

4.2.2 Synthesis of NH_2-CD

NH_2-CD was synthesized by the same procedure as described in Chapter 3.

4.2.3 Introduction of CD to PGA

PGA (1.0 g, 6.62 mmol glutamic acid units) was dissolved in 100 mL of ultra-pure water. EDC (76.2 mg, 0.40 mmol) and NHS (45.7 mg, 0.40 mmol) were added to the aqueous solution with PGA and allowed to react for 1 h at room temperature. NH_2-CD (750.8 mg, 0.66 mmol) was added to the aqueous solution with an activated PGA. The reaction proceeded for 24 h at room temperature (Scheme 4-1). Then, the reaction mixture was poured into seamless cellulose tubing (molecular weight cut off: 3,500) and was dialyzed against ultra-pure water for purification. The resultant CD-PGA was obtained via freeze-drying. The content of CD that was introduced to PGA was determined from the ^{1}H NMR proton integration. The CD-PGA was dissolved in D_2O, and ^{1}H NMR was recorded on JEOL JNM-AL 400 spectrometer using sodium 3-(trimethylsilyl)propionate-2,2,3,3-d_4 as the internal standard.

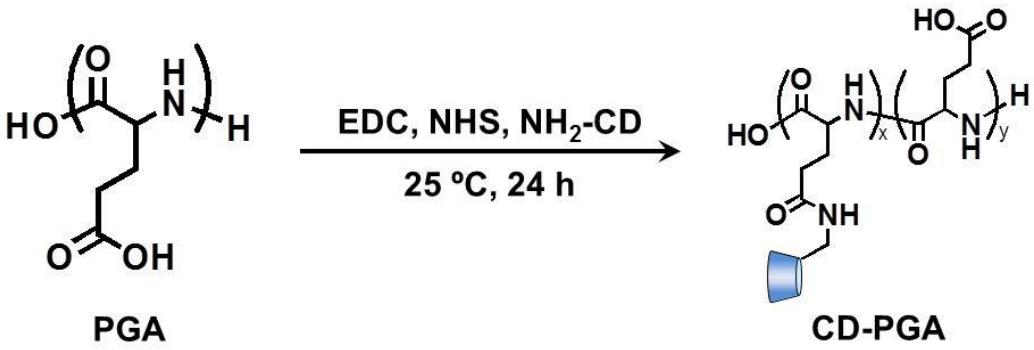

Scheme 4-1. Reaction scheme for the synthesis of CD-PGA.

4.2.4 Preparation of RSV-loaded CD-PGA hydrogels

The RSV-loaded CD-PGA hydrogels were prepared by *pseudo* molecular imprinting, which includes no process for extracting the RSV template shown in scheme 4-2. CD-PGA (100 mg) and PEG-diamine (10 mol% for glutamic acid units) were dissolved in 500 μL of 4-(2-hydroxyethyl)-1-piperazineethanesulfonic acid (HEPES) buffer solution (50 mM, pH 7, 0.5 M NaCl). After 2:1 complex formation between CD and RSV, the resultant CD-PGA was cross-linked by the addition of EDC and NHS (10 mol% for glutamic acid units respectively) in the HEPES buffer solution for 24 hours at 25 °C in the presence of RSV. Here, molds composed of glasses, whose thickness was adjusted with silicon spacers, were used in preparing hydrogels.

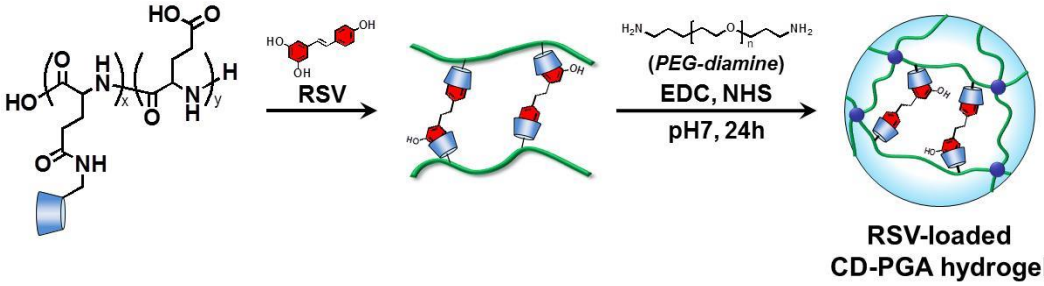

Scheme 4-2. Preparation of RSV-loaded CD-PGA hydrogel.

4.2.5 Circular dichroism

The secondary structures of CD-PGA hydrogels prepared on quartz glass were measured by circular dichroism spectroscopy reported in Chapter 2. The CD-PGA hydrogels on a quartz glass were placed in the 1 mm quartz sandwich cell for CD measurements. The CD-PGA hydrogels in buffer solutions with various pHs were subjected to scanning from 250 nm to 200 nm at 0.1 nm data pitch at the rate of 100 nm/min with background subtracted. To investigate the relationship between pH and the structure of PGA chains, relative α-helix content of the PGA hydrogel was determined from the ellipticity at 222 nm using equation (4-1).

$$\text{Relative } \alpha\text{-helix content } = \frac{\theta_{222}{}^{pH} - \theta_{222}{}^{pH\,3.5}}{\theta_{222}{}^{pH\,3.5} - \theta_{222}{}^{pH\,7}} \times 100 \qquad (4\text{-}1)$$

where $\theta_{222}{}^{pH}$, $\theta_{222}{}^{pH3.5}$, and $\theta_{222}{}^{pH7}$ are the ellipticities (222nm) of the hydrogel in a buffer solution with each pH, pH 3.5, and pH 7, respectively.

4.2.6 Release of RSV from CD-PGA hydrogels

The RSV-loaded CD-PGA hydrogels, which were prepared in tablet form using silicon spacers (ϕ = 5 mm, thickness = 2 mm), were rinsed and attained equilibrium in a HEPES buffer solution at pH 7 and 25 °C. After that, the hydrogels were transferred and kept immersed in CH_3COOH/CH_3COONa (pH 3.5, 4.0, and 4.5), NaH_2PO_4/Na_2HPO_4 (pH 5.0 and 6.0) or HEPES (pH 7.0) buffer solutions at 25 °C. The amount of RSV released from the hydrogels was investigated by measuring the RSV concentration after the immersion in each buffer solutions as follows: Fluorescent intensities of buffer solutions containing RSV at different time intervals were measured in the wavelength range of 300-500 nm with an excitation at 280 nm using spectrofluorophotometer (RF-5300PC, Shimadzu, Kyoto, Japan). The characteristic wavelength for the peaks of fluorescence emission intensity was at 388 nm. The RSV

concentration in the buffer solution was calculated against the calibration curve of the standard RSV solution.

4.2.7 Measurement of swelling ratio changes

Swelling ratio changes of the CD-PGA hydrogels were measured by the same method as described in Chapter 2. The CD-PGA hydrogels for swelling ratio change measurement were prepared in tablet form using silicon spacers (ϕ = 5 mm, thickness = 2 mm). The CD-PGA hydrogels were immersed in 16 mL of CH_3COOH/CH_3COONa, NaH_2PO_4/Na_2HPO_4 and HEPES buffer solutions with various pHs after the swelling of the CD-PGA hydrogels attained equilibrium in a HEPES buffer solution at pH 7. The swelling ratios of the CD-PGA hydrogels (V/V_0) were determined from their diameters in CH_3COOH/CH_3COONa, NaH_2PO_4/Na_2HPO_4 and HEPES buffer solutions with various pHs using the equation (2-1). Where d and d_0 are diameters of the CD-PGA hydrogels in a buffer solution with each pH and pH 7, respectively.

4.3 Results and Discussion

4.3.1 Characterizations of CD-PGA

After the synthesis of a monosubstituted CD derivative possessing an amino group, it was reacted with PGA using EDC and NHS to obtain CD-PGA. The average degree of substitution of the resulting CD-PGA was found to be 0.05 (i.e., on average one CD every 20 glutamic acid units) by ^{1}H NMR analysis (Figure 4-1).

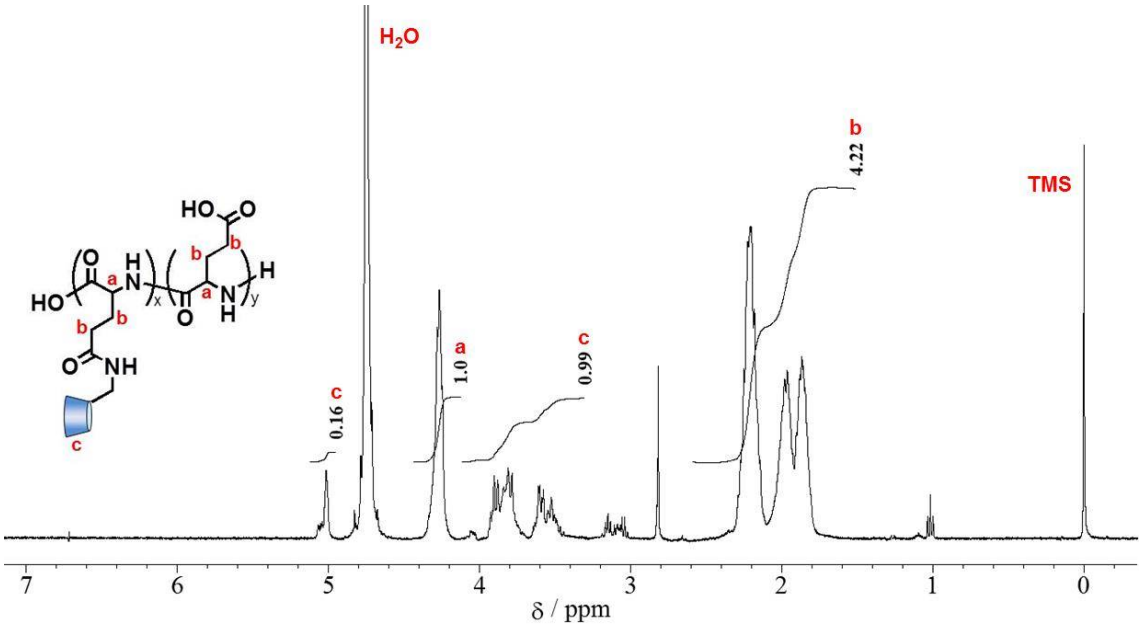

Figure 4-1. ^{1}H NMR spectrum of CD-PGA (D_2O, 400 MHz).

4.3.2 pH-Responsive structural transition of CD-PGA hydrogels

To stabilize molecular complex between CD and RSV that can be regulated by the structural transition of PGA chains as a function of pH, we prepared the CD-PGA hydrogels by cross-linking of CD-PGA chains with random coil structure at pH 7. After the resulting CD-PGA hydrogels were immersed in CH_3COOH/CH_3COONa, NaH_2PO_4/Na_2HPO_4 or HEPES buffer solutions with various pHs for 24 hours, the secondary structures of CD-PGA hydrogels swollen in the buffer solution were investigated with circular dichroism spectroscopy. Figure 4-2 (a) shows the ellipticities of the CD-PGA hydrogel swollen in a buffer solution with various pHs. In a buffer solution with pH 7, circular dichroism spectra of the CD-PGA hydrogel showed a positive cotton effect at 215 nm, which is characteristic to a random coil structure. In the spectra of the CD-PGA hydrogel in buffer solutions with pH less than pH 5, negative cotton effects appeared at 208 nm and 222 nm, which are assigned to α-helix structure. The circular dichroism spectroscopy revealed that the CD-PGA chains of the hydrogel underwent a structural transition from the random coil to α-helix structure when pH of a buffer solution decreased.

Figure 4-2 (b) shows the effect of pH on the relative α-helix content of the CD-PGA hydrogel. In buffer solutions above pH 5, the CD-PGA hydrogel had low α-helix content, meaning that it was composed of a PGA main chain with random coils. However, the relative α-helix content increased dramatically with decreasing pH in the buffer solutions with pHs less than pH 5. These suggest that the PGA main chains of the CD-PGA hydrogel undergo a structural transition from the random coil to α-helix structure at approximately pH 5. The structural transition is attributed to the repulsion between negatively charged carboxy groups, which are generated by the deprotonation above pH 5. Therefore, the PGA network can form the secondary structure that underwent the structural transition between the random coil and α-helix structure after the introduction of CD and cross-linking of PGA.

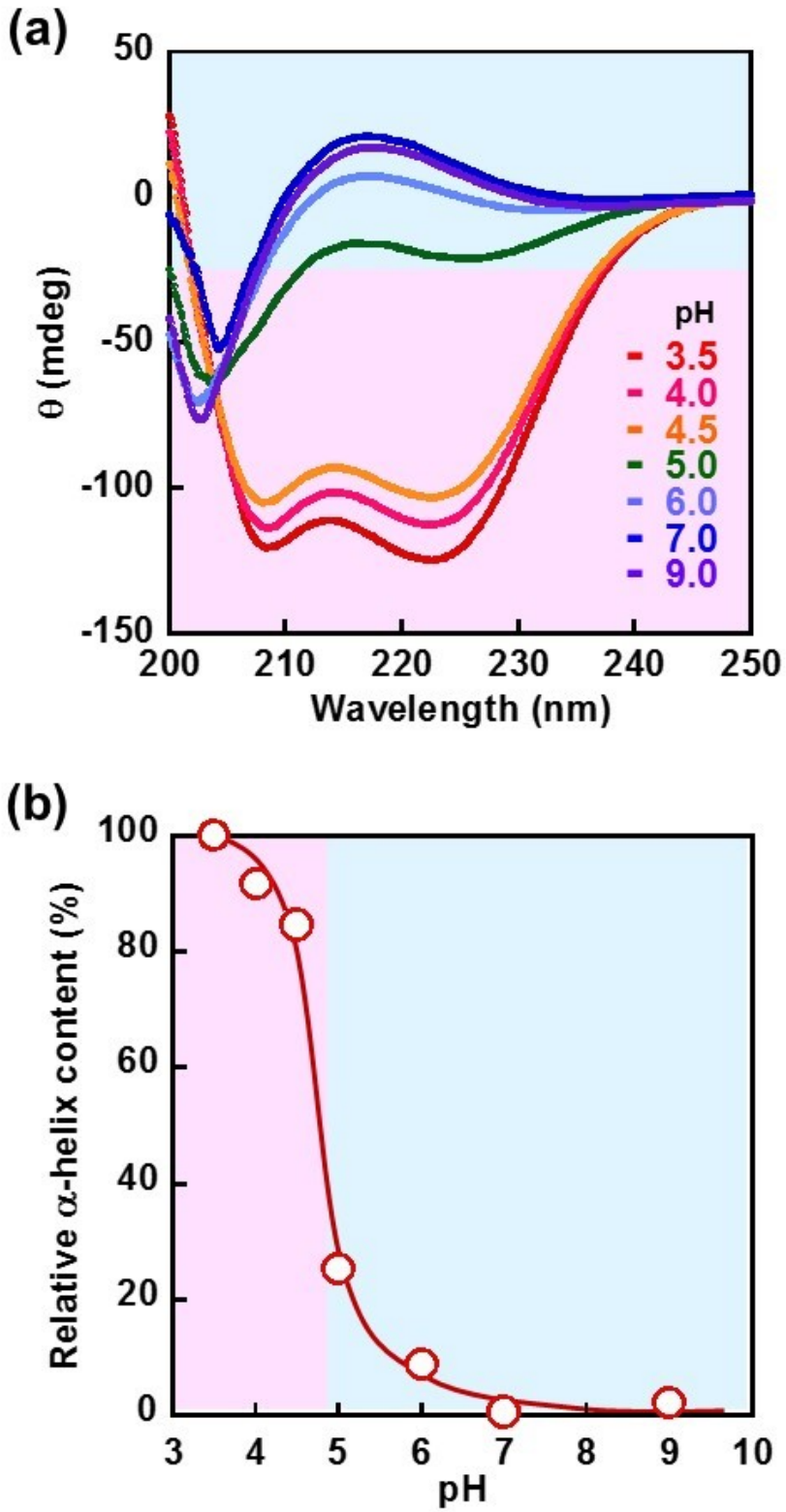

Figure 4-2. (a) Circular dichroism spectra of the CD-PGA hydrogel as a function of pHs. (b) Relationship between pH and relative α-helix content of the CD-PGA hydrogel in a buffer solution with various pHs.

4.3.3 Antioxidant agent release behavior from RSV-loaded CD-PGA hydrogel

To construct novel pH-responsive drug release systems, CDs as ligands for RSV were introduced into PGA, which undergoes a conformational change in response to a pH change. After the resulting CD-PGA formed a CD-RSV-CD complex with RSV in a buffer solution with pH 7, at which the PGA chains form a random coil structure, the BPA-loaded CD-PGA hydrogel with CDs was prepared by cross-linking CD-PGA with PEG-diamine. An important process for the RSV-loaded CD-PGA hydrogel is the complex formation between CD-PGA with a random coil structure and RSV before chemical cross-linking for the network formation.

The release profiles of RSV from the RSV-loaded CD-PGA hydrogels at various pHs are shown in Figure 4-3. The release of RSV from the RSV-loaded CD-PGA hydrogel was suppressed in a buffer solution with neutral pH because of the formation of stable CD-RSV-CD complexes within the hydrogel network designed by *pseudo* molecular imprinting. At acidic condition below pH 5, however, RSV was effectively released from the RSV-loaded CD-PGA hydrogel. The pH dependence of the α-helix content of the CD-PGA hydrogel demonstrates that the structural transition of the CD-PGA chains occurred around pH 5, at which the RSV release from the RSV-loaded CD-PGA hydrogel was drastically enhanced. Therefore, pH-responsive release of RSV is attributed to a destabilization of the CD-RSV-CD complexes by the structural transition of the PGA chains from the random coil to α-helix structure. Figure 4-3b shows the relationship between pH and swelling ratio of the CD-PGA hydrogel, which was determined from their diameters in CH_3COOH/CH_3COONa, NaH_2PO_4/Na_2HPO_4 or HEPES buffer solutions at various pHs, $(d/d_0)^3$. The ionic strength of all buffer solutions was adjusted at 0.5 M by NaCl due to the strong effects on the swelling ratios of polyelectrolyte hydrogels. After the swelling of the CD-PGA hydrogels attained equilibrium in a buffer solution at pH 7, changes in their swelling ratio were measured

in a buffer solution with various pHs. The swelling ratio of the CD-PGA hydrogel in a buffer solution at each pH was normalized by that at pH 7. The swelling ratio of the CD-PGA hydrogel decreased gradually with decreasing pH of a buffer solution. In general, drugs loaded within hydrogels are released by simple diffusion through the swollen network, meaning that drug release is strongly correlated with swelling ratio of hydrogels. In a buffer solution with a pH more than pH 5, the deprotonation of the carboxy groups of CD-PGA chains leads to an increase in the osmotic pressure of the hydrogel, followed by the swelling of the hydrogel network. However, the CD-PGA hydrogel exhibits great shrinkage in a buffer solution with a pH of less than pH 5 because the carboxy groups were protonated. In contrast to the pH-dependence of the swelling ratio, the relative amount of RSV released from the RSV-loaded CD-PGA hydrogel was reduced at pHs more than pH 6 but increased at pHs less than pH 5. It should be noted that the RSV-loaded CD-PGA hydrogels released RSV effectively in spite of their shrinkage with increasing pH. This means that the enhancement in the RSV release at pHs less than pH 5 was not based on the diffusivity of RSV in the hydrogel networks. In the RSV-loaded CD-PGA hydrogel prepared by *pseudo* molecular imprinting without the process for extracting the RSV template, CD ligands are arranged at optimal positions to form CD-RSV-CD complexes with RSV. Importantly, the CD-PGA network has a random coil structure when the CD-PGA chains are chemically crosslinked at pH 7. The stabilization of the CD-RSVA-CD complexes by *pseudo* molecular imprinting prevents RSV from being released from the CD-PGA hydrogel network with a random coil structure at pHs more than pH 6. At pHs less than pH 5, however, the stability of the CD-RSV-CD complexes becomes low because a structural transition of the CD-PGA hydrogel network from a random coil to α-helix structure induces a conformational change of the molecular recognition sites with well-arranged CD ligands for RSV. Therefore, the CD-PGA hydrogel network with random coil structures can retain RSV without leaking at pHs more than pH 6, but

the hydrogel network with the α-helix structure effectively releases it by lowering the stability of the CD-RSV-CD complexes in spite of its shrinkage at pHs less than pH 5. These results about the regulation of releasing RSV derived from the conformational change of the RSV-loaded CD-PGA hydrogel were similar to the results of BPA release from the BPA-loaded CD-PLL hydrogel as describe Chapter 3. In conclusion, release of RSV from the RSV-loaded CD-PGA hydrogel can be regulated by pH because a pH change induced the conformational change of its network with the recognition sites.

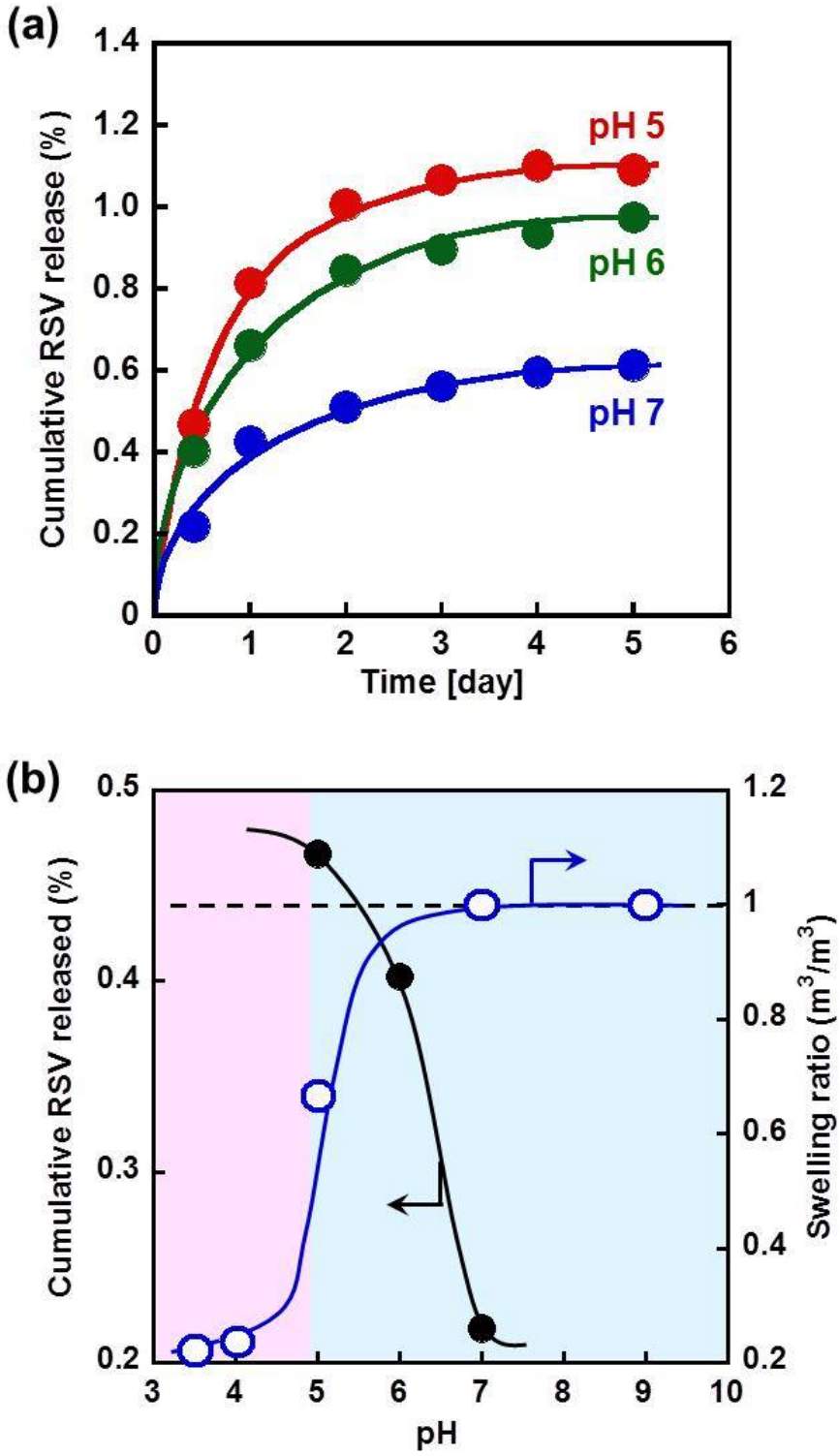

Figure 4-3. (a) Release profiles of RSV from the RSV-loaded CD-PGA hydrogel at pH 5 (●), 6 (●), and 7 (●). (b) Effect of pH on released RSV of the RSV-loaded CD-PGA hydrogel (●) and swelling ratio of CD-PGA hydrogel (○) in a buffer solution with various pHs.

4.4 Conclusions

The RSV-loaded CD-PGA hydrogels that can be prepared from the PGA with random coil structure by *pseudo* molecular imprinting have inclusion complex between CD and RSV. The resulting RSV-loaded CD-PGA hydrogels underwent changes in both the volume and the conformation in response to pH changes. The release of RSV from the RSV-loaded CD-PGA hydrogel was suppressed in a buffer solution with neutral pH because CD ligands are arranged at optimal positions for forming CD-RSV-CD complexes with RSV. With the structural transition of the PGA from the random coil to α-helix structure at slightly acidic condition, the stability of the inclusion complex between CD and RSV became low, followed by the releasing RSV from the RSV-loaded CD-PGA hydrogel. Therefore, the antioxidant agent-loaded PGA hydrogel that was prepared by *pseudo* molecular imprinting method regulated the antioxidant agent-release behavior depending on its conformation. Thus, we designed the drug-loaded CD-PGA hydrogel which regulated the drug release behavior as mimicking Bohr effect of protein. DTX that is a successful agent currently in use for the chemotherapy of cancer also forms a complex with two CD molecules as described in Chapter 3. Additionally, RSV has an ability to sensitize a synergistic cytotoxic activity of DTX in cancer cells. Therefore, the drug-loaded CD-PGA hydrogels that load both DTX and RSV by *pseudo* molecular imprinting method are likely to become promising DDS carriers for anticancer therapy.

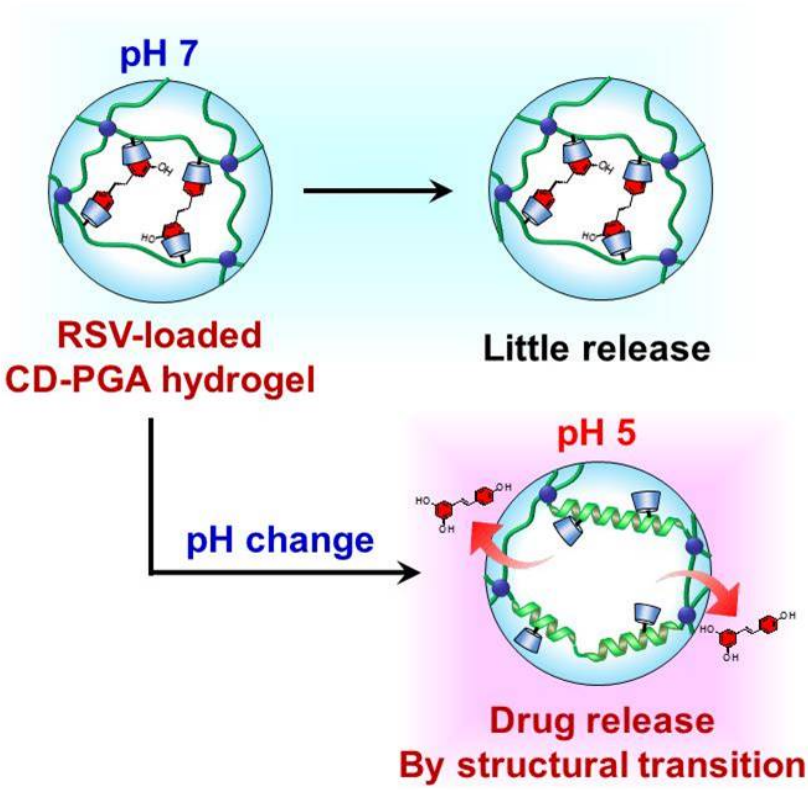

Figure 4-4. Schematic illustration for RSV release from the RSV-loaded CD-PGA hydrogel by its pH-responsive structural transition.

4.5 References

1. B. M. Babior, R. S. Kipnes, J. T. Curnutte, *J. Clin, Invest.*, **52**, 741-744, 1973.
2. J. T. Hancock, R. Desikan, S. J. Neill, Biochemical and Biomedical Aspects of Oxidative Modification, **29**, 345-350, 2001.
3. D. Trachootham, J. Alexandre, P. Huang, *Na.t Rev. Drug. Discov.*, **8**, 579–591, 2009.
4. J. K. Andersen, *Nat. Med.*, **10**, S18–S25, 2004.
5. V. Shukla, S. K. Mishra, H. C. Pant, *Adv. Pharmacol. Sci.*, **2011**, 572634, 2011.
6. T. M. Paravicini, R. M. Touyz, *Cardiovasc. Res.*, **71**, 247–258, 2006.
7. M. C. Haigis, B. A. Yankner, *Mol. Cell.*, **40**, 333–344, 2010.
8. L. Packer, *Annual Reviews of Nutrition*, **16**, 33-50, 1996.
9. C. E. Lister, *Leatherhead Food RA Food Industry Journal*, **2**, 251-264, 1999.
10. P. D. Ray, B. W. Huang, Y. Tsuji, *Cell Signal*, **24**, 981-990, 2012.
11. B. Halliwell, R. Asechbach, J. Loliger, O. I. Aruoma, *Food Chem. Toxicol.*, **33**, 601, 1995.
12. O. I. Aruoma, A. M. Murcia, J. Bitler, B. Halliwell, *J. Agric. Food. Chem.*, **41**, 1880-1885, 1993.
13. J. S. Wright, E. R. Johnson, G. A. DiLabio, *J. Am. Chem. Soc.*, **123**, 1173-1183, 2001.
14. P. Langcake, R. J. Pryce, *Physiol. Plant Pathol.*, **9**, 77-86, 1976.
15. J. Gusman, H. Malonne, G. Atassim, *Carclnogenests*, **22**, 1111-1117, 2001.
16. R. Lu, G. Serrero, *J. Cellular Physiol.*, **179**, 297-304, 1999.
17. S. H. Mitchell, W. Zhu, C. Y. F. Young, *Cancer Research*, **59**, 5892-5895, 1999.
18. C. R. Pace-Asciak, S. Hahn, E. P. Diamandis, G. Soleas, D. M. Goldberg, *Clinica Chimica Acta*, **235**, 207-219, 1995.
19. L. Frémont, *Life Science*, **66**, 663-673, 2000.
20. M. Jangm L. Gai, G. O. Udeani, K. V. Slowing, C. F. Thoms, C. W. W. Beecher, H. H. S. Fong, N. R. Farnsworth, A. D. Kinghorn, R. G. Mehta, R. C. Moon, J. M. Pezzuto, *Science*, **275**, 218-220,1997.
21. B. A. Narayanan, N. K. Narayanan, G. D. Stoner, B. P. Bullock, *Life Sciences*, **70**, 1821-1839, 2002.
22. C. Call, H. Garban, A. Jazirehi, C. Yeh, Y. Mizutani, B. Bonavida, *Curr. Med.*

Chem. Anti-Cancer Agents, **3**, 77-93, 2003.

23. M. Hesloms, J. E. Guillet, *J. Macromol. Sci. Chem.*, **A2**, 1441-1455, 1968.
24. K. Kataoka, G. S. Kwon, M. Yokohama, K. Okano, Y. Sakurai, *J. Control. Release*, **24**, 119-132, 1993.
25. S. W. Kim, Y. H. Bae, T. Okano, *Pharmaceutical Research*, **9**, 283-290, 1992.
26. M. Nagasawa, A. Holtzer, *J. Am. Chem. Sci.*, **86**, 538-543, 1964.
27. G. Ponchel, *Int. J. Pharm.*, **416**, 171-180, 2011.

Chapter 5

Preparation of Molecularly Imprinted Polypeptide Gel Layer for QCM Sensing

5.1 Introduction

BPA has been most commonly used as a monomer in manufacturing polycarbonate plastics and epoxy resins, which are extensively employed in various consumer goods and products. Despite its widespread use, many reports claim that BPA can leach out from plastic products such as food packaging materials and act as an endocrine disrupting chemical. Endocrine disrupting chemicals are exogenous agents that interfere with natural hormones of the body. These hormones are responsible for maintaining homeostasis and regulating developmental processes.[1] High blood levels of BPA are associated with reproduction dysfunction, endometrial hyperplasia, recurrent miscarriages, abnormal karyotypes and polycystic ovarian syndrome.[2-4] In general, gas chromatography and high-performance liquid chromatography have been used for the quantitative determination of BPA in environmental water and packaged food product samples. In particular, a uniquely sensitive sensor of BPA with a less invasive approach for evaluation in environmental and medical fields will be in considerable demand.

Molecularly imprinted polymers with molecular recognition abilities have been significant tools for the development of micro- and multi-analyte sensors.[5–10] The molecular imprinting technique is an effective and robust method for obtaining recognition elements for chemical and biological sensors because it involves the formation of shape-complementary cavities that re-capture the target analyte within the polymer networks. In standard molecular imprinting,[11–14] after prearrangement of ligand monomers around a template molecule (a target molecule) by their specific interaction, ligand monomers are copolymerized with a large number of cross-linkers. Then, molecularly imprinted polymers with molecular recognition sites are obtained by extracting the template molecule from the resulting networks. In molecular imprinting, various functional monomers with carboxy, amino and hydroxy groups have been used as ligand monomers that can form non-covalent hydrogen-bonding interactions with the template molecule. In addition, CDs which have an apolar cavity and a hydrophilic

exterior, have been reported to be useful ligands in designing molecularly imprinted polymers because they form inclusion complexes with a variety of guest molecules.[15] For example, molecularly imprinted polymeric receptors were prepared by cross-linking CD with a large amount of diisocyanate in the presence of various steroids as templates.[16] The significant binding activities and high selectivities of the CD-cross-linked polymeric receptors toward target steroids revealed that the CD ligands are very effective in molecular imprinting.

Stimuli-responsive hydrogels have attracted significant attention as smart soft materials because they can undergo reversible swelling/shrinking in response to external stimuli such as pH[17,18] and temperature.[19–21] Specifically, pH-responsive hydrogels that change their volume due to pH variation can be synthesized by introducing ionizable groups, such as carboxy and amino groups, into the polymer networks. Such stimuli-responsive hydrogels have been investigated for many biomedical uses including sensor systems, drug delivery carriers and actuators.[22–26] Taking advantage of these desirable properties, we functionalized stimuli-responsive hydrogels with biomolecular recognition abilities based on a novel strategy that uses biomolecular complexes as reversible cross-links of their networks.[27–30] Biomolecule-responsive hydrogels, which are designed using this strategy, change their volume in response to target biomolecules such as glucose, enzymes and antigens. Furthermore, the arrangement of ligands within hydrogel networks via molecular imprinting enabled us to prepare biomolecule-responsive hydrogels with molecular recognition sites that can shrink gradually according to the target molecule concentration. Our technique differs from the standard molecular imprinting approach. Specifically, we designed molecularly imprinted hydrogels that shrink by forming complexes between ligands and target molecules using minute amounts of cross-linkers. For example, BPA-imprinted hydrogels that undergo changes in volume in response to BPA were strategically prepared using molecular imprinting that used CDs as ligands for BPA and minute

amounts of cross-linkers.[31] BPA-imprinted hydrogels exhibited a significant shrinkage in the presence of BPA as the formation of an inclusion complex of BPA with two CDs resulted in a cross-linking density increase. Such molecularly imprinted hydrogels with molecular recognition sites can provide useful applications for molecular sensors, separation technology and DDS carriers. Recently, we designed stimuli-responsive hydrogels using polypeptides, such as PLL, as the main chain of a hydrogel network. We used polypeptides because of their well-defined structures and useful functional groups.[32] Previous studies on stimuli-responsive polypeptide hydrogels revealed that polypeptides have high potential as main chains for designing molecularly imprinted hydrogels.

The formation of polymer films with molecular recognition sites on sensor chips is the most important step in fabricating sensors with high sensitivity and selectivity. In general, polymer films are prepared via solvent casting, polymer grafting and vapor deposition.[33,34] Among these methods, electropolymerization is a unique technique for preparing thin polymer films via in situ polymerization from an electrode surface because the thickness, surface growth and morphology can be easily controlled by varying different process parameters (for example, scan rate and potential window).[35,36] π-Conjugated or electrically conducting polymers, whose thin films can be easily formed using electropolymerization, have been investigated as sensors,[37] electro-optical materials[38] and semiconducting devices.[39] In general, electropolymerizable monomers, such as thiophene, aniline, pyrrole and carbazole, have been widely used to form π-conjugated or electrically conducting polymer films in electro-optical applications.[40] For example, electropolymerization of terthiophene leads to the formation of highly electrochromic and conducting polythiophenes.[41–43] The mechanism is based on a radical cation coupling that can be accessed using potentiodynamic or potentiostatic methods. Conjugated polymer films that are prepared via surface modification of conducting films with functional polymers provide several opportunities for taking

advantage of the properties of both polymers.

In this study, we prepared BPA-imprinted polypeptide gel layers on a conducting polymer via chemical cross-linking of CD-PLL and investigated their molecular recognition behaviors. This paper focuses on the preparation of BPA-imprinted CD-PLL gel layers on polyterthiophene modified quartz crystal microbalance (QCM) sensor chips. Electrochemical QCM (EQCM) was used to probe in situ electropolymerization of polyterthiophene on the Au-electrode surface. The BPA-imprinted CD-PLL gel layers were strategically prepared via molecular imprinting using CD as a ligand on a polyterthiophene surface that was produced using electropolymerization. The resulting polymer thin films were characterized using atomic force microscopy (AFM), Fourier transform infrared reflection absorption spectrometry (FT-IR-RAS), ellipsometry and static water contact angle measurements. The sensitivity and selectivity of BPA-imprinted CD-PLL gel layers for BPA were evaluated using the QCM technique, which has been used to detect nanomolar to micromolar masses. This paper demonstrates that the combination of QCM and molecular imprinting enables us to fabricate highly selective and sensitive sensor devices with commercialization potential.

5.2 Experimental

5.2.1 Materials

PLL hydrobromide (12,000 MWCO) and EGDE were purchased from Peptide Ins. Co. Ltd (Osaka, Japan) and Tokyo Chemical Ind. Co. Ltd (Tokyo, Japan), respectively. All aqueous solutions were prepared with ultra-pure water (Milli-Q, 18.2 MΩ cm). The other solvents and reagents were of analytical grade, were obtained from commercial sources and were used without further purification.

5.2.2 Synthesis of carboxy-CD

The carboxy-CD was synthesized by the same procedure as described in Chapter 3.

5.2.3 Introduction of CD to PLL

The CD-PLL was synthesized by the same procedure as described in Chapter 3.

5.2.4 Preparation of poly(G03T-COOH) films

After 2-(2,5-di(thiophen-2-yl)thiophen-3-yl)acetic acid (G03T-COOH) was synthesized using a previously described method,[42] its electropolymerization was performed on a QCM sensor chip via cyclic voltammetry (CV) in acetonitrile with 0.1 M tetrabutylammonium hexafluorophosphate. Polyterthiophene-carboxylic acid films, poly(G03T-COOH), were prepared via electropolymerization of G03T-COOH using EQCM (Q-Sense E4 and E1, Molecularly imprinted polypeptide layers on QCM chips Meiwa Fosis Co. Ltd, Tokyo, Japan). An AT-cut polished QCM sensor chip (4.95 MHz) with a 14-mm diameter, a Ag/AgCl electrode (Dri-Ref, World Precision

Instrument Inc., Sarasota, FL, USA) and a Pt sheet were used as a working electrode, a reference electrode and a counter electrode, respectively. QCM crystals were cleaned in a Piranha solution (a mixture of 98% H_2SO_4 and 30% H_2O_2, 3:1 v/v) at 70 °C for 5 min, rinsed with ultra-pure water and dried under nitrogen flow. The QCM sensor chips were cleaned using a ultraviolet ozone cleaner (BioForce Nanoscience, Inc., Ames, IA, USA) for 10 min before use. The poly(G03T-COOH) films were formed by scanning the potential between 0 and 1100 mV at a scan rate of 100 mV s^{-1} for 40 cycles using CV techniques. Mass changes on the QCM sensor chips were monitored using EQCM to in situ evaluate oxidation/reduction during the electrochemical processes. Electropolymerization of conducting monomers was confirmed by increasing reduction-oxidation (redox) peaks (~1.0 V) of poly(G03T-COOH) while the potential was swept from 0 to 1100 mV from cycle 1 to 10.

5.2.5 Preparation of BPA-imprinted CD-PLL gel layers

The BPA-imprinted CD-PLL gel layers were prepared using the method shown in Scheme 5-1. First, EDC (1.0 g, 5.22 mmol) and NHS (1.0 g, 8.69 mmol) were dissolved in 20 ml of ultra-pure water. Then, to activate carboxy groups on the surface of poly(G03T-COOH) films, the poly(G03T-COOH) films were immersed in the EDC/NHS solution for 1 h at room temperature. The films were rinsed with ultra-pure water and dried with a nitrogen flow. To form the CD-BPA-CD complexes, CD-PLL (100 mg) and BPA were dissolved in 10 ml of ultra-pure water and stirred for 24 h at room temperature. By immersing the activated poly(G03T-COOH) films in the resultant CD-PLL solution for 2 h, CD-PLL chains that form complexes with BPA were grafted onto the film surfaces, and COOH was activated with NHS. Then, the resultant CD-PLL gel layers were cross-linked via immersion in water that contained ethylene glycol diglycidyl ether (10 wt%) for 24 h at 35 °C in the presence of template BPA.

BPA-imprinted CD-PLL gel layers were obtained by extracting the template BPA from the films using a water/acetone (70/30) mixture. Furthermore, non-imprinted CD-PLL gel layers were prepared by cross-linking CD-PLL gel layers in a similar manner without the template BPA. To prepare a reference sensor chip, CD was directly immobilized on a sensor chip using a standard amino coupling method without using poly(G03T-COOH) and CD-PLL. First, to introduce carboxy groups onto a QCM sensor chip, the chip was immersed in ethanol that contained containing 5 mM 3, 3'-dithiopropionic acid. Then, the sensor chip was washed with ethanol. Carboxy groups, which were introduced on the sensor chip, were activated with EDC (1.0 g) and NHS (1.0 g) in 20 ml of ultra-pure water for 1 h. After washing with water, the surface-activated sensor chip was immersed in 10 mg ml^{-1} of water that contained NH2-CD to obtain the directly CD-immobilized sensor chip.

5.2.6 Characterizations of gel layers on QCM sensor chips

The BPA-imprinted and non-imprinted CD-PLL gel layers were characterized using FT-IR-ATR, AFM and ellipsometry. FT-IR-RAS measurements were performed using a Spectrum 100 spectrometer (Perkin Elmer, Waltham, MA, USA) equipped with Refractor 2 (Harrick Scientific Inc., Pleasantville, NY, USA) with a single Brewster's angle silicon polarizer plate (grazing angle, 75°) and a liquid nitrogen-cooled MCT (Mercury–Cadmium–Telluride) detector (Perkin Elmer, Waltham, MA, USA). The spectra were referenced to a bare gold chip spectrum. All FT-IR-RAS measurements were performed at room temperature under dried air. In addition, the surface structure of BPA-imprinted CD-PLL gel layers was observed with AFM in the tapping mode using SPI3800/SPA400 (SII nanotechnology, Tokyo, Japan) by taking 256 points in a 5000× 5000 nm area with a 0.1 Hz scan rate at room temperature. The thickness of electropolymerized films on QCM sensor chips was determined using an M-2000

ellipsometer (JA Woollam Co., Lincoln, NE, USA) equipped with a laser with 250-1000 nm wavelengths (at 70°, 75° and 80° angle of incidence).

5.2.7 QCM measurements

The adsorption of BPA, bisphenol E (BPE, 4,4'-ethylidenebisphenol) and bisphenol F (BPF, 4,4'-methylenebisphenol) into the BPA-imprinted and nonimprinted CD-PLL gel layers was evaluated with in situ QCM-D (model E1, Q-sense, Meiwa Fosis Co., Ltd, Tokyo, Japan). The changes in frequency and dissipation were monitored during the ultra-pure water flow. After the baseline was established, an aqueous solution of 400 μM BPA, BPE or BPF was flown over the QCM sensors at a flow rate of 50 μl min^{-1} at 25 °C for 80 min. The frequency of the third overtone (F3) and dissipation (D3) was recorded. The subsequent changes in frequency were used to calculate the mass change due to BPA adsorption onto the film using the Sauerbrey equation.[48]

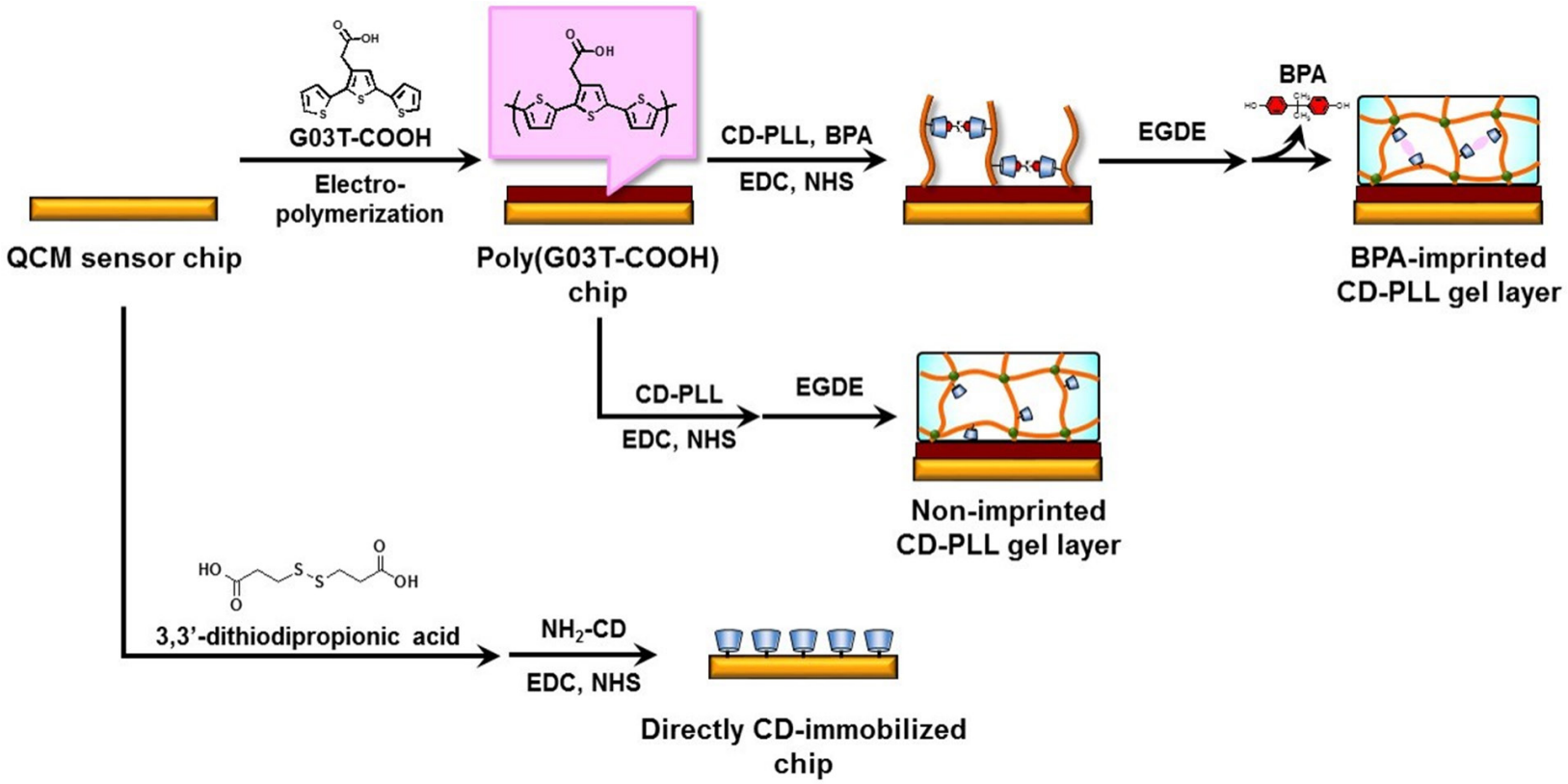

Scheme 5-1. Preparation of the BPA-imprinted CD-PLL gel layer chip, non-imprinted CD-PLL gel layer chip, and directly CD-immobilized chip.

5.3 Results and Discussion

5.3.1 Characterizations of poly(G03T-COOH) films

Cyclic voltammogram of 10mM G03T-COOH on QCM sensor chips in acetonitrile with 0.1 M tetrabutylammonium hexafluorophosphate is shown in Figure 5-1a. In the first cycle, the onset of the first anodic peak assigned as the oxidation of terthiophene pendant groups was observed at E_{pa} 1.05 V versus Ag/AgCl as a reference electrode. A cathodic peak was observed at 0.75 V versus Ag/AgCl. The oxidation and reduction peak currents increased gradually as the number of cyclic scans changed, which suggested a stepwise polyterthiophene film growth. Furthermore, the oxidation peak potential shifts in anodic direction and the reduction peak potential shifts in cathodic direction were observed on subsequent CV cycles.

The combination of CV with QCM allows us to monitor in situ the polymerization of G03T-COOH on QCM sensor chips through changes in the resonant frequency of the quartz crystal electrode. The negative value of the frequency change (ΔF) in Figure 5-1b denotes that G03T-COOH was adsorbed onto the QCM crystal by electropolymerization and that the thickness of the formed film increased with CV cycles. QCM measurements revealed that ΔF and the energy dissipation factor (ΔD) were shifted during the oxidation and reduction process. From both the QCM microgram and the CV diagram, we concluded that G03T-COOH was deposited to form a poly(G03T-COOH) film on a gold sensor chip. The thickness of the poly(G03T-COOH) film formed on the QCM sensor chip via electropolymerization was measured using ellipsometry. The poly(G03T-COOH) film prepared using CV (40 cycles) had an average thickness of 14.1 nm. This means that a single CV scan resulted in the formation of a poly(G03T-COOH) film with an average thickness of 0.35 nm, which is equal to the theoretical molecular thickness of G03T-COOH (~0.39 nm). Considering the strong interactions between sulfur moieties of the polyterthiophene

backbone and the gold substrate, the closely related theoretical and experimental values suggest that a monolayer of poly(G03T-COOH) deposits on the gold substrate after each CV scan. Therefore, electropolymerization of G03T-COOH using CV enables us to form poly(G03T-COOH) films with a controlled thickness and to easily introduce functional carboxy groups onto QCM sensor chips. The modified QCM sensor chips with carboxy groups are very useful in fabricating highly sensitive QCM sensor chips with various ligands for a target molecule.

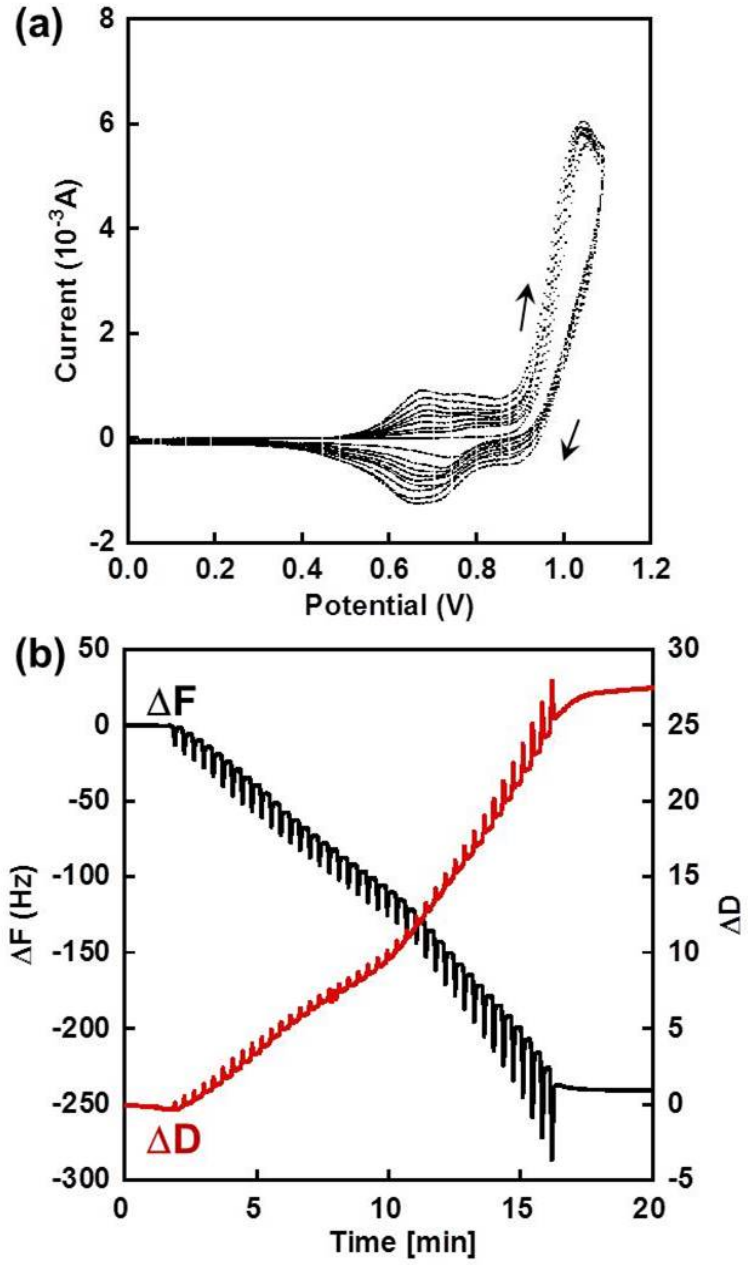

Figure 5-1. Cyclic voltammogram (a) and QCM response (b) of 03T-COOH on a QCM sensor chip in acetonitrile with 0.1 M tetrabutylammonium hexafluorophosphate. The concentration of G03T-COOH in acetonitrile was 10 mM. Electropolymerization of G03T-COOH was performed by sweeping the potential from 0 to 1100 mV vs the Ag/AgCl reference electrode.

5.3.2 Characterization of BPA-imprinted CD-PLL gel layers

In this study, BPA was chosen as a target molecule because it has high possibility of exhibiting endocrine disrupting chemical behavior. The QCM technique is a powerful tool for detecting minute amounts of target biomolecules such as DNAs and proteins. However, QCM has a disadvantage in detecting small molecules with a very low molecular weight. Our strategy for detecting a small molecule, such as BPA, is to form molecularly imprinted gel layers on QCM sensor chips. In this study, CD-PLL was used to form BPA-imprinted gel layers on QCM sensor chips because amino groups of PLL can easily react with carboxy groups of poly(G03T-COOH) films on QCM sensor chips. After the complex formation between CD-PLL and BPA, CD-PLL was grafted onto the poly(G03T-COOH) films of QCM sensor chips. Then, the BPA-imprinted CD-PLL gel layers were obtained by extracting template BPA from the CD-PLL gel layers. To extract BPA from the layers, the resulting sensor chips were immersed in a water/acetone mixture with an acetone concentration of 30 vol%. The resultant BPA-imprinted CD-PLL gel layers were characterized using static water contact angle measurements, FT-IR-RAS spectroscopy, AFM and ellipsomery.

The water contact angles on a bare Au QCM sensor chip and a poly (G03T-COOH) film were found to be 46.3° and 69.1°, respectively. After the formation of a BPA-imprinted CD-PLL gel layer on a poly(G03T-COOH) film on a QCM sensor chip, the water contact angle decreased from 69.1° to 35.8°. The decrease in water contact angle implies that a hydrophilic CD-PLL gel layer was formed on a less hydrophilic poly(G03T-COOH) film by the reaction of CD-PLL with poly(G03T-COOH) in molecular imprinting. Figure 5-2 shows the FT-IR-RAS spectra of the poly(G03T-COOH) film and BPAimprinted CD-PLL gel layer. The poly(G03T-COOH) film FT-IR spectrum displays a peak at ~ 1200 cm^{-1}, which is assigned to the C–C stretching vibration, and peaks at 1456 cm^{-1} and 1510 cm^{-1}, which are assigned to the C=C stretching vibration bands of thiophene rings. Another strong

peak at 1715 cm^{-1} was assigned to the carbonyl stretch vibration. In the spectrum of BPA-imprinted CD-PLL gel layer, there were strong absorption bands at 1540 cm^{-1} and 1650 cm^{-1} that corresponded to amide bonds of PLL. In addition, the surface structure of BPA-imprinted CD-PLL gel layer was observed with AFM in the tapping mode at room temperature. Figure 5-3 shows AFM images of the bare QCM sensor chip, the poly(G03T-COOH) film and the BPA-imprinted CD-PLL gel layer. The AFM observation revealed that the poly(G03T-COOH) film and the BPA-imprinted CD-PLL gel layer with a large surface area were formed on the QCM sensor chip that was functionalized using electropolymerization of terthiophene. Ellipsometry revealed that the thicknesses of BPA-imprinted CD-PLL gel layer and non-imprinted CD-PLL gel layer on the QCM sensor chip were 15.7 and 19.5 nm, respectively. The fact that the thickness of BPA-imprinted CD-PLL gel layer was approximately the same as that of non-imprinted CD-PLL gel layer implies that the same amount of CD-PLL was immobilized on the QCM sensor chips. Thus, we can design the BPA-imprinted CD-PLL gel layers in which CD ligands for the target BPA were arranged at optimal positions to form CD-BPA-CD complexes via molecular imprinting. The next section focuses on the BPA adsorption behavior of BPA-imprinted CD-PLL gel layers on QCM sensor chips.

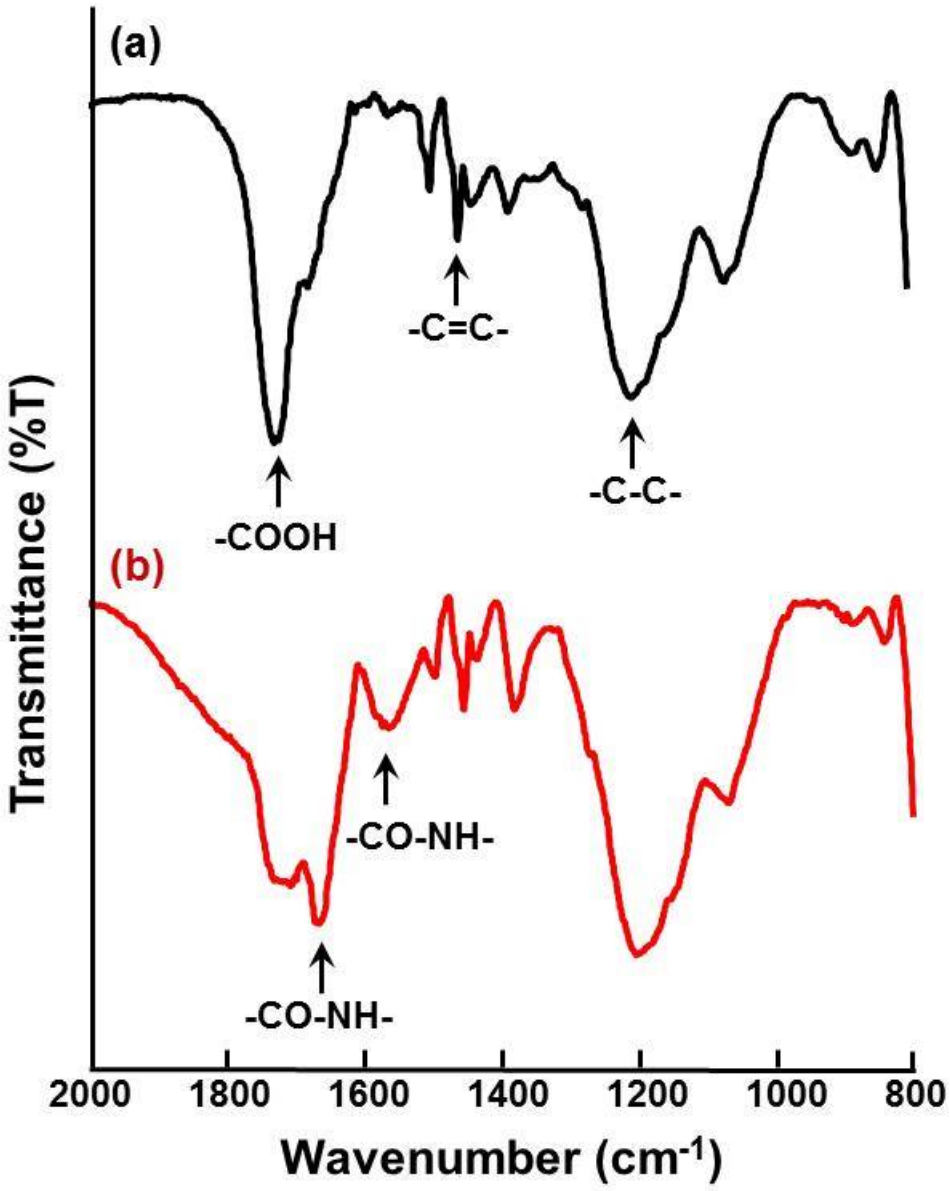

Figure 5-2. FT-IR-RAS spectra of a poly(G03T-COOH) film (a) and a BPA-imprinted CD-PLL gel layer (b).

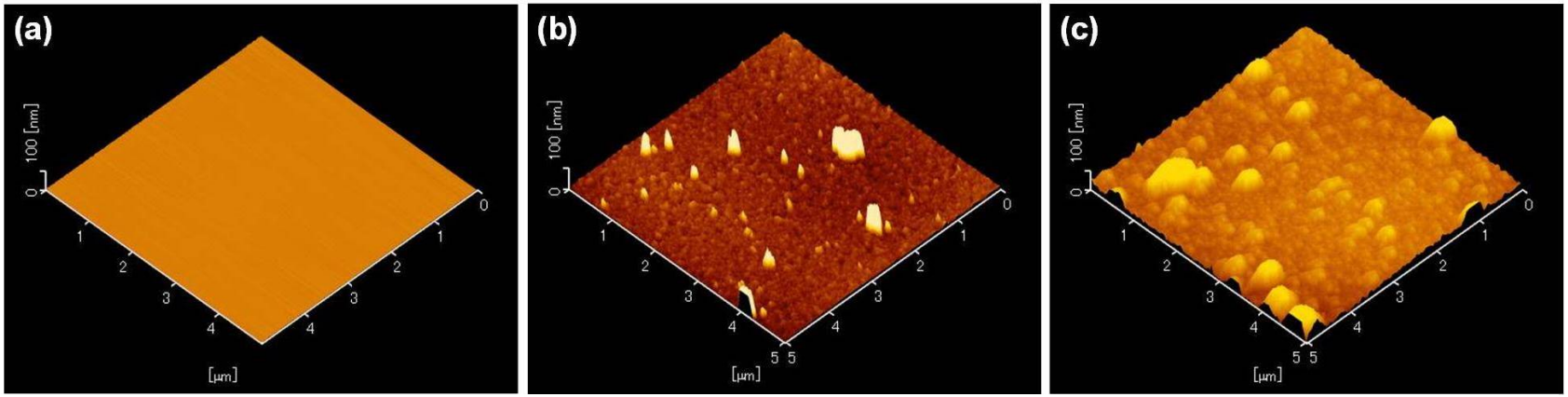

Figure 5-3. AFM images of a bare QCM sensor chip (a), a poly(G03T-COOH) film (b) and a BPA-imprinted CD-PLL gel layer (c).

5.3.3 BPA recognition behavior of BPA-imprinted CD-PLL gel layers

QCM is a powerful tool for monitoring molecular recognition events such as binding of lectins with carbohydrate and formation of DNA duplexes. In QCM techniques, molecular recognition events are monitored by weight changes that are induced by the adsorption of target biomolecules onto QCM sensor chips. Therefore, QCM has disadvantages in detecting a small molecule with a low molecular weight such as BPA. The BPA-imprinted CD-PLL gel layers on QCM sensor chips are expected to have many capacities for BPA adsorption because molecular recognition sites for a target BPA are effectively formed within PLL hydrogel networks by molecular imprinting using CDs as ligands. Therefore, BPA-imprinted CD-PLL gel layers on QCM sensor chips have a high possibility in detecting BPA even though BPA has a low molecular weight of 228 g mol^{-1}. In this study, the adsorption behavior of BPA into BPA-imprinted CD-PLL gel layers was evaluated using in situ QCM-D measurements.

Figure 5-4 demonstrates QCM micrograms of a BPA-imprinted CD-PLL gel layer chip, a non-imprinted CD-PLL gel layer chip, a directly CD-immobilized chip and a bare chip in water that contained target BPA. The QCM measurements revealed that ΔF of the BPA-imprinted CD-PLL gel layer chip decreased more than that of the non-imprinted CD-PLL gel layer chip that was prepared without a template BPA and the directly CD-immobilized chip. A larger decrease in ΔF of the BPA-imprinted CD-PLL gel layer chip suggests that BPA-recognition sites were created via molecular imprinting using CD ligands. The ΔF decrease of BPA-imprinted CD-PLL gel layer chip and non-imprinted CD-PLL gel layer chip corresponds to a mass gain of 205.8 ng cm^{-2} and 30.8 ng cm^{-2}, respectively. This is attributed to the fact that molecular imprinting enabled CD ligands to be arranged at optimal positions for binding the target BPA even though our molecular imprinting used minute amounts of cross-linkers to form the gel layer (Figure 5-5). Furthermore, the sensitivity of QCM sensor chips may

be improved by the large surface area of poly(G03T-COOH) films prepared via electropolymerization of terthiophene.

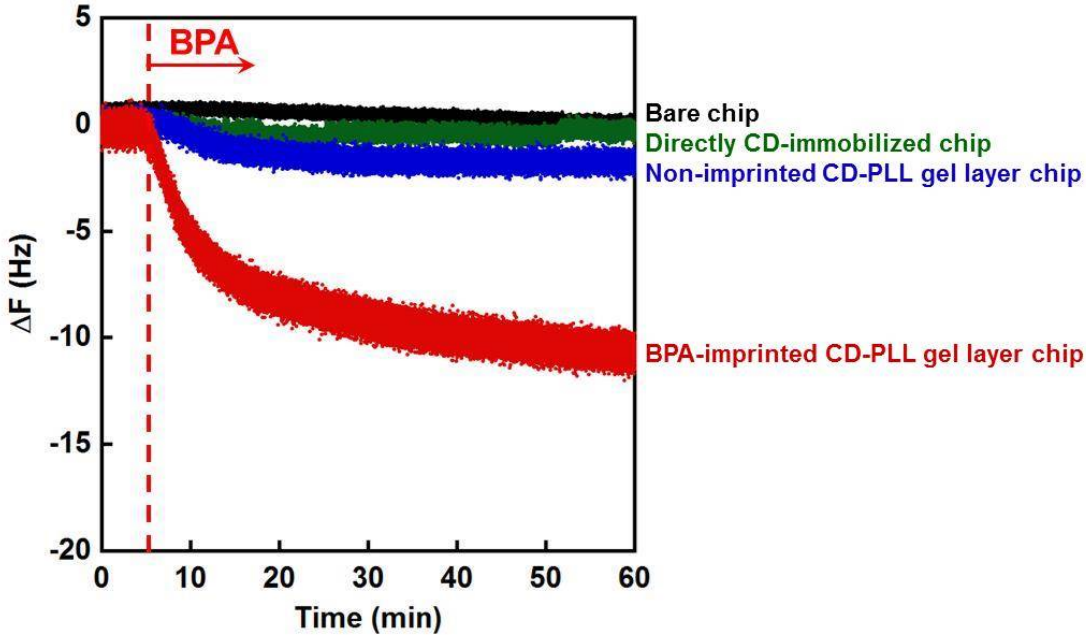

Figure 5-4. QCM responses of a BPA-imprinted CD-PLL gel layer chip, a non-imprinted CD-PLL gel layer chip, a directly CD-immobilized chip and a bare chip after the injection of an aqueous 400 μM BPA solution.

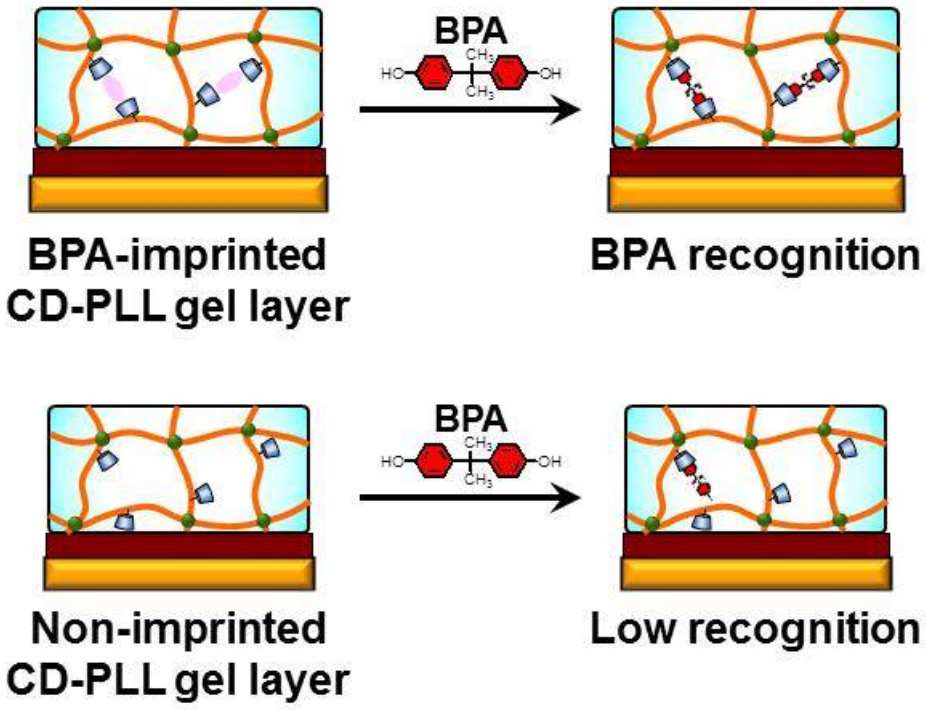

Figure 5-5. Schematic illustration of BPA recognition of the BPA-imprinted CD-PLL gel layer and the non-imprinted CD-PLL gel layer.

The sensitivity of BPA-imprinted CD-PLL gel layer on a QCM sensor chip was investigated by measuring ΔF as a function of BPA concentration (Figure 5-6). In an aqueous solution with a BPA concentration of <400 μM, ΔF of the BPA-imprinted CD-PLL gel layer chip gradually increased with increasing BPA concentration in water. A calibration plot showing linearity between the BPA concentration and ΔF in the concentration range between 0 and 400 μM was obtained using the Pearson's correlation R^2 value of 0.9782. The limit of detection (equal to (3 ρ/m)) and the limit of quantification (equal to (10 ρ/m)) in quantitative determination of BPA are 24.499 and 81.664 μM, respectively, where ρ is the standard deviation and m is the calibration curve slope. These values suggest that the BPA-imprinted CD-PLL gel layer chip is applicable to a QCM sensor device for detecting BPA in water. Notably, the BPA-imprinted CD-PLL gel layer chip exhibited ~ 7 times greater ΔF than the

non-imprinted CD-PLL gel layer chip. Furthermore, in an aqueous solution with <200 μM BPA, ΔF of the non-imprinted CD-PLL gel layer chip became constant, which is different from the BPA-imprinted CD-PLL gel layer chip. This finding implies that the BPA-imprinted CD-PLL gel layer has a large molecular recognition capacity than the non-imprinted gel layer. The greater sensitivity of the BPAimprinted CD-PLL gel layer chip is attributed to the formation of BPA-recognition sites within its gel layer via molecular imprinting using the CD ligands. In addition, in our previous paper, we reported that BPA-imprinted bulk hydrogels that were prepared using poly(acrylamide) as the main chain exhibited a significant shrinkage in response to the target BPA.31 In BPA-imprinted bulk hydrogels, the BPA-recognition sites were formed via the optimal arrangement of ligand CDs. Therefore, the target BPA was preferentially absorbed into BPA-imprinted bulk hydrogels, which is similar to the BPA-imprinted CD-PLL gel layers on QCM sensor chips reported in this paper. However, BPA adsorption onto BPA-imprinted bulk hydrogels required a large amount of an aqueous BPA solution and several hours to attain equilibrium. In contrast, the BPA-imprinted CD-PLL gel layers on QCM sensor chips could rapidly detect the target BPA with a small amount of an aqueous BPA solution. Thus, the BPA-imprinted CD-PLL gel layers on QCM sensor chips provide useful platforms to fabricate molecular sensors that enable us to monitor BPA in aqueous solutions.

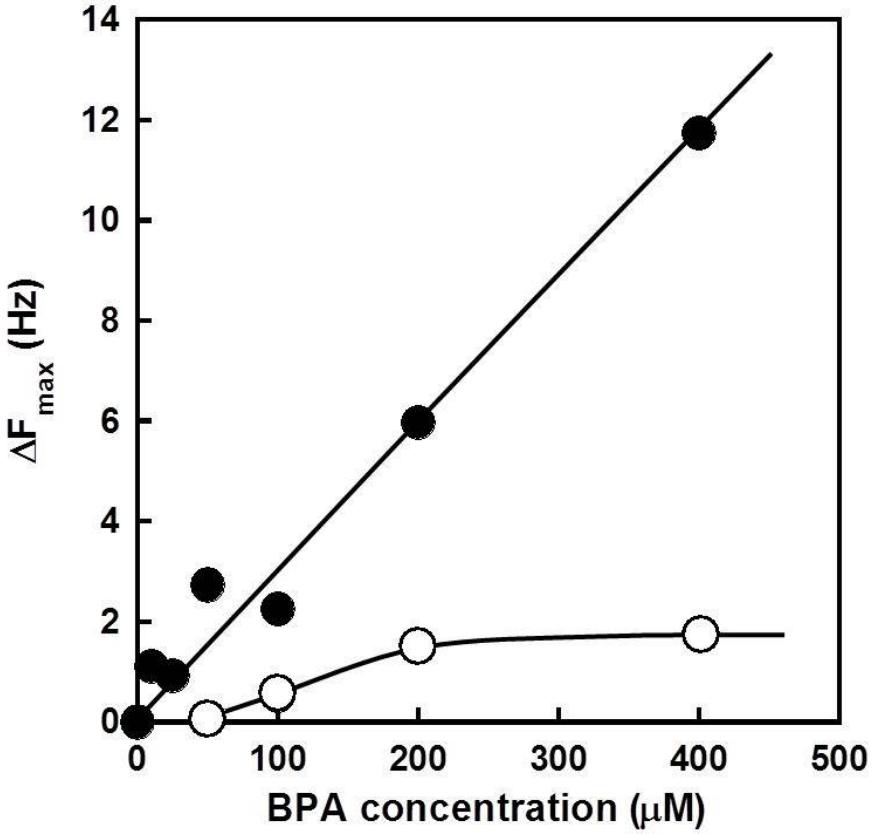

Figure 5-6. Relationship between BPA concentration in water and QCM responses of the BPA-imprinted CD-PLL gel layer chip (●) and non-imprinted CD-PLL gel layer chip (○) after the injection of an aqueous BPA solution.

Molecular imprinting enables ligands to be arranged at optimal positions for a target molecule, followed by the formation of complementary cavities as molecular recognition sites. Standard molecular imprinting requires a large amount of cross-linkers to fix ligands at the optimal positions. However, because the BPA-imprinted CD-PLL gel layers on QCM sensor chips were weakly cross-linked using minute amounts of cross-linkers, they had flexible molecular recognition sites. We investigated the molecular recognition ability of BPA-imprinted CD-PLL gel layers by measuring ΔF in an aqueous solution containing BPE and F (BPF) that have similar structures to BPA. QCM responses of the BPA-imprinted and non-imprinted CD-PLL gel layer chips toward the injection of BPA, BPE and BPF are shown in Figure 5-7. The BPA-imprinted CD-PLL gel layer chip exhibited a much greater ΔF than the non-imprinted CD-PLL gel layer chip in response to BPA, BPE and BPF. Because CD ligands in the BPA-imprinted CD-PLL gel layer were arranged at optimal positions for simultaneously binding two aromatic groups of BPA via molecular imprinting, the recognition sites that were formed using the template BPA also bonded BPE and BPF effectively. Thus, BPA and its derivatives were more efficiently adsorbed into the BPA-imprinted CD-PLL gel layer than into the non-imprinted CD-PLL gel layer. Notably, ΔF of the BPA-imprinted CD-PLL gel layer chip for BPA was greater than that for BPE and BPF, even though the molecular structures of BPE and BPF are similar to that of BPA. We designed the BPA-imprinted CD-PLL gel layer chip via molecular imprinting using a minute amount of cross-linkers, which is differing from a standard molecular imprinting that requires a large amount of cross-linkers. The fact that BPA was more efficiently adsorbed into the BPA-imprinted CD-PLL gel layer than BPE and BPF reveals that the recognition sites formed by molecular imprinting can recognize a small difference between BPA and BPE/BPF. This may be attributed to the molecular recognition ability of CDs and to the important role of amino groups of PLL main chains. The high recognition ability and multiple interactions in molecular imprinting

enable the resulting gel layers to recognize target molecules selectively and sensitively despite weak cross-linking. Although further research is required to clarify the molecular recognition behavior of BPA-imprinted CD-PLL gel layers, the molecularly imprinted gel layers that are weakly cross-linked on QCM sensor chips are likely to become promising sensor chips for monitoring small amounts of BPA and its derivatives slightly in aqueous solutions. Molecular imprinting using PLL and minute amount of cross-linkers will contribute significantly to the fabrication of highly sensitive and selective QCM sensor systems.

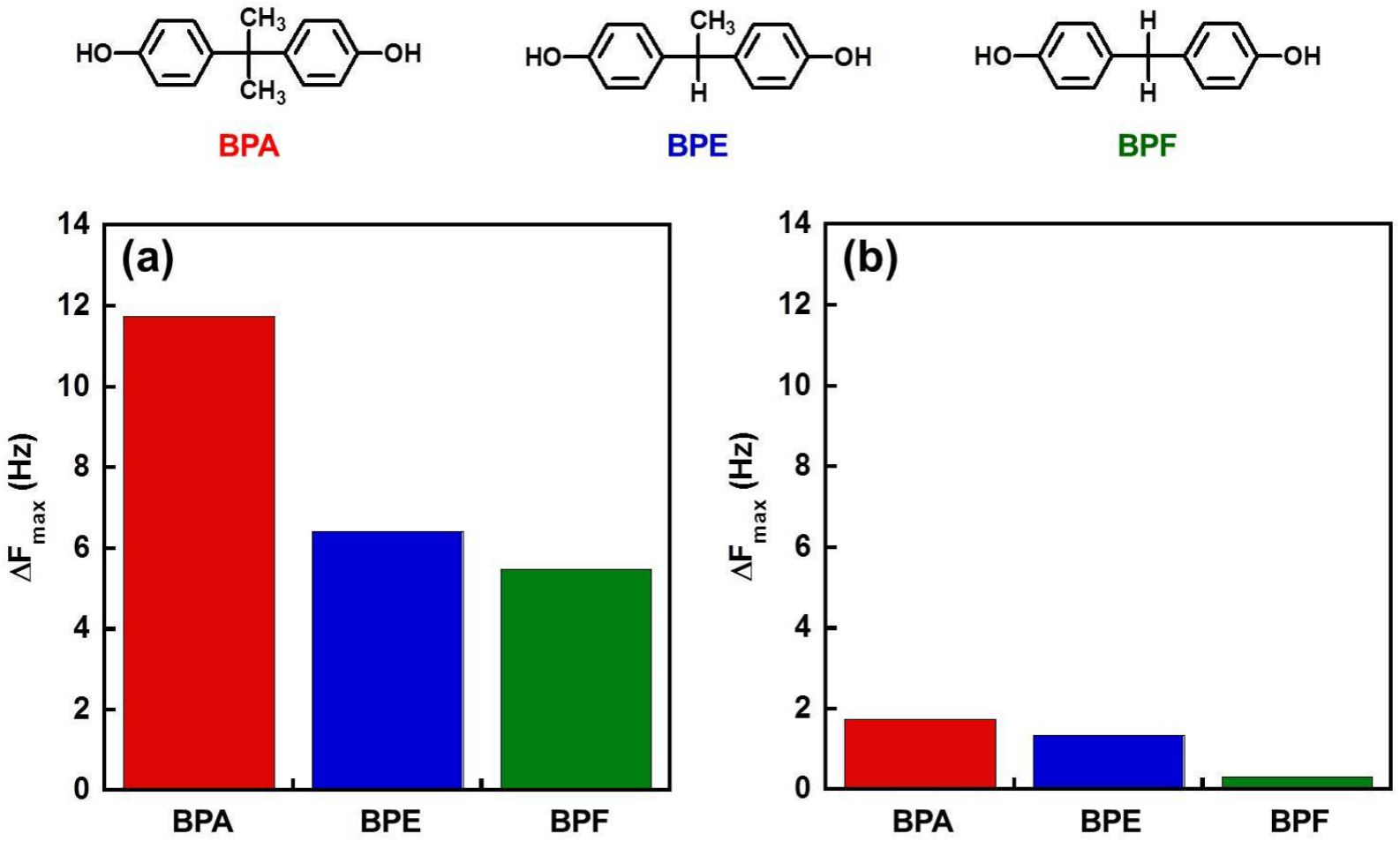

Figure 5-7. QCM responses of the BPA-imprinted CD-PLL gel layer chip (a) and non-imprinted CD-PLL gel layer chi after the injection of an aqueous solution of 400 mM BPA, BPE and BPF.

5.4 Conclusions

This paper describes the preparation of molecularly imprinted polypeptide gel layers with molecular recognition sites on QCM sensor chips by combining electropolymerization with molecular imprinting. Electropolymerization of G03T-COOH was performed to form poly(G03T-COOH) films on QCM sensor chips. The process was monitored using in situ EQCM measurements. The BPA-imprinted CD-PLL gel layers with molecular recognition sites were prepared on the poly(G03T-COOH) films of QCM sensor chips via chemical cross-linking of PLL and molecular imprinting that used CDs as ligands for the template BPA. In QCM measurements, the BPA-imprinted CD-PLL gel layer chip showed a greater ΔF in response to BPA than the non-imprinted CD-PLL gel layer chip and the directly CD-immobilized chip. This is attributed to a large surface area produced by electropolymerization and the arrangement of CD ligands at optimal positions for forming CD-BPA-CD complexes via molecular imprinting. The QCM microgram demonstrated a very good linear relationship between the BPA concentration and ΔF in the concentration range between 0 and 400 μM. The BPA-imprinted CD-PLL gel layers that are weakly cross-linked on QCM sensor chips are likely to become promising sensor chips for monitoring BPA and its derivatives with small amounts in aqueous solutions.

5.5 References

1. R. J. Kavlock, G. P. Daston, C. DeRosa, P. Fenner-Crisp, L. E. Gray, S. Kaattari, G. Lucier, M. Luster, M. J. Mac, C. Maczka, R. Miller, J. Moore, R. Rolland, G. Scott, D. M. Sheehan, T. Sinks, H. A. Tilson, *Environ Health Perspect*, **104**, 715-740, 1996.
2. H. S. Kim, S. Y. Han, S. D. Yoo, B. M. Lee, K. L. Park, *J. Toxicol. Sci.*, **26**, 111-118, 2001.
3. W. Li, M. Seifert, Y. Xu, B. Hock, *Environ. Int.*, **30**, 329-335, 2004.
4. A. Suzuki, A. Sugihara, K. Uchida, T. Sato, Y. Ohta, Y. Kats, H. Watanabe, T. Iguchi, *Reprod. Toxicol.*, **16**, 107-116, 2002.
5. C. Malitesta, I. Losito, P. G. Zambonin, *Anal. Chem*., **71**, 1366-1370, 1999.
6. F. L. Dickert, O. Hayden, K. P. Halikias, *Analyst*, **126**, 766-771, 2001.
7. J. M. Lin, M. Yamada, *Analyst*, **126**, 810-815, 2001.
8. D. Apodaca, R. Pernites, R. Ponnapati, F. Del Mundo, R. C. Advincula, *ACS Appl. Mater. Interfaces*, **3**, 191-203, 2011.
9. R. Pernites, R. Ponnapati, R. C. Advincula, *Macromolecules*, **43**, 9724-9735, 2010.
10. R. Pernites, R. Ponnapati, J. Felipe, R. C. Advincula, *Biosens. Bioelectron.*, **26**, 2766-2771, 2011.
11. K. Mosbach, *Trends. Biochem. Sci.*, **19**, 9-14, 1994.
12. K. J. Shea, *Trends. Polym. Sci.*, **2**, 166-184, 1994.
13. G. Wulff, *Angew. Chem. Int. Ed.*, **34**, 1812-1832, 1995.
14. M. E. Byrnea, K. Parka, N. A, Peppas, *Adv. Drug Delivery Rev.*, **54**, 149-161, 2002.
15. H. Asanuma, T. Hishiya, M. Komiyama, *Adv. Mater.*, **12**, 1019-1030, 2000.
16. T. Hishiya, M. Shibata, M. Kakazu, H. Asanuma, M. Komiyama, *Macromolecules*, **32**, 2265-2269, 1999.
17. T. Tanaka, D. Fillmore, S-T. Sun, I. Nishio, G. Swislow A. Shah, *Phys. Rev. Lett.* **45**, 1636-1644, 1980.
18. M. Annaka, T. Tanaka, *Nature*, **335**, 430-432, 1992.
19. T. Amiya, Y. Horikawa, Y. Hirose, Y. Li, T. Tanaka, *J. Chem. Phys.*, **86**, 2375-2379, 1987.
20. G. Chen, A. S. Hoffman, *Nature*, **373**, 49-52, 1995.
21. R. Yoshida, K. Uchida, T. Kaneko, K. Sakai, A. Kikuchi, Y. Sakurai, T. Okano, T.

Nature, **374**, 240-242, 1995.

22. T. Tanaka, *Sci. Am.*, **244**, 124-136, 1981.
23. K. Dusek, "Responsive Gels: Volume Transitions I", *Adv. Polym. Sci.*, **109**, Springer, Berlin, 1993.
24. K. Dusek, "Responsive Gels: Volume Transitions II", *Adv. Polym. Sci.*, **110**, Springer, Berlin, 1993.
25. T. Okano, "Biorelated Polymers and Gels", Academic Press, Boston, 1998.
26. A. S. Hoffman, *Macromol. Symp.*, **98**, 645-664, 1995.
27. T. Miyata, *Polym. J.*, **42**, 277-289, 2010.
28. T. Miyata, N. Asami, T. Uragami, *J. Polym. Sci. Part B: Polym. Phys.*, **47**, 2144-2157, 2009.
29. T. Miyata, M. Jige, T. Nakaminami, T. Uragami, T. *Proc. Natl. Acad. Sci. U.S.A.*, **103**, 1190-1193, 2006.
30. T. Miyata, N. Asami, T. Uragami, *Nature*, 1999, **399**, 766-769, 1999.
31. A. Kawamura, T. Kiguchi, T. Nishihata, T. Uragami, T. Miyata, *Chem. Commun.*, **50**, 11101-11103, 2014.
32. K. Matsumoto, A. Kawamura, T. Miyata, *Chem. Lett.*, **44**, 1284-1286, 2015.
33. R. C. Advincula, B. Brittain, J. Ruhe, K. Caster, "Polymer Brushes: Synthesis Characterizations, Applications", Wiley- VCH, Weinheim, Germany, 2004.
34. H. Duran, K. Ogura, K. Nakao, S. Vianna, H. Usui, R. C. Advincula, W. Knoll, *Langmuir*, **25**, 10711-10718, 2009.
35. X. Wang, Y. Kim, C. Drew, B. Ku, J. Kumar, L. Samuelson, *Nano Lett.*, **4** (2), 331-334, 2004.
36. R. Pernites, S. Venkata, B. Tiu, A. Yago, R. C. Advincula, *Small*, **8**, 1669-1674, 2012.
37. J. Park, R. Pernites, N. Estillore, T. Hyakutake, R. Ponnapati, B. Tiu, H. Nishide, R. C. Advincula, *Chem. Commun*. **47**, 8871-8873, 2011.
38. H. Tong, L. Wang, X. Jing, F. Wang, *Macromolecules*, **36** (8), 2584–2586, 2003.
39. R. McCullough, P. Ewbank, R. Loewe, *J. Am. Chem. Soc.*, **119**, 633-634, 1997.
40. B. Tiu, R. Pernites, E. Foster, R. C. Advincula, *J. Colloid Interf. Sci*., **459**, 86-96, 2015.
41. U. Evans-Kennedy, J. Clohessy, V. J. Cunnane, *Macromolecules*, **37**, 3630-3634, 2004.

42. G. Zotti, R. Marin, M. Gallazzi, *Chem. Mater.*, **9**, 2945-2950, 1997.
43. P. Taranekar, T. Fulghum, A. Baba, D. Patton, R. C. Advincula, *Langmuir*, **23**, 908-917, 2007.
44. H. S. Byun, R. Bittman, *Tetrahedron Lett.*, **42**, 1839-1841, 2001.
45. M. Prabaharan, J. F. Mano, *Drug*. *Macromol. Biosci.*, **5**, 965-973, 2005.
46. T. Girek, W. Ciesielski, *J. Incl. Phenom. Macrocycl. Chem.*, **69**, 439-444, 2011.
47. F. Adrian, T. Budtova, E. Tarabukina, M. Pinteala, S. Mariana, C. Peptu, V. Harabagiu, B. C. Simionescu, *J. Incl. Phenom. Macrocycl. Chem.*, **64**, 83-94, 2009.
48. G. Z. Sauerbrey, *Phys. A Hadrons Nucl.*, **155**, 206-222, 1959.

Chapter 6

Molecule-Triggered Structural Transition of Molecularly Imprinted Polypeptide Hydrogel

6.1 Introduction

Polypeptides usually form a stable three-dimensional structure to function as a protein under physiological conditions.[1,2] Bryngelson and Wolynes suggested that the energy landscape for protein folding can be described as rugged funnels.[3-6] Near the top of the funnel, the protein has denatured structures due to high enthalpy and entropy. In contrast, an individual native structure reaches the lowest energy structure and becomes thermally occupied at the bottom of the funnel. Equilibrium structure of the protein is a trade-off between the retention of randomness of polypeptide chain (maximization of entropy) and the folding of the chain (minimization of enthalpy). Many interactions that are defined by amino acid sequence inevitably make the protein fold in its low energy structure. On one hand, a synthetic polymer that does not have several kinds of intramolecular interactions displays a large number of possible conformations in good solvents. The maximization of the total number of ways to arrange polymer chains (or entropy) usually plays an important role in the stabilization of three-dimensional structure of synthetic polymer.

Molecular imprinting method using a target molecule as a template, ligand monomers that interact with it, and cross-linkers enables us to easily create the molecular recognition sites within polymer network and hydrogel network.[7-13] The network conformation of as-prepared hydrogel designed by molecular imprinting is the most stable because a spatial arrangement of monomers is thermodynamically optimized in the solution.[14-17] The cross-linking during polymer network restricts the freedom of polymer chains and freezes the host monomers in the most preferable position to interact with the target molecule. Namely, the minimization of the energy attributes to creating the molecular recognition sites.

Chapter 2 describes that the α-helix structure induced by intramolecular hydrogen bonding is stabilized by cross-linking of polypeptide chains. These indicate that molecularly imprinted polypeptide hydrogels are able to memorize both the molecular

recognition sites and the α-helix structure.[18,19] The conformation of the as-prepared hydrogel with α-helix structure is in the ground state of the funnel. In contrast, the conformation with neither the molecular recognition sites nor the α-helix structures of the as-prepared hydrogel is around the top of the energy funnel. In the presence of the target molecule in the solution, a decrease in enthalpy induced by its binding to the ligands allows the hydrogel to fall into funnel-like energy landscape and to reach the lowest energy network structure. This suggests that the structural transition of the molecularly imprinted polypeptide hydrogels can be induced by binding of the target molecule.

In this study, we prepared molecularly imprinted polypeptide hydrogels that underwent molecule-triggered structural transition from random coil to α-helix in response to the presence of the target molecules, similar to the allosteric proteins. The molecularly imprinted polypeptide hydrogels with α-helix structure were strategically prepared by chemical cross-linking of CD-PGA or CD-PLL in the presence of BPA as a template molecule. The BPA-imprinted CD-polypeptide hydrogels memorized as-prepared conformation involving both α-helix structure and molecular recognition sites. The pH of structural transition of polypeptide chain was shifted due to stabilization of α-helix structure by chemical cross-linking. Similarly, it is conceivable that the molecular complex also can stabilize the α-helix structure of PGA chains (Figure 6-1) and PLL chains (Figure 6-2). The PGA chains of the hydrogel under acidic condition (pH_1) suggest energy landscapes that are funneled, and then their conformation forms minimally frustrated α-helix structure. On the other hand, the energy landscape of the PGA chains in neutral pH (pH_2) would be rough without deep metastable minima of α-helix structure. In a particular pH range (pH_3) that shows the BPA-dependent shift in the equilibrium of secondary structure between α-helix and random coil structure, the complex formation in the presence of a target molecule can lead to funneled energy landscapes. Therefore, the formation of the sandwich-like

CD-BPA-CD complexes under the certain conditions would cause a structural transition of the BPA-imprinted CD-polypeptide hydrogel.

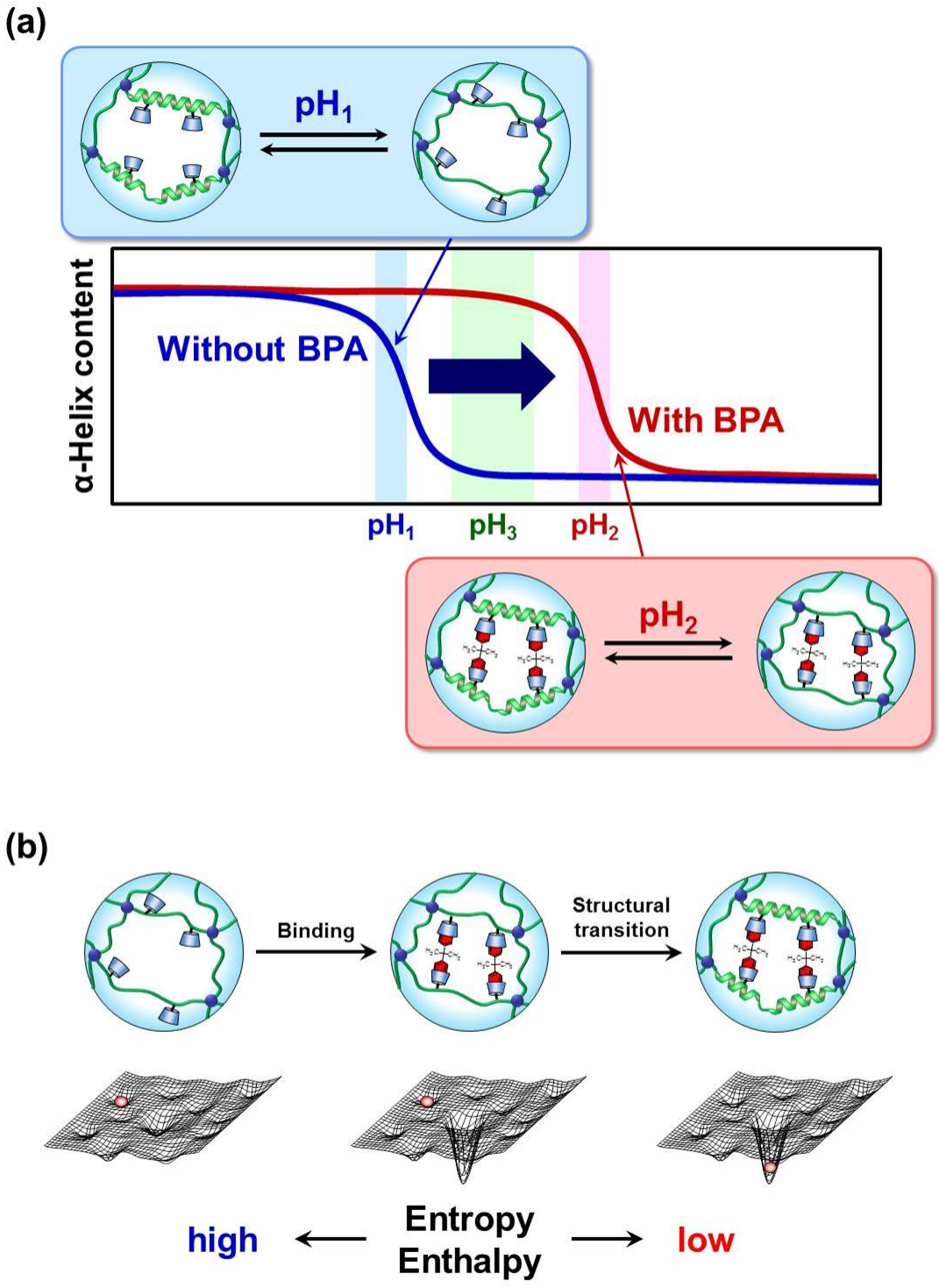

Figure 6-1. (a) Schematic illustration for pH-responsive structural transition behavior of the BPA-imprinted CD-PGA hydrogel in a buffer solution or an aqueous BPA solution. (b) Schematic illustration for BPA-triggered structural transition behavior of the BPA-imprinted CD-PGA hydrogel in a particular pH (pH_3).

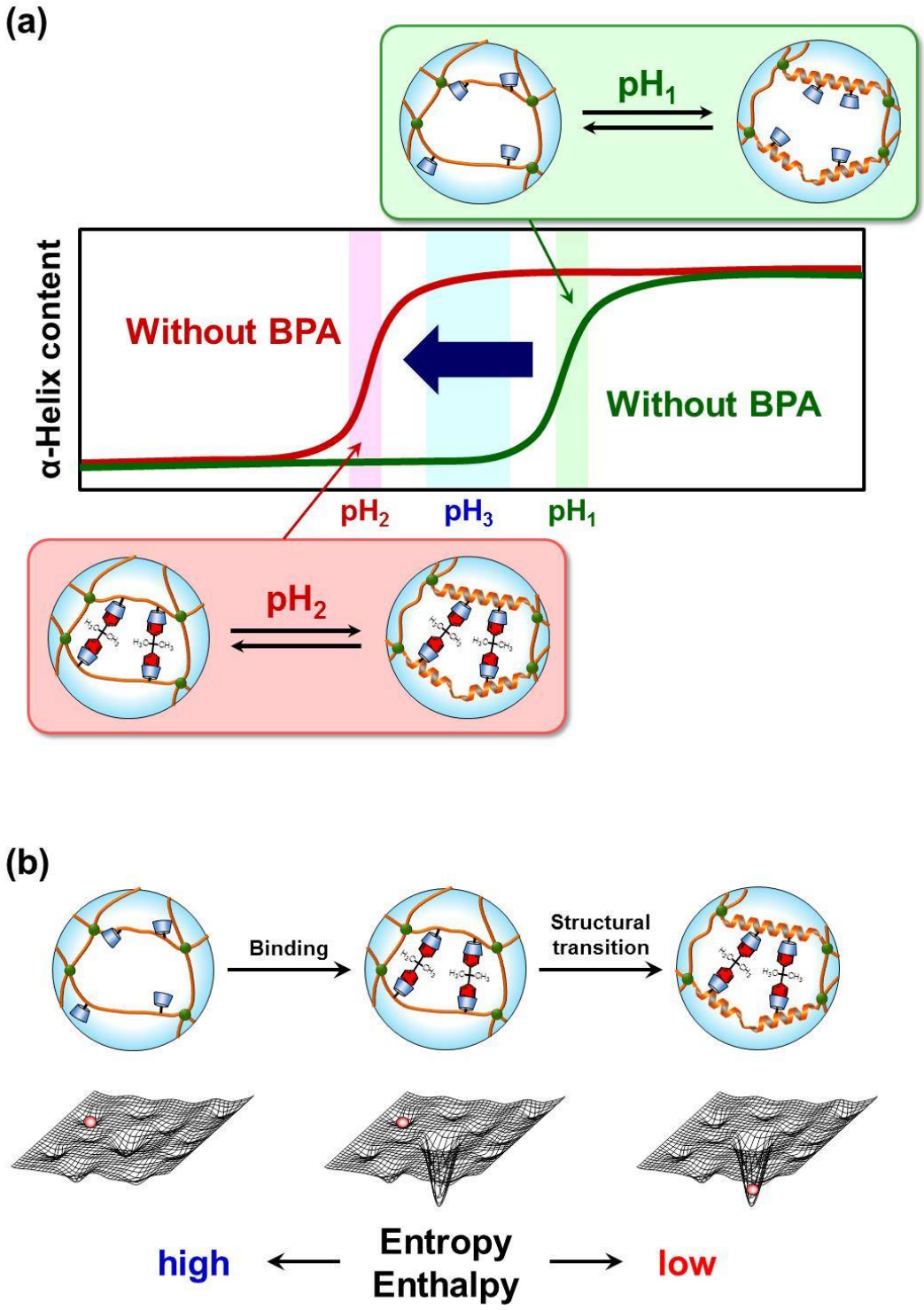

Figure 6-2. (a) Schematic illustration for pH-responsive structural transition behavior of the BPA-imprinted CD-PLL hydrogel in a buffer solution or an aqueous BPA solution. (b) Schematic illustration for BPA-triggered structural transition behavior of the BPA-imprinted CD-PLL hydrogel in a particular pH (pH_3).

6.2 Experimental

6.2.1 Materials

PGA sodium sat (12,000 MWCO) and PLL hydrobromide (12,000 MWCO) was purchased from Peptide Ins. Co. Ltd. (Osaka, Japan). Pentaerythritol tetra(mercaptoethyl) polyoxyethylene (Tetra-PEG-SH) and PEGDE (Mw = 500) were purchased from NOF Co. Ltd (Tokyo, Japan) and , respectively. All aqueous solutions were prepared with ultra-pure water (Milli-Q, 18.2 MΩ cm). The other solvents and reagents of analytical grade were obtained from commercial sources and were used without further purification.

6.2.2 Synthesis of NH_2-CD and carboxy-CD

The NH_2-CD and the carboxy-CD were synthesized by the same procedure as described in Chapter 3.

6.2.3 Introduction of CD and allyl group to PGA

PGA (1.0 g, 6.62 mmol glutamic acid units) was dissolved in 100 mL of ultra-pure water. EDC (317.3 mg, 1.66 mmol) and NHS (190.5 mg, 1.66 mmol) were added to the aqueous solution with PGA and allowed to react for 1 h at room temperature. NH_2-CD (300.3 mg, 0.26 mmol) and allylamine (94.5 mg, 1.66 mmol) were added to the aqueous solution solution with activated PGA. The reaction proceeded for 24 h at room temperature (Scheme 6-1). Then, the reaction mixture was poured into seamless cellulose tubing (molecular weight cut off: 3,500) and was dialyzed against ultra-pure water for purification. The resultant CD- and allyl group-modified PGA (CD-AA-PGA) was obtained via freeze-drying. The contents of CD and allyl group that were introduced to PGA were determined from the ^{1}H NMR proton integration. CD-AA-PGA was dissolved in D_2O, and ^{1}H NMR was recorded on

JEOL JNM-AL 400 spectrometer using sodium 3-(trimethylsilyl)propionate-2,2,3,3-d_4 as the internal standard.

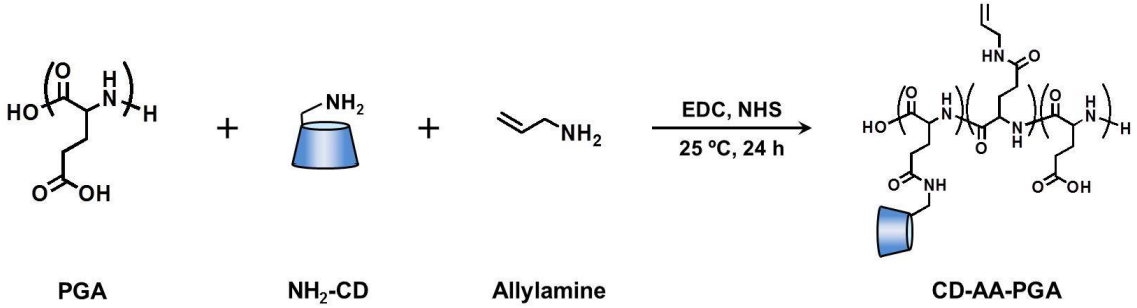

Scheme 6-1. Introduction of CD and allyl group into PGA.

6.2.4 Preparation of BPA-imprinted CD-PGA hydrogel

The BPA-imprinted CD-PGA hydrogels were prepared by the method shown in Scheme 6-2. CD-AA-PGA (100.0 mg), Tetra-PEG-SH (25.4 mg) and BPA (3.1 mg) were dissoluble in 500 μL of CH_3COOH/CH_3COONa buffer solution (ABS, 50 mM, pH 3, 0.5 M NaCl). The CD-AA-PGA solution was kept for 24 hours at room temperature so that PGA chains could form α-helix structure. After the formation of 2:1 complex between CD and BPA, 2,2'-azobis(2methylpropion amidine) dihydrochloride (v-50, 6.9 mg) was added to the solution. The solution was injected into the molds composed of a quartz glass and silicon wafer by capillary action. While the mixture solution was exposed to UV light (λ = 365 nm) for 6 hours, CD-AA-PGA was chemically cross-linked by thiol-ene reaction in the ABS for 24 hours at 35 °C in the presence of template BPA. The BPA-imprinted CD-PGA hydrogels were immersed in ABS/acetone (70/30) mixture to extract template BPA and then were immersed in ABS until the equilibrium swelling was achieved.

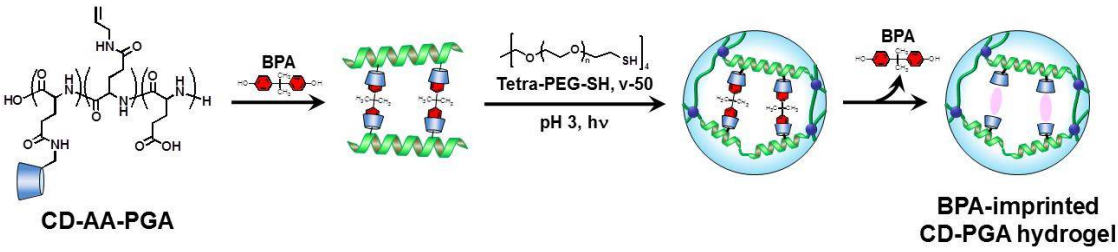

Scheme 6-2. Preparation of BPA-imprinted CD-PGA hydrogel.

6.2.5 Introduction of CD to PLL

The CD-PLL was synthesized by the same procedure as described in Chapter 3. Carboxy-CD (1.77 g, 1.33 mmol) was dissolved in 80 mL of ultra-pure water. EDC (1.37 g, 6.67 mmol) and NHS (0.82 g, 6.67 mmol) were added to the aqueous solution containing carboxy-CD and allowed to react for 1 hour at room temperature. PLL (0.5 g, 2.4 mmol primary amines), which was dissolved in 20 mL of ultra-pure water, was added to the aqueous solution containing an activated carboxy-CD. The reaction proceeded for 4 hours at room temperature (Scheme 1). Then, the reaction mixture was poured into a seamless cellulose tubing (molecular weight cut off: 3,500) and was dialyzed against ultra-pure water for purification. The resultant CD-PLL was obtained by freeze-drying. The content of CD introduced to PLL was determined from ^{1}H NMR proton integration. CD-PLL was dissolved in D_2O, and ^{1}H NMR was recorded on a JEOL JNM-AL 400 spectrometer using sodium 3-(trimethylsilyl)propionate-2,2,3,3-d_4 as the internal standard. The average degree of substitution of the resulting CD-PLL was determined to be 0.30 by ^{1}H NMR analysis.

6.2.6 Preparation of BPA-imprinted CD-PLL hydrogel

The BPA-imprinted CD-PGA hydrogels were prepared by the same procedure as described in Chapter 3.

6.2.7 Circular dichroism

The circular dichroism spectra of the CD-PGA solution (100 μg/mL), the BPA-imprinted CD-PGA and CD-PLL hydrogels were measured using a circular dichroism spectrometer reported in Chapter 2. The hydrogels for circular dichroism measurements were prepared using molds composed of a quartz glass and silicon wafer. After the hydrogel formation, the silicon wafer was peeled off from the surface of the resulting BPA-imprinted CD-PGA and CD-PLL hydrogels. The BPA-imprinted CD-PGA and CD-PLL hydrogels on a quartz glass were placed in a quartz sandwich cell of 1 mm for the circular dichroism measurements. The CD-PGA linear polymer, the BPA-imprinted CD-PGA and CD-PLL hydrogels in buffer solutions and aqueous BPA solution with various pHs were subjected to scanning from 250 nm to 200 nm at 0.1 nm data pitch at the rate of 100 nm/min with background subtracted. To investigate the relationship between pH and the structure of PGA chains, relative α-helix content of the CD-PGA linear polymer, the BPA-imprinted CD-PGA and CD-PLL hydrogels was determined from the ellipticity at 222 nm using equation (4-1) and (2-2).

6.3 Results and Discussion

6.3.1 Characterizations of CD-AA-PGA

NH_2-CD and allylamine were reacted with PGA using EDC and NHS to obtain CD-AA-PGA. The average degree of substituted CD and allyl group of the resulting CD-AA-PGA was found to be 0.03 (i.e., on average one CD every 33 glutamic acid units) and 0.21 (i.e., on average one allyl group every 5 glutamic acid units) by ^{1}H NMR analysis (Figure 6-3), respectively.

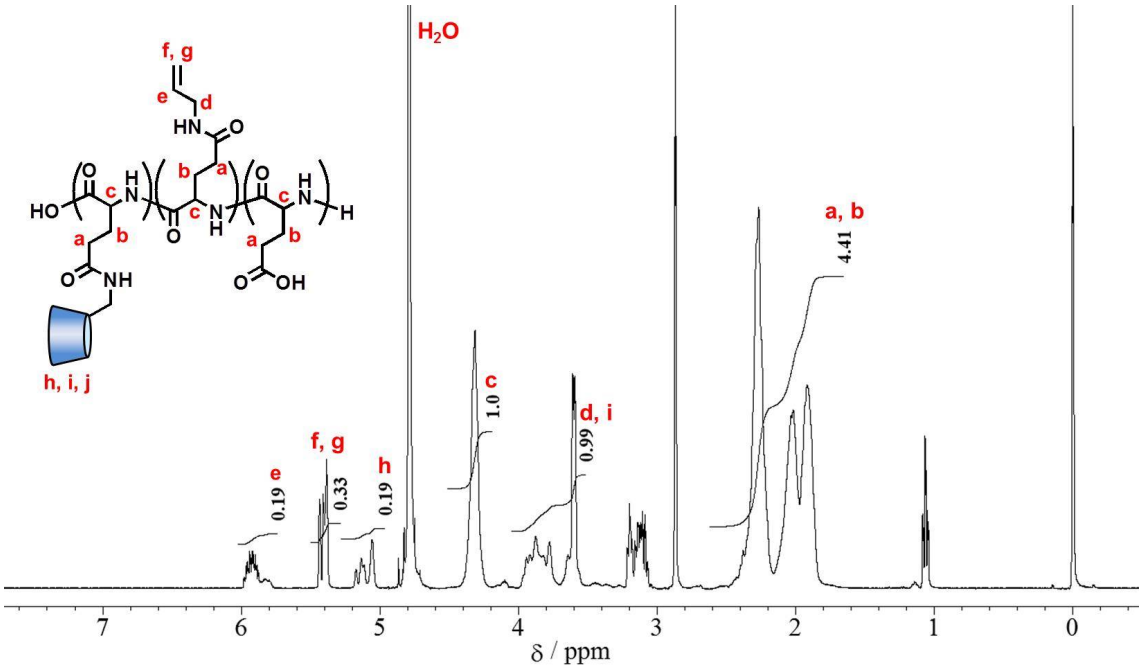

Figure 6-3. ^{1}H NMR spectrum of CD-AA-PGA (D_2O, 400 MHz).

6.3.2 Circular dichroism spectra of PGA in a BPA solution

A PGA linear polymer forms the α-helix structure at pH below 5 but undergoes a structural transition to the random coil structure at pH above 5. The structural transition of the PGA linear polymer from α-helix to random coil is attributed to the repulsion between negatively charged carboxy groups generated by the deprotonation at pH above 5. To focus on the structural transition of the PGA chains in response to the presence of BPA, pH-responsive structural transition behavior of the PGA linear polymer in an aqueous BPA solution was investigated using circular dichroism spectroscopy. First of all, the circular dichroism spectra of the PGA linear polymer in an aqueous BPA solution as a function of BPA concentration were measured to scanning from 250 nm to 200 nm because an aqueous BAP solution has an absorption in a wavelength range of 200-250 nm (Figure 6-4). In an aqueous solution with less than 10 mg/mL BPA, meaningful spectra of PGA linear polymer did not be recorded because enough light could not reach the detector. The HT value in an aqueous solution with 4 mg/mL BPA was suppressed within the range between 209 nm and 250 nm.

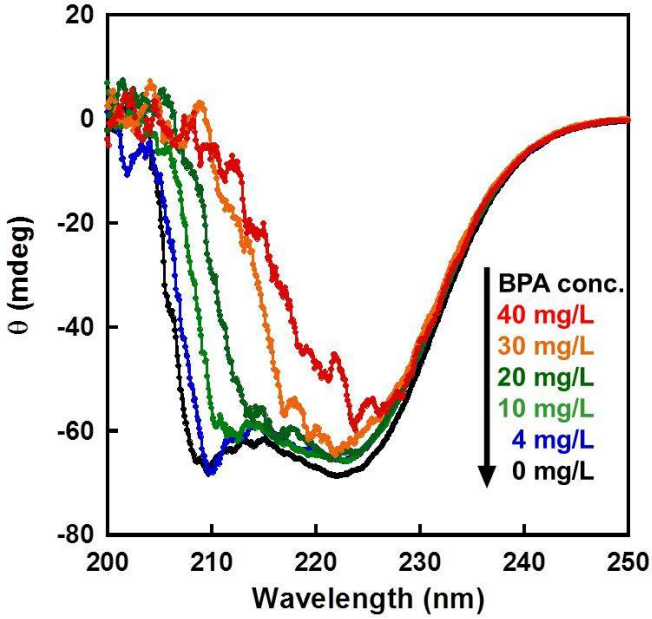

Figure 6-4. Circular dichroism spectra of the PGA linear polymer in a buffer solution with various BPA concentrations.

6.3.3 pH-Responsive structural transition of CD-PGA solution

To investigate the stabilization of the α-helix structure by complex formation between BPA and CD, the secondary structures of the CD-PGA linear polymer, the BPA-imprinted CD-PGA and CD-PLL hydrogels in the presence of target BPA were measured by circular dichroism spectroscopy. Figure 6-5a and b show the ellipticities of the CD-PGA linear polymer in buffer solutions and aqueous BPA solutions with various pHs, respectively. In a buffer solution and an aqueous BPA solution at pH 3, the circular dichroism spectra of the CD-PGA linear polymer showed negative peaks at 208 nm and 222 nm, which are assigned to the α-helix structure. In the spectra of the CD-PGA linear polymer with more than pH 6, positive peak appeared at 215 nm, which is characteristic to the random coil structure. Figure 6-5c shows the effect of pH on the relative α-helix content of the CD-PGA linear polymer in buffer solutions and aqueous BPA solutions with various pHs. In solutions below pH 5, the CD-PGA linear polymer had high α-helix content. However, the relative α-helix content decreased dramatically with increasing pH in solutions above pH 5. These suggest that the PGA undergo a structural transition from α-helix to random coil at approximately pH 5. It should be noted that the CD-PGA linear polymers in both buffer solution and aqueous BPA solution underwent structural transition around pH 5.

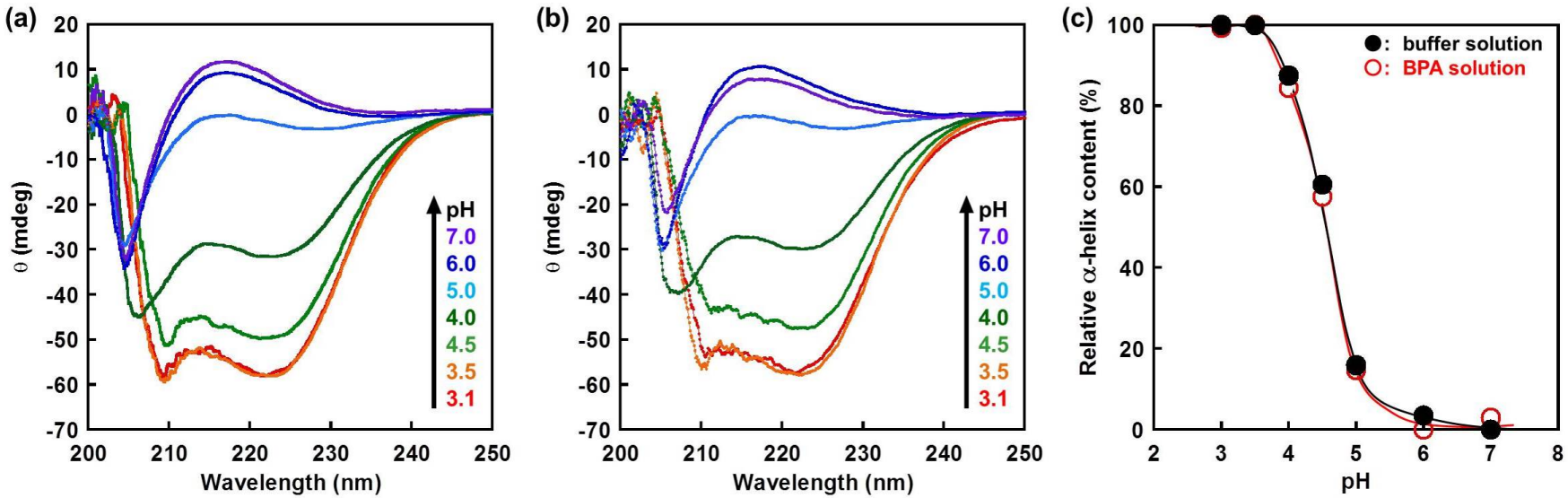

Figure 6-5. Circular dichroism spectra of the CD-PGA linear polymer (a) in a buffer solution and (b) in an aqueous BPA solution as a function of pHs. (c) Relationship between pH and relative α-helix content of the CD-PGA linear polymer in a buffer solution and an aqueous BPA solution with various pHs.

6.3.4 pH-Responsive structural transition of BPA-imprinted CD-PGA hydrogel and BPA-imprinted CD-PLL hydrogel

Figure 6-6 shows the effect of pH on relative α-helix content of the BPA-imprinted CD-PGA hydrogel in aqueous BPA solutions with various pHs. The BPA-imprinted CD-PGA hydrogel formed the α-helix structure in aqueous BPA solutions below pH 4.5 but the α-helix content decreased dramatically with increasing pH in aqueous BPA solutions above pH 4.5. This result suggests that the PGA main chains of the BPA-imprinted CD-PGA hydrogel with sandwich-like CD-BPA-CD complexes undergo a structural transition from the α-helix to random coil structure at approximately pH 4.5. The α-helix structure of the PGA chains was not stabilized by the chemical cross-linking and the formation of sandwich-like CD-BPA-CD complexes. This is attributed to a decrease in the number of cross-linking for the stabilization of the α-helix structures of the PGA chains because of low reactivity of the thiol-ene reaction in acidic conditions.

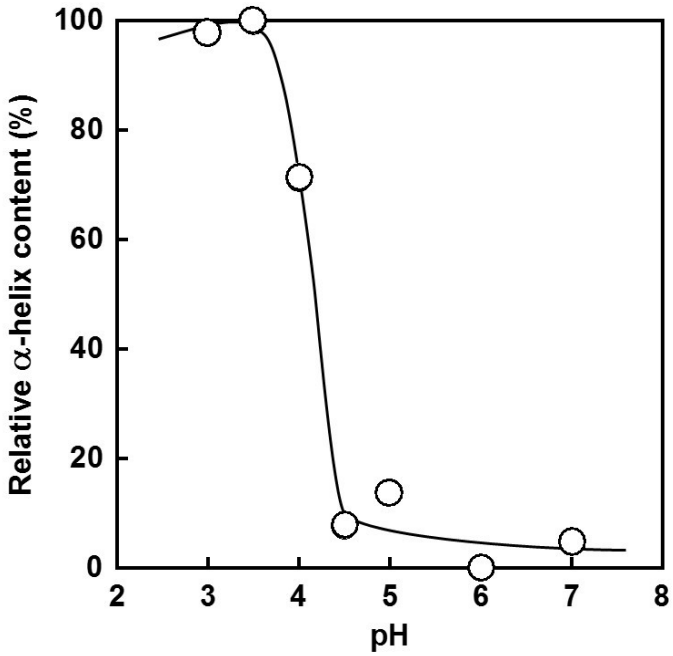

Figure 6-6. Relationship between pH and relative α-helix content of the BPA-imprinted CD-PGA hydrogels in an aqueous BPA solution with various pHs.

Our strategy for preparing molecularly imprinted polypeptide hydrogels that undergo molecule-triggered structural transition was also to utilize PLL as a main chain in the hydrogel network. To investigate the stabilization of α-helix structure by complex formation between CD and BPA, the secondary structures of BPA-imprinted CD-PLL hydrogel in the presence of target BPA were measured by circular dichroism spectroscopy. To enhance the effect of the dynamic cross-linking between CD and BPA, high-substituted CD-PLL was employed to prepare the BPA-imprinted CD-PLL hydrogels. Figure 6-7a and b show ellipticities of the BPA-imprinted CD-PLL hydrogels in buffer solutions and aqueous BPA solutions with various pHs, respectively. In a buffer solution and an aqueous BPA solution with pH 12, the circular dichroism spectra of the BPA-imprinted CD-PLL hydrogels showed negative peaks at 208 nm and 222 nm, which are assigned to the α-helix structure. The spectra of the BPA-imprinted CD-PLL hydrogels with more than pH 9.5 demonstrates a positive peak at 215 nm, which is characteristic to the random coil structure. Figure 6-5c shows the effect of pH on relative α-helix content of the BPA-imprinted CD-PLL hydrogels in buffer solutions and aqueous BPA solutions with various pHs. In solutions above pH 10, the BPA-imprinted CD-PLL hydrogels had high α-helix content. Furthermore, the relative α-helix content of the BPA-imprinted CD-PLL hydrogels in an aqueous BPA solution with pH 10.5 was higher than that in a buffer solution with the same pH. These means that the BPA-imprinted CD-PLL hydrogels in an aqueous BPA solution can maintain the α-helix structure in a wider pH than those in the absence of BPA. The formation of sandwich-like CD-BPA-CD complexes can stabilize the α-helix structure of the BPA-imprinted CD-PLL hydrogels because it inhibits a structural transition from the α-helix to random coil structure. However, the range of shifted pH in the structural transition by complex formation between CD and BPA was much lower than that by the chemical cross-linking as described in Chapter 2. This is attributed to lowering the interaction between CD and BPA for the stabilization of the α-helix structures of the

PLL chains. Utilizing stronger interaction between a target molecule and ligands will induce the molecule-triggered structural transition more effectively.

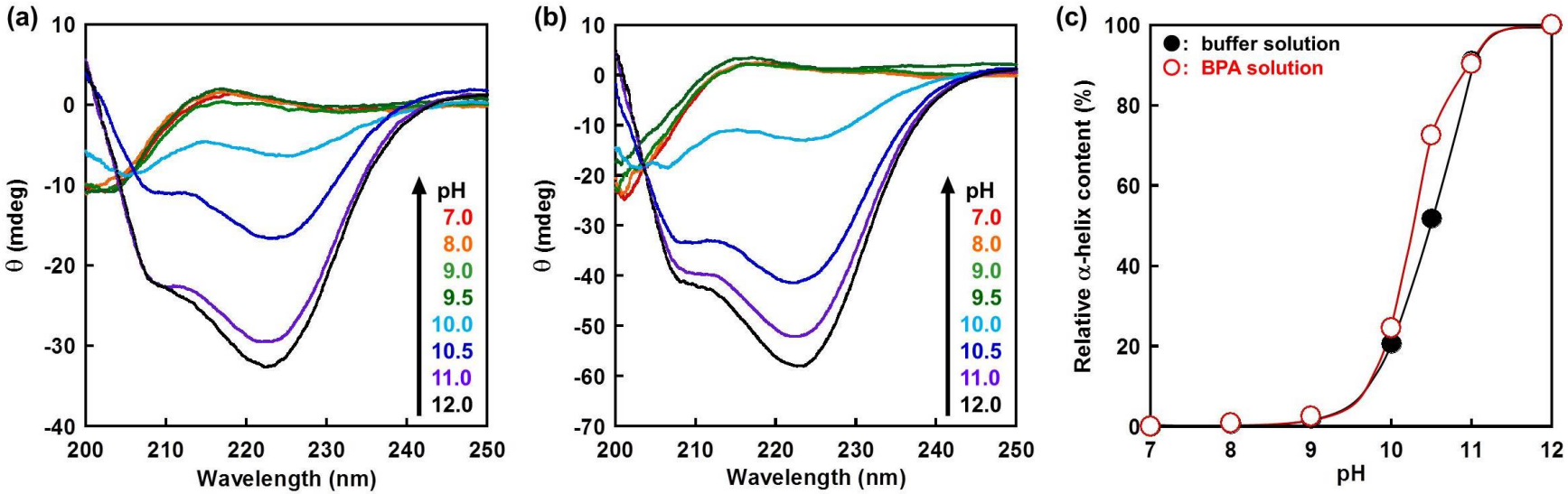

Figure 6-7. Circular dichroism spectra of the BPA-imprinted CD-PLL hydrogel (a) in a buffer solution and (b) in an aqueous BPA solution as a function of pHs. (c) Relationship between pH and relative α-helix content of the BPA-imprinted CD-PLL hydrogel in a buffer solution and an aqueous BPA solution with various pHs.

6.3.5 BPA-Triggered structural transition of BPA-imprinted CD-PLL hydrogel

The BPA-triggered structural transition behavior of the BPA-imprinted CD-PLL hydrogel was investigated in a buffer solution containing BPA at pH 10.5. The BPA-imprinted CD-PLL hydrogel was kept immersed in 5 mL of Na_2HPO_4/NaOH (pH 10.5) buffer solutions until equilibrium was reached at 25 °C. Afterwards, the hydrogel was transferred and kept immersed in an aqueous BPA solution (4 mg/L) at 25 °C. Figure 6-8a shows change in the circular dichroism spectra of the BPA-imprinted CD-PLL hydrogel in response to BPA. In the spectra of the BPA-imprinted CD-PLL hydrogel, negative Cotton effects were observed at 208 nm and 222 nm, which are assigned to the α-helix structure. The negative Cotton effects of the BPA-imprinted CD-PLL hydrogel in the presence of BPA was somewhat stronger than in the absence of BPA. Figure 6-b shows change in the relative α-helix content of the BPA-imprinted CD-PLL hydrogel in aqueous BPA solutions at pH 10.5. The BPA-imprinted CD-PLL hydrogels gave relative α-helix content of 67 % in a buffer solution. When the BPA-imprinted CD-PLL hydrogel was immersed in a buffer solution containing BPA, the relative α-helix content rose to 80 %. These mean that the formation of sandwich-like CD-BPA-CD complexes induced structural transition of the CD-PLL chains to the α-helix structure. As the BPA-imprinted CD-PLL hydrogel was prepared by molecular imprinting at pH 12, as-prepared conformations involving both α-helix structure and molecular recognition sites for BPA were memorized within hydrogel networks. A decrease in enthalpy, which is induced by the formation sandwich-like CD-BPA-CD complex, allows the BPA-imprinted CD-PLL hydrogel to reach the lowest energy network structure. As a result, α-helix content of the BPA-imprinted CD-PLL hydrogel increased in response to BPA due to stabilization of the α-helix structures by the dynamic cross-linking. Therefore, the structural transition of the BPA-imprinted CD-PLL hydrogel can be induced by BPA because the as-prepared

conformations with α-helix structure are the most stable, which is similar to the native three-dimensional structure of proteins.

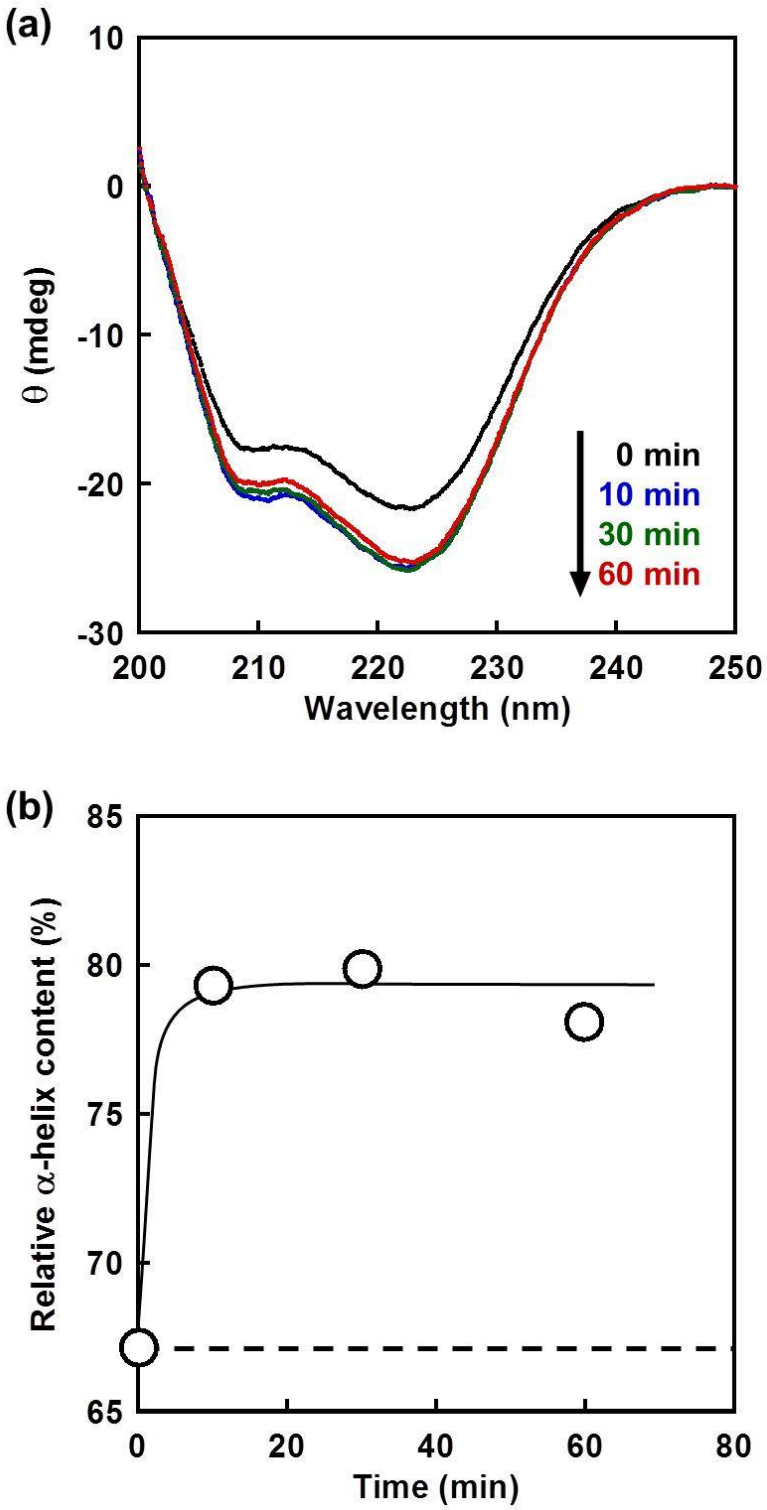

Figure 6-8. (a) Circular dichroism spectra of the BPA-imprinted CD-PLL hydrogels in an aqueous BPA solution at pH 10.5. (b) Change in relative α-helix content of the BPA-imprinted CD-PLL hydrogels as a function of time after immersion in an aqueous BPA solution at pH 10.5.

6.4 Conclusions

The BPA-imprinted CD-PGA and CD-PLL hydrogels can be prepared from PGA and PLL with the α-helix structures by molecular imprinting using complex formation between CD and BPA. The α-helix structure of the BPA-imprinted CD-PGA hydrogels chains was not stabilized by chemical cross-linking and complex formation between CD and BPA because of low reactivity of the thiol-ene reaction in acidic conditions. In contrast, the BPA-imprinted CD-PLL hydrogel exhibited BPA-triggered structural transition behavior due to memorization of as-prepared conformation involving both the molecular recognition sites and the α-helix structure. Utilizing stronger interaction between a target molecule and ligands will induce the molecule-triggered structural transition more effectively. Chapter 3 reveals that the molecular recognition sites during the molecularly imprinted polypeptide hydrogel disappear due to structural transition of polypeptide chains.[20] Thus, the molecule-triggered structural transition system will significantly contribute to design of allosteric protein-mimicking intelligent hydrogels.

6.5 References

1. B. Alberts, Q, Johnson, J. Lewis, M. Raff, K. Roberts, P. Walter, "Molecular Biology of the Cell 4th ed.", Garland, New York, 2002.
2. G. A. Petsko, D. Ringe, "Protein Structure and Functions" Oxford Univ. Press, 2008.
3. J.D. Bryngelson, P. G. Wolynes, *Proc. Natl. Acad. Sci. USA*, 84, 7524-7528, 1987
4. J.D. Bryngelson, P. G. Wolynes, *J. Phys. Chem.*, **93**, 6902-6915, 1989.
5. J.D. Bryngelson, J. N. Onuchic, N. D. Socci, P. G. Wolynes, *Proteins: Struct., Funct., Genet.*, **21**, 167-195, 1995.
6. P. G. Wolynes, *Biochimie*, **119**, 218-230, 2015.
7. G. Wulff, A. Sarhan, K. Zabrocki, *Tetrahedron Lett.*, **14**, 4329-4332, 1973.
8. B. Sellergren, M. Lepistoe, K. Mosbach, *J. Am. Chem. Soc.*, **110**, 5853-5860, 1988.
9. K. Mosbach, *Trends Biochem. Sci.*, **19**, 9-14, 1994.
10. K. J. Shea, *Trends. Polym. Sci.*, **2**, 166-173, 1994.
11. G. Wulff, *Angew. Chem. Int. Ed.*, **34**, 1812-1832, 1995.
12. M. Byrne, K. Park, N. A. Peppas, *Adv. Drug Deliv. Rev.*, **54**, 149-161, 2002.
13. N. M. Bergmann, N. A. Peppas, *Prog. Polym. Sci.*, **33**, 271-288, 2008.
14. S. Dniach, J. Bascle, T. Garel, H. Orland, *J. Mol. Biol.*, **254**, 960-967, 1995.
15. E. Shakhnovich, A. Gutin, *J. Chem. Phys.*, **93**, 5967-5971, 1990.
16. V. S. Pande, A. Y. Grosberg, T. Tanaka, *Proc. Natl. Acad. Sci. USA*, **91**, 12976-12979, 1994.
17. V. S. Pande, A. Y. Grosberg, T. Tanaka, *Rev. Mod. Phys.*, **72**, 259-314, 2000.
18. K. Matsumoto, A. Kawamura, T. Miyata, *Chem. Lett.*, **44**, 1284-1286, 2015.
19. A. Harada, S. Ichimura, E. Yuba, K. Kono, *Soft Matter*, **7**, 4629-4635, 2011.
20. K. Matsumoto, A. Kawamura, T. Miyata, *J. Am. Chem. Soc.*, *submitted*.

Chapter 7

Concluding remarks

This thesis describes design and applications of intelligent hydrogels with controllable molecular recognition. In the present work, the author focused on polypeptide as a main chain of intelligent hydrogel (Chapter 2). Two strategies were employed to construct an allosteric regulation of molecularly imprinted polypeptide hydrogels: (1) Regulation of the binding capacity by the structural transition and (2) inducement of the structural transition by molecular recognition. The regulation of the binding capacity of the molecularly imprinted polypeptide hydrogels was accomplished by conformational change of their networks (Chapter 3). The polypeptide hydrogels with controllable molecular recognition were developed as DDS carrier (Chapter 4) and sensor systems (Chapter 5). Furthermore, the inducement of the structural transition in response to target molecule was proposed (Chapter 6).

In Chapter 2, by chemical cross-linking of PLL that exhibits helix-to-coil transition, we prepared a PLL hydrogel that underwent changes in conformation in response to pH changes. In addition, the chemical cross-linking enabled effective stabilization of the α-helix structure of the PLL chains, which was directly correlated with the pH-responsive change in swelling ratio of the PLL hydrogel.

In Chapter 3, BPA-imprinted CD-PLL hydrogels, which can be prepared from PLL with random coil structures by molecular imprinting using complex formation, have molecular recognition sites for specific molecules. Upon a structural transition of PLL from the random to α-helix structure, the molecular recognition sites created by molecular imprinting are conformationally changed. As a result, the binding capacity of the BPA-imprinted CD-PLL hydrogel can be regulated by a pH-responsive structural transition of the PLL chains, similar to the allosteric effect. Furthermore, the BPA-loaded CD-PLL hydrogel that were prepared by *pseudo* molecular imprinting can also regulate the BPA release in response to a small change in pH because a pH change

induced a reduction in the stability of CD-BPA-CD complexes within the hydrogel networks

In Chapter 4, the RSV-loaded CD-PGA hydrogels that can be prepared from the PGA with random coil structure by *pseudo* molecular imprinting have inclusion complex between CD and RSV. The release of RSV from the RSV-loaded CD-PGA hydrogel was suppressed in a buffer solution with neutral pH because CD ligands are arranged at optimal positions for forming CD-RSV-CD complexes with RSV. With structural transition of PGA from the random coil to α-helix structure, the stability of the inclusion complex between CD and RSV was decrease, followed by releasing the RSV form the RSV-loaded CD-PGA hydrogel. Therefore, antioxidant agent-loaded PGA hydrogel that was prepared by *pseudo* molecular imprinting method regulated the antioxidant agent-release behavior depending on its conformation.

In Chapter 5, molecularly imprinted polypeptide gel layers with molecular recognition sites were prepared on QCM sensor chips by combining electropolymerization with molecular imprinting. A large surface area produced by electropolymerization and the arrangement of CD ligands at optimal positions for forming CD-BPA-CD complexes via molecular imprinting contributed significantly to the fabrication of highly sensitive and selective QCM sensor systems.

In Chapter 6, The BPA-imprinted CD-PGA hydrogels and the BPA-imprinted CD-PLL hydrogels can be prepared from PGA and PLL with the α-helix structures by molecular imprinting using complex formation. The α-helix structure of the BPA-imprinted CD-PGA hydrogels chains did not be stabilized by chemical cross-linking and complex formation between CD and BPA, because of low reactivity of the thiol-ene reaction in acidic conditions. In contrast, the BPA-imprinted CD-PLL

hydrogel exhibited BPA-triggered structural transition behavior due to memorization of as-prepared conformation involving both the molecular recognition sites and the α-helix structure.

In conclude, intelligent hydrogels with controllable molecular recognition were fabricated by utilizing polypeptide as a main chain of the hydrogel. The intelligent hydrogels proposed in the study are applicable for various stimuli and molecules by replacing polypeptide chains and CD with other polypeptides and other ligand molecules, respectively. The underlying concepts in our results will assist others in preparing new materials for molecular sensor, separations, drug delivery, and many other fields. The author believes that the intelligent hydrogel with controllable molecular recognition opens the new field as protein-mimicking intelligent materials.

Appendix

List of publication

Original papers

1) Kazuya Matsumoto, Takashi Miyata

生体分子機能を利用した刺激応答性ゲル

Kobunshi Ronbunshu, **71**, 125-142 (2014)

2) Kazuya Matsumoto, Akifumi Kawamura, Takashi Miyata

Structural Transition of pH-responsive Poly(L-lysine) Hydrogel Prepared via Chemical Crosslinking

Chem. Lett., **44**, 1284-1286 (2015)

3) Kazuya Matsumoto, Brylee David B. Tiu, Akifumi Kawamura, Rigoberto C. Advincula, Takashi Miyata

QCM sensing of bisphenol A using molecularly imprinted hydrogel/conducting polymer matrix

Polymer J., **48** 525-532 (2016)

4) Kazuya Matsumoto, Akifumi Kawamura, Takashi Miyata

Conformationally Regulated Molecular Binding and Release of Molecularly Imprinted Polypeptide Hydrogels that Undergo Helix-Coil Transition

submitted

5) Kazuya Matsumoto, Nobuki Sakikawa, Takashi Miyata

Thermo-Responsive Gels That Absorb Moisture and Ooze Water

submitted

6) Kazuya Matsumoto, Yoshinori Ito, Akifumi Kawamura, Takashi Miyata
Antioxidant Agent-Loaded Polypeptide Hydrogels and Their Release Behavior by Conformational Change
in preparation

7) Kazuya Matsumoto, Akifumi Kawamura, Takashi Miyata
Molecule-Triggered Structural Transition of Molecule-Imprinted Polypeptide Hydrogel
in preparation

List of presentation

International conferences

1) Kazuya Matsumoto, Akifumi Kawamura, Takashi Miyata, Tadashi Uragami
Swelling-Shrinking Behavior of pH-Responsive Polypeptide Hydrogels That Undergo Conformational Change
9th International Gel Symposium, Tsukuba (Japan), October 2012, Poster

2) Kazuya Matsumoto, Akifumi Kawamura, Tadashi Uragami, Takashi Miyata
Preparation of Molecularly Imprinted Polypeptide Hydrogels and Their Swelling-Shrinking Behavior
8th International Symposium in Science and Technology at Kansai University 2013, Suita (Japan), August 2013, Oral

3) Kazuya Matsumoto, Akifumi Kawamura, Tadashi Uragami, Takashi Miyata
Design of Molecularly Stimuli-Responsive Polypeptide Hydrogels with Controllable Molecular Recognition Sites
International Symposium on Smart Biomaterials ～2nd Hoffman Family Symposium～, Tsukuba (Japan), March 2014, Poster

4) Kazuya Matsumoto, Akifumi Kawamura, Tadashi Uragami, Takashi Miyata
Structural Control of Molecular Recognition Sites within Molecularly Imprinted Polypeptide Hydrogels
9th International Symposium in Science and Technology at Cheng Shiu University 2014, Kaohsiung (Taiwan), August 2014, Poster

5) Kazuya Matsumoto, Akifumi Kawamura, Tadashi Uragami, Takashi Miyata

Regulation of Molecular Recognition Ability in Stimuli-Responsive Polypeptide Hydrogels

22nd Polymer Networks Group Meeting and 10th Gel Symposium (PN&G 2014), Tokyo (Japan), November 2014, Poster

6) Kazuya Matsumoto, Akifumi Kawamura, Takashi Miyata

Preparation of Molecularly Imprinted Polypeptide Hydrogels with Controllable Molecular Recognition Sites

The 5th International Workshop on Nanogrid Materials, Busan (Korea), December 2014, Poster

7) Kazuya Matsumoto, Akifumi Kawamura, Tadashi Uragami, Takashi Miyata

Drug Release Behavior from Stimuli-Responsive Hydrogels with Controllable Molecular Recognition Sites

The 10th SPSJ International Polymer Conference, Tsukuba (Japan), December 2014, Poster

8) Kazuya Matsumoto, Akifumi Kawamura, Takashi Miyata

Loading of Drug within Molecularly Imprinted Polypeptide Hydrogels and Its Controlled Release

IUPAC 11th International Confernce on Advanced Polymers via Macromolecular Engineering, Yokohama (Japan), October 2015, Poster

9) Kazuya Matsumoto, Akifumi Kawamura, Takashi Miyata

Controlled Drug Release from Molecularly Imprinted Polypeptide Hydrogels by Structural Transition of Their Network

The International Chemical Congress of Pacific Basin Societies 2015, Honolulu (USA), December 2015, Poster

10) Kazuya Matsumoto, Brylee David B. Tiu, Akifumi Kawamura, Rigoberto C. Advincula, Takashi Miyata

Design of Molecularly Imprinted Polypeptide Gel Films on Sensor Chips and Their Target Molecule-Responsive Behavior

The International Chemical Congress of Pacific Basin Societies 2015, Honolulu (USA), December 2015, Oral

11) Kazuya Matsumoto, Yoshinori Ito, Akifumi Kawamura, Takashi Miyata

Controlled Drug Release from Molecularly Imprinted Polypeptide Hydrogels by Structural Transition of Their Network

Polymer Networks Group Meeting 2016, Stockholm (Sweden), June 2016, Poster

12) Kazuya Matsumoto, Brylee David B. Tiu, Akifumi Kawamura, Rigoberto C. Advincula, Takashi Miyata

QCM Sensing of Bisphenol A Using Molecularly Imprinted Gel Layers on Electropolymerized Terthiophene Films

The 10th Conference of Aseanian Membrane Society, Nara (Japan), July 2016, Poster

13) Kazuya Matsumoto, Yoshinori Ito, Akifumi Kawamura, Takashi Miyata

Loading of Drugs within Polypeptide Hydrogels via Molecular Imprinting and Their Controlled Release

The 11th SPSJ International Polymer Conference, Fukuoka (Japan), December 2016, Poster

Domestic conferences

1) Kazuya Matsumoto, Takashi Miyata, Tadashi Uragami

Preparation of polypeptide hydrogels that undergo structural transition and their stimuli-responsive behavior

61th SPSJ Annual Meeting, Yokohama, May 2012, Poster

2) Kazuya Matsumoto, Brylee David B. Tiu, Akifumi Kawamura, Tadashi Uragami, Rigoberto C. Advincula, Takashi Miyata

Preparation of Molecularly Imprinted Polypeptide Hydrogel Film that Formed Honeycomb Structure and Applied Molecular Sensor System

The 7th Fusion Materials Young School, Sendai, January 2013, Poster

3) Kazuya Matsumoto, Akifumi Kawamura, Tadashi Uragami, Takashi Miyata

Introduction of molecular recognition sites in stimuli-responsive gels that undergo conformational changes

62th SPSJ Annual Meeting, Kyoto, May 2013, Oral

4) Kazuya Matsumoto, Tomoya Katoh, Masanori Takee, Yuya Konishi, Akifumi Kawamura, Tadashi Uragami, Takashi Miyata

分子認識能を有する刺激応答性有機-無機ハイブリッド材料の創製

58th Summer College, Hiroshima, July 2013, Poster

5) Kazuya Matsumoto, Akifumi Kawamura, Tadashi Uragami, Takashi Miyata

Conformational Change and Responsive Behavior of Stimuli-Responsive Polypeptide Hydrogels That Recognize Target Molecules

62th Symposium on Macromolecules, Kanazawa, September 2013, Oral

6) Kazuya Matsumoto, Akifumi Kawamura, Tadashi Uragami, Takashi Miyata
標的分子に応答するポリペプチドゲルの合成
Gel Workshop in Kaga, Kaga, September 2013, Poster

7) Kazuya Matsumoto, Brylee David B. Tiu, Akifumi Kawamura, Tadashi Uragami, Rigoberto C. Advincula, Takashi Miyata
構造転移を示す刺激応答性ゲルの合成と分子認識挙動
The 8th Fusion Materials Young School, Gamagori, November 2013, Poster

8) Kazuya Matsumoto, Akifumi Kawamura, Tadashi Uragami, Takashi Miyata
構造転移により分子認識能を変化させるポリペプチドゲルの分子応答収縮挙動
25th Symposium on Polymer Gels, Tokyo, January 2014, Oral

9) Kazuya Matsumoto, Akifumi Kawamura, Takashi Miyata
構造転移を示す分子応答性ポリペプチドゲルの合成とその分子認識挙動
New Polymeric Materials Based on Element-Blocks, Hyogo, March 2014, Poster

10) Kazuya Matsumoto, Akifumi Kawamura, Tadashi Uragami, Takashi Miyata
Molecular Recognition Controlled by Conformational Changes of Polypeptide Hydrogels
63h SPSJ Annual Meeting, Nagoya, May 2014, Oral (English)

11) Kazuya Matsumoto, Akifumi Kawamura, Tadashi Uragami, Takashi Miyata
Synthesis of Stimuli-Responsive Polypeptide Hydrogels that Regulate Molecular Recognition Abilities
The 65th Division Meeting on Colloid & Interface Chemistry, Tokyo, September 2014, Poster

12) Kazuya Matsumoto, Akifumi Kawamura, Tadashi Uragami, Takashi Miyata
Preparation of Stimuli-Responsive Hydrogels That Change Molecular Recognition Ability by Structural Transition and Their Molecule Release Behaviors
63th Symposium on Macromolecules, Nagasaki, September 2014, Oral

13) Kazuya Matsumoto, Akifumi Kawamura, Tadashi Uragami, Takashi Miyata
ポリペプチドゲルの構造転移に伴う認識能変化
Gel Workshop in Nagasaki, Nagasaki, September 2014, Poster

14) Kazuya Matsumoto, Akifumi Kawamura, Tadashi Uragami, Takashi Miyata
分子インプリント法を用いたポリペプチドゲル薄膜の調製とその分子認識挙動
Membrane Symposium 2014, Kobe, November 2014, Poster

15) Kazuya Matsumoto, Akifumi Kawamura, Takashi Miyata
分子応答性を変化させる分子インプリントポリペプチドゲルの合成
The 11th Fusion Materials Young School, Kitakyushu, January 2015, Oral

16) Kazuya Matsumoto, Akifumi Kawamura, Takashi Miyata
Molecular Recognition and Responsive Behavior of Molecularly Imprinted Polypeptide Hydrogels That Undergo Helix-Coil Transition
64th SPSJ Annual Meeting, Sapporo, May 2015, Oral (English)

17) Kazuya Matsumoto, Yoshinori Ito, Akifumi Kawamura, Takashi Miyata
Design of Molecularly Imprinted Polypeptide Hydrogels for Drug Delivery
25th Annual Meeting of MRS-J, Yokohama, December 2015, Poster

18) Kazuya Matsumoto, Brylee David B. Tiu, Akifumi Kawamura, Rigoberto C. Advincula, Takashi Miyata
Preparation of Molecularly Imprinted Gel Layers on QCM Sensor Chips and Their Molecular Adsorption Behavior
38th Annual Meeting of Membrane Society of Japan, Tokyo, May 2016, Oral

19) Kazuya Matsumoto, Yoshinori Ito, Akifumi Kawamura, Takashi Miyata
Controlled Molecular Release from Molecularly Imprinted Polypeptide Hydrogels That Undergo Helix-Coil Transition
65th SPSJ Annual Meeting, Kobe, May 2016, Oral (English)

20) Kazuya Matsumoto, Brylee David B. Tiu, Akifumi Kawamura, Rigoberto C. Advincula, Takashi Miyata
Preparation of Molecularly Imprinted Polypeptide Gel Films and Their Molecular Adsorption Properties
65th SPSJ Annual Meeting, Kobe, May 2016, Poster

21) Kazuya Matsumoto, Yoshinori Ito, Akifumi Kawamura, Takashi Miyata
Regulation of Molecular Adsorption and Release by Structural Transition of Molecular Recognition Polypeptide Hydrogels Designed via Molecular Imprinting
65th Symposium on Macromolecules, Yokohama, September 2016, Oral

Award

1) Excellent Poster Award

Gel Workshop in Kaga, Kaga (Japan), September 2013

2) Poster Presentation Award

9th International Symposium in Science and Technology at Cheng Shiu University 2014, Kaohsiung (Taiwan), August 2014

3) Excellent Poster Award

The 65th Division Meeting on Colloid & Interface Chemistry, Tokyo, September 2014

4) Excellent Poster Award

Membrane Symposium 2014, Kobe, November 2014

5) Poster Award

65th SPSJ Annual Meeting, Kobe, May 2016

6) IPC 2016 Young Scientist Poster Award

The 11th SPSJ International Polymer Conference, Fukuoka, December 2016

Acknowledgment

The present research work was carried out under the direction of Professor Dr. Takashi Miyata of Department of Chemistry and Materials Engineering, Faculty of Chemistry, Materials, Bioengineering, Kansai University during 2011-2016. The author would like to express his sincere gratitude to Professor Dr. Takashi Miyata for his continuous guidance, fruitful discussions and encouragement throughout this study. He also gave him many chances to attend the domestic conferences, international conferences, and studying abroad. They were great experiences to expand his knowledge and perspective.

The author wishes to express his thanks to Assistant Professor Dr. Akifumi Kawamura, Department of Chemistry and Materials Engineering, Faculty of Chemistry, Materials, Bioengineering, Kansai University, for his useful discussions, advice and encouragement. Through his much valuable advice, the author learned a great deal of scientific thinking.

The author also expresses his deepest gratitude to Professor Dr. Yoshiaki Hirano, Professor Dr. Yuichi Ohya and Professor Dr. Yasuhiko Iwasaki, Department of Chemistry and Materials Engineering, Faculty of Chemistry, Materials, Bioengineering, Kansai University, for their valuable discussions.

The author is very indebted to Professor Dr. Rigoberto C. Advincula, Department of Macromolecular Science and Engineering, Case Western Reserve University, for giving exciting chances of collaboration works.

The author is also grateful to Professor Dr. Tadashi Uragami, Department of Chemistry and Materials Engineering, Faculty of Chemistry, Materials, Bioengineering,

Kansai University, for his valuable guidance.

The author wishes to thanks clerical staffs and cleanings staff of Kansai University, for giving pleasant university life.

The author would also like to thank his fellow labmates in Miyata laboratory for hearty discussing, for working together, and for all the fun in the last six years.

The author is also grateful to Mr. Yasuyuki Yoshida, Mr. Yoshinori Ito, Department of Chemistry and Materials Engineering, Faculty of Chemistry, Materials, Bioengineering, Kansai University, Dr. Allan C. Yago, Dr. Brylee David B. Tiu, Department of Macromolecular Science and Engineering, Case Western Reserve University, for letting defense be an enjoyable moment, and for their continuous encourage.

Last but not least, the author would also like to say a heartfelt thank you to his parents, Mr. Takayuki Matsumoto and Mrs. Sachiko Matsumoto, for helping in whatever way they could in every situation. *“最後に，あらゆる場面であたたかく応援してくれた両親に深く感謝いたします。”*

Kazuya Matsumoto
Integrated Science and Engineering Major
Graduate School of Science and Engineering
Kansai University
March 2017